THE EFFECTS OF DEPOSITION CONDITIONS ON THE LOW ENERGY ABSORPTION SPECTRUM OF MICROCRYSTALLINE SILICON THIN FILMS PREPARED BY HWCVD METHOD

Nebile IŞIK

İzmir Institute of Technology
July, 2005

THE EFFECTS OF DEPOSITION CONDITIONS ON THE LOW ENERGY ABSORPTION SPECTRUM OF MICROCRYSTALLINE SILICON THIN FILMS PREPARED BY HWCVD METHOD

A Thesis Submitted to
the Graduate School of Engineering and Science of
İzmir Institute of Technology
in Partial Fulfillment of Requirements for the Degree of

MASTER OF SCIENCE

in Physics

by
Nebile IŞIK

July 2005
İZMİR

We approve the thesis of **Nebile IŞIK**

Date of Signature

……………………………………. **04 July 2005**

Assoc. Prof. Mehmet GÜNEŞ
Supervisor
Department of Physics
İzmir Institute of Technology

……………………………………. **04 July 2005**

Asst. Prof. Yusuf SELAMET
Department of Physics
İzmir Institute of Technology

…………………………………. **04 July 2005**

Prof. Mustafa EROL
Department of Physics Education
Dokuz Eylül University

…………………………………. **04 July 2005**

Prof. Durmuş Ali DEMİR
Head of Department of Physics
İzmir Institute of Technology

……………………………………

Assoc. Prof. Semahat ÖZDEMİR
Head of the Graduate School

ACKNOWLEDGEMENTS

I am grateful to my advisor, Assoc. Prof. Mehmet Güneş for his help, kindly and scientific approach during this thesis.

I am also thankful to the other members of my thesis committee, Assoc. Prof. Yusuf Selamet, and Prof. Dr. Mustafa Erol for their comments and suggestions.

I would like to thank Dr. Reinhard Carius, Dr. Fridhelm Finger from Jülich Research Center, Germany, for their help, comments and suggestion and to Josef Klomfass for PSD, CPM measurements and calculations of fringe free absorption coefficient spectra for the films.

I am thankful to my boy friend and my family for their love.

Special thanks go to all my friends at Izmir Institute of Technology.

ABSTRACT

The optical and electronic properties of hydrogenated microcrystalline silicon films deposited by HWCVD method were investigated using steady state photoconductivity (SSPC), dual beam photoconductivity (DBP) and transmission spectroscopy methods to understand the effects of deposition conditions such as silane concentration and filament temperature on the low absorption coefficient spectrum, α (hν). The α (hν) spectrum obtained from the detailed optical calculation using the relative DBP and transmission spectra were compared with that independently measured on the same samples using photothermal deflection spectroscopy (PDS) and constant photocurrent method (CPM) techniques. The results were found to be in agreement with those of PDS and CPM at higher energy part of spectrum. On the other hand some differences exist among the spectra at lower energies. These differences were discussed to be consistent with underlying the physics of these methods.

The effect of silane concentration on the sub-bandgap α (hν) spectrum was found to be substantial. At highest SC of 10% the α (hν) spectrum similar to that of a-Si: H is obtained. As SC decreases to 7%, microcrystalline phase becomes dominant. Further decrease of SC, the low energy α (hν) decreases and given a minimum around SC of 5%. For the lower SC's, highly crystalline μc-Si: H films are obtained but the α (hν) values increases to higher values indicating an increase in the defect densities present in the microstructure.

The effect of filament temperature was investigated for a constant SC of 10%. It was found that at 1700ºC and 1800ºC, fully amorphous films are obtained but 1800ºC results in higher α (hν) values at lower energies. At 1880ºC, microcrystalline phase becomes dominant and the α (hν) spectrum becomes similar to that of single crystal silicon.

Finally, due to inhomogeneous microstructure of μc-Si: H, there are left fringes on calculated α (hν) spectrum on same samples. The degree of the inhomogeneity was investigated by front and back ac illumination of DBP measurements. It was found that there exists a substantial differences on the spectra measured on the same sample indicating importance of inhomogeneous film growth on optoelectronic measurements and its evaluation.

ÖZET

HW-CVD methodu ile büyütülmüş mikrokristal silisyum filmlerin optik ve elektronik özellikleri durağan hal ışıl iletkenlik, iki demetli ışıl iletkenlik (DBP) methodları kullanılarak incelenmiş ve hazırlık koşullarının mikrokristal silisyum filmlerin düşük enerjilerdeki ışıl soğurma katsayısına etkileri anlaşılmaya çalışılmıştır. Girişim saçaksız ışıl soğurma katsayısı spektrumu iki demetli ışıl iletkenlik (DBP) kullanılarak elde edimiş ve elde edilen sonuçlar bağımsiz olarak ışıl ışın saptırma izgegözlem (PDS) ve sabit ışılakım (CPM) teknikleri kullanılarak elde edilen sonuçlarla karşılaştırılmıştır. PDS, CPM ve DBP methodlarından elde edilen soğurma spektrumun bant enerjisine kadar uyumlu olduğu gözlenmiş ve bant enerjisinin altında meydana gelen farklılıklar ise tekniklerin farklı fiziksel yapıya sahip oluşuyla açıklanmıştır.

Silane konsantrasyonunun düşük enerji bölgesinde elde edilen soğurmaya önemli etkileri olduğu gözlenmiştir. Yüksek silane konsantrasyonunda elde edilen soğurma katsayısı spektrumunun a-Si:H filmlerin sahip olduğu soğurma spektrumuna benzer olduğu ve silane konsantrasyonunun azalması ile malzemenin yapısında mikrokristal fazın baskın hale geldiği gözlenmiştir. Silane konsantrasyonunun daha fazla azaltılması ile düşük enerji bölgesinde elde edilen soğurma katsayısının azaldığı ve SC=5% olduğunda en düşük değeri verdiği gözlenmiştir. En düşük silane konsantrasyon değerinde ise yüksek kristal yapıya sahip filmler elde edilmiş fakat elde edilen yüksek soğurma katsayı değerleri mikro yapının içerisinde bulunan kusur yoğunluğunun artması ile ilişkilendirilmistir.

Filament sıcaklığının soğurma katsayısına etkileri sabit silane konsantrasyonunda (SC=10%) büyütülmüş filmler kullanılarak incelenmistir. 1700ºC ve 1800ºC filament sıcaklıklarında büyütülmüş filmlerin amorf yapıda olduğu anlaşılmış fakat 1800ºC filament sıcaklığında büyütülmüş filmin düşük enerji bölgesinde yüksek soğurma verdiği gözlenmiştir. 1880ºC filament sıcaklığında ise micro yapıda mikrokristal fazın baskın olduğu ve elde edilen soğurma spektrumun tek kristal yapıdaki silisyumun soğurma spektrumuna benzer olduğu gözlenmiştir.

İncelenen mikrokristal silisyum filmlerin çoğu için elde edilen soğurma spektrumlarında kalıcı saçaklar gözlenmiş ve bu saçaların oluşması malzemenin homojen olmayan yapısı ile ilişkilendirilmiştir. Homojen olmayan yapının etkilerinin incelenmesi için DBP deneyleri tekrenk ışık ön ve alttabaka cam tarafından geçecek şekilde yapılmıştır.

TABLE OF CONTENTS

LIST OF FIGURES viii

LIST OF TABLES xii

CHAPTER 1. INTRODUCTION 1

1.1. Thesis Objectives 7

CHAPTER 2. EXPERIMENTAL..8

2.1. Sample Preparation 8

2.2. Characterization Techniques...11

2.2.1.Steady State Photoconductivity 11

2.2.2.Dual Beam Photoconductivity Spectroscopy 14

2.2.2.1. Flux Calibration..19

2.2.2.2. Transmission Spectrum 20

2.2.2.3. Dual Beam Photoconductivity Yield Spectrum, Y_{DBP} 21

2.2.3. Fringe Free Optical Absorption Coefficients Spectrum From DBP Yield Spectrum 23

2.2.4. Photothermal Deflection Spectroscopy 27

2.2.5. Constant Photocurrent Method 29

CHAPTER 3. EXPERIMENTAL RESULTS OF HYDROGENATED MICROCRYSTALLINE SILICON THIN FILMS DEPOSITED BY HWCVD METHOD..32

3.1. Introduction 32

3.2. The Effects of Silane Concentration...32

3.2.1. Steady State Photoconductivity Results 33

3.2.2. Sub-Bandgap Absorption Spectrum 35

3.2.2.1. Comparison of PDS, DBP, and CPM Absolute Absorption Coefficient Spectra 55

3.3. The Effects of Filament Temperature...58

3.3.1. The Effect on Steady State Photoconductivity 59

3.3.2. The Effect on The Sub-Bandgap Absorption Spectrum 61
3.4. The Effects of Microstructure on Dual Beam Photoconductivity Method 67
3.5 Conclusions..72

CHAPTER 4. DISCUSSIONS AND CONCLUSIONS 74

REFERENCES 81

APPENDICES
APPENDIX A. COMPUTER PROGRAM USED FOR DBP MEASUREMENTS 87
APPENDIX B. COMPUTER PROGRAM FOR CALCULATION OF $\alpha(h\nu)$ SPECTRUM 95

LIST OF FIGURES

Figure **Page**

Figure 2.1. a) Sample geometry for DBP measurement is shown. b) The top view of the sample geometry is shown. c) Sample geometry for PDS measurement is shown 10

Figure 2.2. Schematic diagram of steady state photoconductivity measurement system 13

Figure 2.3. Schematic diagram of dual beam photoconductivity system....................18

Figure 2.4. Flux spectrum of white light obtained using pyroelectric detector 19

Figure 2.5. A typical transmission spectra of a μc-Si: H thin film 20

Figure 2.6. Normalized photocurrent and raw spectra of μc-Si: H thin films measured by DBP method 21

Figure 2.7. DBP yield spectra of a μc-Si: H thin film deposited HWCVD method for high and low dc bias light intensities 22

Figure 2.8. The calculated absolute α (hν) spectra of a μc-Si: H thin film deposited by HWCVD method obtained from PDS, CPM, and DBP measurements. In the inset the corresponding transmission spectra of three methods are shown 26

Figure 2.9. Schematic diagram of photothermal deflection spectroscopy system 28

Figure 3.1. a) σph versus generation rate for μc-Si: H thin films deposited by HWCVD method at filament temperature 1700 ºC. b) $\mu_n\tau_n$ -product versus rate of the generation same μc-Si: H thin films.............................34

Figure 3.2. a) DBP yield spectrum for high and low bias light intensities for μc-Si: H thin films deposited by HWCVD method with SC=10 % and 1700 ºC. The phases of both measurements are shown. b) Corresponding transmission spectrum is exhibited.............................37

Figure 3.3. The calculated absolute α (hν) spectra of DBP for high and low bias light measurements of μc-Si: H thin films deposited by HWCVD method with SC=10 %..39

Figure 3.4. The calculated absolute α (hν) spectra of PDS and DBP for high and low bias light measurements of μc-Si: H thin films deposited by HW-CVD method with SC=10 %. In the inset, the phase of PDS, DBP are presented 41

Figure 3.5. a) Yield DBP signals measured at two different dc bias light intensities are shown. In the inset the phase of DBP signals are shown. b) The corresponding transmission spectrum is given for a μc-Si: H thin film deposited with SC=7% 42

Figure 3.5. c) The calculated absolute α (hν) spectra of DBP for high and low bias light measurements of μc-Si: H thin films deposited by HW-CVD method with SC=7 % 43

Figure 3.5. d) The calculated absorption coefficient spectra obtained from DBP low bias light intensity for two μc-Si: H thin films deposited by HW-CVD with SC=10% and SC=7% 44

Figure 3.6. a) Yield DBP signals measured at two different dc bias light intensities are shown. In the inset the phase of DBP signals are shown. b) The corresponding transmission spectrum is given for a μc-Si: H thin film deposited with SC=6% 46

Figure 3.6. c) The calculated absolute α (hν) spectra of DBP for high and low bias light measurements of μc-Si: H thin films deposited by HWCVD method with SC=6% 47

Figure 3.6. d) The calculated absolute α (hν) spectra of PDS and DBP for low bias light measurements of μc-Si: H thin films deposited by HWCVD method with SC=6 %. In the inset, the phase of PDS, DBP are presented 48

Figure 3.7. a) Yield DBP signals measured at two different dc bias light intensities are shown. In the inset the phase of DBP signals are shown. b) The corresponding transmission spectrum is given for a μc-Si: H thin film deposited with SC=5% 49

Figure 3.7. c) The calculated absolute α (hν) spectra of DBP for high and low bias light measurements of μc-Si: H thin films deposited by HWCVD method with SC=5% 50

Figure 3.7. d) The calculated absolute α (hν) spectra of PDS and DBP for low bias light measurements of μc-Si: H thin films deposited by HWCVD method with SC=5 %. In the inset, the phase of PDS, DBP are presented 51
Figure 3.8. a) Yield DBP signals measured at two different dc bias light intensities are shown. In the inset the phase of DBP signals are shown. b) The corresponding transmission spectrum is given for a μc-Si: H thin film deposited with SC=2% 52
Figure 3.8. c) The calculated absolute α (hν) spectra of DBP for high and low bias light measurements of μc-Si: H thin films deposited by HWCVD method with SC=2% 53
Figure 3.8. d) The calculated absolute α (hν) spectra of PDS and DBP for low bias light measurements of μc-Si: H thin films deposited by HWCVD method with SC=2 %. In the inset, the phase of PDS, DBP are presented 54
Figure 3.9. Absolute absorption coefficients versus the SC measured by PDS and DBP front ac illumination (low bias light) for μc-Si: H thin films prepared using HWCVD method at filament temperature 1700ºC 55
Figure 3.10. The calculated α (hν) spectra independently obtained the PDS, CPM, and low bias light DBP measurements for a μc-Si: H thin film deposited with SC=6%. In the inset the phase of PDS, CPM, and DBP low bias light signals are shown 57
Figure 3.11. The calculated α (hν) spectra independently obtained the PDS, CPM, and low bias light DBP measurements for a μc-Si: H thin film deposited with SC=10%. In the inset the phase of PDS, CPM, and DBP low bias light signals are shown 58
Figure 3.12. a) σ_{ph} versus generation rate for μc-Si: H thin films deposited by HW-CVD method at filament temperatures 1700 ºC, 1800ºC, and 1880 ºC With SC=10%. b) $\mu_n\tau_n$ -product versus generation rate of the same μc-Si: H thin films 60

Figure 3.13 a) DBP yield spectrum for high and low bias light intensities for μc-Si: H thin films deposited by HWCVD method with SC=10 % and filament temperature of 1700 ºC. b) Corresponding transmission spectrum is exhibited 63
Figure 3.14. a) DBP yield spectrum for high and low bias light intensities for μc-Si: H thin films deposited by HWCVD method with SC=10 % and filament temperature of 1800 ºC. b) Corresponding transmission spectrum is exhibited 64
Figure 3.15 a) DBP yield spectrum for high and low bias light intensities for μc-Si: H thin films deposited by HWCVD method with SC=10 % and filament temperature of 1880 ºC. b) Corresponding transmission spectrum is exhibited 65
Figure 3.16. The calculated absolute α (hv) spectra obtained from DBP low bias intensities for three thin films deposited at filament temperatures of 1700 ºC, 1800 ºC, and 1880 ºC 66
Figure 3.17. a) DBP yield spectra for μc-Si: H thin film with SC=10% for ac light incident from film side and substrate side. Inset of the figure, transmission spectrums of both measurements are shown. b) The calculated absolute α (hv) spectrum of both measurements are shown. In the inset, the phases of both measurements signals are presented 68
Figure 3.18. a) DBP yield spectra for μc-Si: H thin film with SC=6% and filament temperature 1700 ºC for ac light incident from film side and substrate side. Inset of the figure, transmission spectrum of the sample is shown. b) The calculated absolute α (hv) spectrum of both measurements are shown. In the inset, the phases of both measurements signals are presented 69
Figure 3.19. a) DBP yield spectra for μc-Si: H thin film with SC=2% and filament temperature 1700 ºC for ac light incident from film side and substrate side. Inset of the figure, transmission spectrum of the sample is shown. b) The calculated absolute α (hv) spectrum of both measurements are shown. In the inset, the phases of both measurements signals are presented 71

LIST OF TABLES

Table **Page**

Table 2.1 Deposition parameters and thickness of μc-Si: H thin films deposited with 1700 ºC, 1800 ºC, and 1880 º C filament temperatures used in this thesis 10

CHAPTER 1

INTRODUCTION

Hydrogenated microcrystalline silicon (μc-Si: H) is a material that has recently become of prime interest for thin film solar cells, flat panel, optical sensors and other thin film devices because of its properties such as a larger long-wavelength response, high stability against light-induced degradation, higher conductivities and mobilities which are important for technological applications when compared to hydrogenated amorphous silicon (a-Si: H) (Vetterl et al 2002a, Shah et. al 2003a, Klein et. al 2004a). One of the most used approaches to grow device quality hydrogenated microcrystalline silicon layers at low substrate temperature and on very cheap materials is Plasma Enhanced Chemical Vapor Deposition (PECVD) (Vetterl et. al 2002a, Klein et. al 2004a, Carius et al 2003a). Radio Frequency Plasma Enhanced Chemical Vapor Deposition (RF-PECVD) technique produces electronic quality of μc-Si: H thin films in lab scale, however, large area fabrication can not be possible in this technique. The standard excitation frequency of plasma is 13.56 MHz but with increasing frequency of the plasma higher deposition rates and better film properties can be acquired. Therefore, Very High Frequency Plasma Enhanced Chemical Vapor Deposition (VHF-PECVD) technique has become popular for thin films device technologies. However, in this technique created ions play important role on the nature of the films (Rath 2001). On the other hand, Hot Wire Chemical Vapor Deposition (HWCVD) (Yamamoto et. al 2002, Schroop 2004, Klein et. al 2001b) has been attracted considerable attention in recent years as an alternative deposition method for hydrogenated microcrystalline silicon (μc-Si: H) thin films because of satisfying high quality solar cells at high deposition rates, and large area fabrication.

Hydrogenated microcrystalline silicon (μc-Si: H) shows different morphological microstructures from the crystalline silicon (c-Si) and amorphous silicon (a-Si: H). The microstructure of μc-Si: H consists of randomly oriented crystalline grains, varied volume fractions of amorphous phase, grain boundaries and voids which depend critically on deposition conditions and are important for understanding the electronic and optical properties of μc-Si: H. Using a special kind of plasma deposition

technique, hydrogenated microcrystalline silicon (μc-Si: H) was first fabricated in 1968 by Veprek and Maracek (Veprek et. al 1986a). Since then, using a strong dilution of silane (SiH_4) in hydrogen as an original source gas so as to activate formation of a microcrystalline growth rather than amorphous silicon. μc-Si: H microcrystalline silicon layers have been obtained by radio frequency glow discharge technique reported by some groups (Usui et. al 1987). The deposition rates were achieved well below 1 Å/s in these experiments.

Hydrogenated microcrystalline silicon (μc-Si: H) has a relatively low absorption coefficient than that of hydrogenated amorphous silicon (a-Si: H) in the visible part of solar spectrum due to its indirect bandgap. The absorption coefficient of μc-Si: H is very high in high energy region when compared crystalline silicon (c-Si). μc-Si: H also exhibits significant absorption well below the bandgap of crystalline silicon than that of crystalline silicon. To acquire sufficient absorption and photogeneration in the corresponding wavelength range, the required thicknesses of μc-Si: H layers can be kept a few μm. As well as above reason, poor grain boundary passivation in the material is considered to be a main obstacle for electronic transport in microcrystalline silicon layers. Because of above reasons, using hydrogenated microcrystalline silicon as an active photogeneration layer within a thin film silicon solar cells took several years (Shah et. al 2003a). First attempts results were reported by Lucovsky et al. (Lucovsky et. al 1991), and Faraji et al. (Faraji et. al 1992). Afterward, using the very high frequency (VHF) glow discharge method, completely microcrystalline p-i-n and n-i-p type-silicon solar cells were fabricated (Meier et. al 1994, Fluckiger et. al 1992, Feitknecht et. al 2001). To obtain higher efficiencies, very high frequency PECVD (Vetterl et. al 2002a, Shah et. al 2003a, Finger et. al 1994a), RF-PECVD (Nasuno et. al 2000) and Hot Wire CVD (Schroop et. al 2004, Klein et. al 2004a, Klein et. al 2001b, Carius et. al 2003a) techniques were used. Combining the advantageous of microcrystalline silicon (μc-Si: H) and amorphous silicon (a-Si: H) in a tandem concept, micromorph solar cell has been achieved (Meier et. al 1994). Thus far, micromorph tandem cell efficiencies in the range of 10-14% which are higher than that of single junction solar cells have been reported (Proceedings, Vetterl et. al 2002a). Because of its excellent and sufficient properties, hydrogenated microcrystalline silicon has received growing attention in the field of thin film semiconductor technology.

A broad variety of methods has been applied to investigate unpredictable physical properties of μc-Si: H, which was not straightforward to determine till now. The microstructure of μc-Si: H is the most important consideration for determining its properties. It consists of crystalline and amorphous phases, grain boundaries, cracks, voids, etc. The most common parameter to control the microstructure of μc-Si: H is silane concentration (SC= $[SiH_4]/[SiH_4+H_2]$), which has a universal influence on the material properties. Depending on decreasing or increasing of silane concentration in whatever deposition process such as PECVD (Plasma Enhanced Chemical Vapor Deposition) or HW CVD (Hot Wire Chemical Vapor Deposition) is known to cause changing in the microstructure of μc-Si: H from the growth of amorphous to microcrystalline material (Matsuda 1983). If the silane concentration (SC) is decreased, the crystalline growth starts. Afterward, with further decrease of silane concentration (SC), the crystalline volume fraction increases and morphological transitions from amorphous to microcrystalline are observed. Optical, structural and electrical properties of μc-Si: H thin films deposited by HW CVD method are changed not only by silane concentration (SC) but also by other deposition conditions such as filament temperature, deposition rate and substrate temperature. One of the most important process parameter in HW CVD method is filament temperature which affects both the deposition rate and optical and structural properties of the films. For the silane concentration in amorphous region, at higher filament temperature an amorphous to microcrystalline transition is observed (Jadkar et. al 2003).

The changes in the structural properties of μc-Si: H thin films are characterized by Raman spectroscopy (Vetterl et. al 2002a, Ray et. al 2002, Neto et. al 2002, Luysberg et. al 1997, Klein et. al 2004a, Houben et. al 1998). Focusing on inelastic scattering of photons caused by interaction of photons and phonons (lattice vibration) is the basic principle of this technique for investigation of the properties of materials. The measurements are generally functioned in the back-scattering configuration. For excitation, 514 nm line of an Ar laser strongly absorbed or 633 nm line of a HeNe laser, less absorbed, is used as the excitation source (Houben et. al 1998, Carius et. al 2001b). The Raman spectrum of a- Si: H films with a width (full width at half maximum; FWHM) of 60 cm^{-1} centered at 480 cm^{-1} are used. The symmetric and narrow spectrum of c- Si film is located at about 520 cm^{-1} with a FWHM of about 3.5 cm^{-1}. The μc- Si: H film exhibits an asymmetric spectrum centered at 518 cm^{-1} with a FWHM of 12 cm^{-1}

and a tail interpreted as an amorphous phase in the material. With changing silane concentration the Raman spectra of the material alters. Depending on the differences between the absorption of amorphous and crystalline phases and the Raman cross sections, a unique measurement of the structure of films can not obtained by the Raman spectra (Ossadnik et. al 1999, Carius et. al 2001b). The ratio of the integrated scattering intensity of the crystalline phase to the total scattering intensity given $I_{CRS} = I_C/ (I_A+I_C)$ (where $I_c=I_{520}+I_{500}$ and $I_a= I_{480}$ and I denotes the area of Gaussian peaks that were fitted to the spectra), can be considered as a semiquantitative measure for the crystalline volume fraction.

To obtain information about the crystalline structure and phase content of μc-Si: H thin films, X– Ray Diffraction (XRD) is also used (Houben et. al 1998, Carius et. al 2001b). The diffractograms of microcrystalline silicon thin films can be characterized by sharp peaks at diffraction angles $2\,\Theta_{hkl} = 28.4\,^{o}$, $47.30\,^{o}$ and 56.1^{o} corresponding to {111}, {220} and {311} lattice plane reflections from crystalline silicon. Amorphous silicon can be characterized by two board peaks centered at slightly lower angle than the position of {111} reflection and in between the {220} and {311} reflections. The crystalline volume fraction of the microcrystalline silicon thin films can be determined by the scattering intensities of amorphous and crystalline peaks (Carius et. al 2001b). With increasing silane concentration the amorphous phase dominates in the spectra.

The microstructure of μc-Si: H thin films can be investigated, by using the diffraction of high energy electrons, by transmission electron microscopy (TEM). The TEM results show that crystal nucleation and grain growth and also the evolution of microstructure of μc-Si: H thin films can be affected by changing the silane to hydrogen ratio in the plasma (Shah et. al 2003a, Houben et. al 1998, Carius et. al 2001b). At lower hydrogen dilution, at high silane concentration, the crystalline growth begins at nucleation centers. During the growth, the size of crystalline grains strongly depend on the deposition parameters and the substrate increase. As a result, the crystalline grains occur in a conical shape near the substrate surface. However, these crystalline grains are not perfectly single crystalline, they show a large number of twin defects (Houben et. al 1998). Either amorphous or voids can fill the space between the crystalline columns. A disordered phase can only be found in the shape of grain boundaries between the crystalline columns. Thus, the volume fraction of amorphous is low. In the transition from crystalline to fully amorphous growth, the diameter of crystalline grains decreases

when amorphous phase dominates. The microstructure of hydrogenated microcrystalline silicon thin films is altered by varying of deposition parameters. Silane concentration plays an important role to determine the electronic, optical and structural properties of material.

The optical absorption coefficient is one of the main quality properties of the PV materials. Absorption studies show that the measured optical absorption of microcrystalline silicon thin films is in general higher than that of crystalline silicon thin films in visible region of solar spectrum (Vanacek et. al 1998, Shah et. al 2000b). The enhanced absorption at higher energies (hν >1.8 eV) is mainly due to light scattering by the rough surface of the μc-Si: H layers, also a contribution from the amorphous phase at high amorphous volume fractions present in the μc-Si: H thin films (Poruba et. al 2000). The absorption coefficient at energies below the 1. 8 eV down to bandgap of silicon (1.12 eV) is commonly attributed to strain effects in the grain and grain boundaries (Jun et. al 2002). In this region it gives higher absorption coefficient spectrum higher than that of pure amorphous silicon. The sub-bandgap absorption (at photon energies < 1.2 eV) of microcrystalline silicon thin films can be attributed to the defect densities in the material.

Hydrogenated microcrystalline silicon is an inhomogeneous thin film material consisting of highly disordered morphology reflected by several localized bandgap states. These states are tail states which are present in high concentration in energetic proximity to the band edges and deep band gap states are included by silicon dangling bonds. A variety of techniques have been used to investigate these electronic states in the mixed-phase material hydrogenated microcrystalline silicon. These techniques are electron spin resonance (ESR), steady state photoconductivity, dark conductivity and optical absorption measurement techniques especially photothermal deflection spectroscopy (PDS), constant photocurrent method (CPM) and dual beam photoconductivity method (DBP).

To obtain valuable information about charge carrier recombination process of the electronic states, in particular defect states, present in μc-Si: H thin films, electron spin resonance method (ESR) has been used successfully in recent year. Extended investigations by ESR techniques have been performed by many research groups to determine the paramagnetic defects present in μc-Si: H thin films (Neto et. al 2002a, Lips et. al 2003, Lima et. al 2002, Finger et. al 1998b, Finger et. al 2004c, Boehme et. al

2004). The ESR measurements show that μc-Si: H reveals a signal with an asymmetric-line shape associated with the presence of two different centers. One of them is supposed to be a silicon dangling bond (Si DB) with a g value (gyromagnetic ratio) of 2.0052. The other center with g value of 2.0043 is explained by the electrons trapped in the conduction band tails of the amorphous phase, but this center is a puzzling phonemenon for researchers. The g- value is given by $g=h\upsilon/\mu_b B$ where h is the Planck constant, υ is the microwave frequency at resonance, μ_b is the Bohr magneton and B is the magnetic field at resonance. The signal of μc-Si: H is very different from that of a-Si: H (Lima et. al 2002, Finger et. al 2004c). There is another important signal observed in μc-Si: H with g value of 1.998 is ascribed to free electron in the crystalline region in the material.

Three optical absorption measurement techniques, namely photothermal defection spectroscopy (PDS) (Jackson et. al 1981a, Jackson and Amer 1982b), constant photocurrent method (CPM) (Vanacek et. al 1995b) and dual beam photoconductivity (DBP) (Wronski et. al 1982, Lee et. al 1998, Gunes and Wronski 1992a) are commonly used to measure the absolute optical absorption coefficient, (α), in the visible and infrared region. Photothermal deflection spectroscopy (PDS) is based on the heating of a sample by the absorbed light energy and has been used as complementary technique to obtain the absorption coefficient spectrum of μc-Si: H thin films (Klein et. al 2001b, Poruba et. al 2000b). Although PDS can give information about surface states, it can not allow acquiring information about the accurate absorption coefficient below the bandgap energy of microcrystalline silicon thin films because of substrate absorption effect. Constant photocurrent method (CPM), both in standard and absolute mode (Vanacek et. al 1983c) has also been used to obtain absolute absorption coefficient spectrum of μc-Si: H thin films (Beck et. al 1996). In CPM, only the electron occupied defect states below the Fermi level can be detected because of using low generation rate of monochromatic light which satisfies the lifetime of the electron is almost constant. Dual beam photoconductivity (DBP) method is another relative method to derive the absorption coefficient spectrum from the photoconductivity spectrum like CPM. Using two different bias light intensities in DBP can satisfy to detect gap states because DBP spectrum at low energies depends on the bias light intensity used during the measurements. Increasing bias light intensities more information about the defect states in the gap of μc-Si: H thin films can be obtained compared to CPM.

1.1 Thesis Objectives

Hydrogenated microcrystalline silicon (μc-Si: H) has attracted considerable attention as a device quality material for solar cells and thin film device technology due to some of its unique properties. Monitoring the changes of material parameters such as an optical absorption coefficient spectrum and defect states in the material with filament temperature and silane concentration is important from a practical point of view.

The objective of this thesis is to understand the effects of deposition parameters, especially filament temperature and silane concentration, and to learn the effect of inhomogeneous structure of material on the low energy absorption coefficient spectrum of μc-Si: H thin films deposited HW-CVD method. Especially, the α (hν) at sub-bandgap energies are taken as a comparison criteria for the effect of deposition parameters on the defect states present in the material. In this study, steady state photoconductivity (SSPC), dual beam photoconductivity (DBP) and transmission spectroscopy will be used to investigate the effects of deposition conditions on the microstructure of the material. DBP and transmission spectra have been used to obtain interference fringe free absolute absorption coefficient spectrum using Ritter and Weiser theory (Ritter and Weiser 1986). Then the resulting absolute absorption coefficient spectrum will be compared with those independently measured PDS and CPM methods.

To understand the effect of silane concentration on sub-bandgap absorption coefficient spectrum, μc-Si: H thin films deposited with different silane concentrations and at filament temperature 1700ºC will be used. By changing silane concentration, the substantial differences in the microstructure of the material will be investigated.

The effect of filament temperature on sub-bandgap absorption coefficient spectrum was investigated for a constant SC of 10% with filament temperature changing between 1700-1880ºC. The behaviors of the material will be investigated by changing filament temperature.

Finally, to investigate the effects of inhomogeneous structure of material on the sub-bandgap absorption coefficient spectrum, DBP measurements will be carried out by illuminated ac monochromatic light through the film and the substrate side at the same dc bias light intensity. The interference fringes left on the α (hν) spectra will be attributed to inhomogeneous structure of microcrystalline silicon thin films.

CHAPTER 2

EXPERIMENTAL

2.1 Sample Preparation

Hydrogenated microcrystalline silicon (μc-Si: H) thin films have been deposited by several fabrication techniques such as radio frequency (RF) plasma enhanced chemical vapor deposition at 13 MHz, very high frequency plasma enhanced chemical vapor deposition (VHF-PECVD) (Kondo 2003), and hot wire chemical vapor deposition technique (HW-CVD) (Schroop 2004).

RF-PECVD has been widely employed for the fabrication of μc-Si: H thin films. In RF-PECVD system, an rf voltage is applied between two parallel electrodes and the substrate is located at the grounded electrode. The standard frequency is 13.56 MHz and the silane (SiH_4) diluted by hydrogen has been used as a source gas for μc-Si: H fabrication. For large area deposition RF-PECVD is preferred since it provides better thickness uniformity than that of VHF-PECVD.

VHF-PECVD, in the range between 13.56-110 MHz, has become so popular because of creating a high hydrogen density in the plasma, which is very important for the growth of μc-Si: H thin films (Rath 2002). VHF-PECVD technique is one of the most used approaches to grow device quality material within a short fabrication time. However, this technique has difficulties for large area deposition because of wavelength comparable to the cell size.

HW=CVD is a new developed method to fabricate device quality μc-Si: H thin films (Matsumura 1986, Mahan et. al 1991). In HW-CVD process, the source gases are effectively cracked into atomic radicals at the surface of the filament. Especially, tungsten or tantalum wires are used as filaments. The temperature of the filament is held at higher than 1500 º C in the system. The decomposed radicals of the silane gas thermally diffuse to and are deposited on the substrate. Thus, the filament is one of the most important process parameters in the HW-CVD system to determine the optical and electronic properties of the deposited thin films. Compared to PECVD technique, HW-CVD technique has some important advantages. First of all, there is no plasma, so there

is no dust in HW-CVD system. Secondly, no ions are created in the system so there are no ionic species to disturb the nucleation process. Finally, very efficient radical production can be obtained in HWCVD system which leads to a high deposition rate (Schroop 2004).The large area capabilities can be physically determined in HWCVD technique by increasing the number of wires in the system. In addition, it is a low cost production method for silicon based thin films.

The deposition parameters, especially filament temperature, silane concentration (SC), and substrate temperature affect the deposition rate, the crystalline volume fraction, and optical and electronic properties of HW-CVD deposited μc-Si: H thin films (Schroop 2004). The crystalline volume fraction depends on the silane concentration. The Raman and XRD measurements show that with increasing the silane concentration the crystalline volume fraction decreases (Houben et. al 1998, Carius 2002a). At higher SC's, amorphous phase is dominant in the structure. As the silane concentration decreases, the crystalline regions increase and for very low silane concentration, highly crystalline intrinsic films are grown in a columnar structure (Vetterl et. al 2002b). Thus, the complex structure of the microcrystalline silicon containing the crystalline grains and amorphous region occurs (Houben et. al 1998). The deposition rate increases with increasing the filament temperature because the filament temperature plays important role on the breaking of the silane molecules. At higher silane concentration and at higher filament temperature a transition from amorphous to microcrystalline is observed (Jadkar et. al 2003).

In this thesis, hydrogenated microcrystalline silicon (μc-Si: H) thin films were prepared using hot-wire chemical vapor deposition (HW-CVD) system at Research Center Jülich, Germany, on a borosilicate glass substrates, with varying silane concentration (SC) (gas flow ratio, SC= [SiH4] / [SiH4 + H2]) from 2% to 10% and with different filament temperatures. Samples are typically 554 -1100 nm thick were used in this study. Coplanar Ag electrodes 0.5 mm wide and 0.5 cm long were evaporated on the μc-Si: H samples. For the hot wire 2-3 tantalum filaments with 0.5 mm diameter were used. The filament temperatures were between 1700 and 1880 ºC and the substrate temperature was mainly kept unchanged around 220 ºC±10 ºC. Coplanar μc-Si: H samples were used to measure dark and photoconductivity, constant photocurrent method, and dual beam photoconductivity spectrum. To measure PDS

Table 2.1 Deposition parameters and thickness of μc-Si: H thin films deposited with 1700ºC, 1800 ºC, and 1880 ºC filament temperatures used in this thesis.

HW-CVD THIN FILMS				
Sample name	Silane Concentration (SC)	Thickness (T) (nm)	Filament Temperature (ºC)	Substrate Temperature (ºC)
02c310	2	887	1700	215
02c312	7	1100	1700	215
02c332	10	685	1700	215
02c458	6	554	1700	230
02c466	5	634	1700	230
02c303	10	986	1800	230
02c367	10	740	1880	227

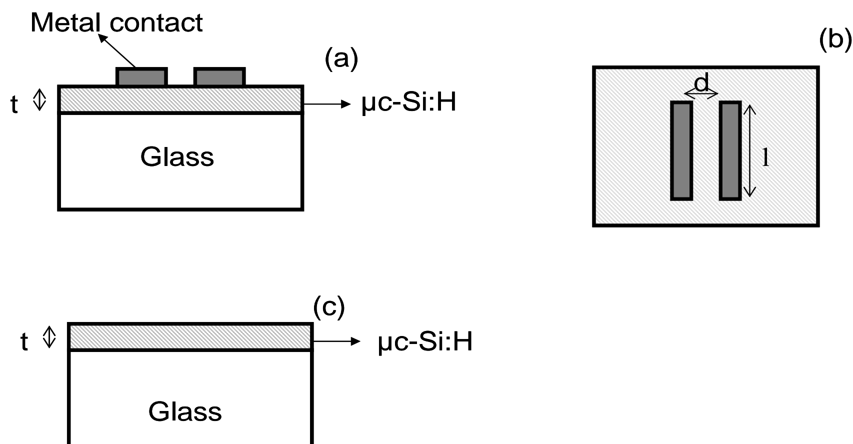

Figure 2.1 a) Sample geometry for DBP measurement is shown. b) The top view of the sample geometry is shown. c) Sample geometry for PDS measurement is shown.

spectrum, samples deposited on glass substrate without Ag contacts were used. Hydrogenated microcrystalline silicon thin films used in this thesis listed in Table 2.1. The sample geometries for DBP and PDS system are given in Figure 2.1.

2.2 Characterization Techniques

In this thesis, the effects of deposition conditions on the electronic and optical properties of intrinsic hydrogenated microcrystalline silicon thin films are characterized using steady state photoconductivity (SSPC), dual beam photoconductivity (DBP), and optical transmission spectroscopy techniques. The absolute absorption coefficient spectrum at wider energy region is obtained using the relative DBP and transmission spectra measured on the same sample. Then, the resulting absolute α (hν) spectrum is compared with those measured by photothermal deflection spectroscopy (PDS), and constant photocurrent method (CPM).

2.2.1 Steady State Photoconductivity

Steady state photoconductivity is a complex process of carrier generation across the bandgap, carrier transport of the band edges and recombination of photogenerated carriers through the defect states present in the bandgap of semiconductor. It is generally expressed as a function of the electron and hole concentrations and mobilities.

$$\sigma_{ph} = q\mu_n n + q\mu_p p \qquad (\Omega cm)^{-1} \qquad (2.1)$$

where n and p are the densities of free electrons and holes in the conduction band (CB) and the valance band (VB), respectively, μ_n and μ_p are electrons and holes mobilities. In intrinsic microcrystalline silicon thin films, the mobility lifetime product of holes are much smaller than that of electrons (Wyrsch et. al 1995a). Therefore photoconductivity is dominated by a single carrier electron. Thus, the photoconductivity formula can be written as,

$$\sigma_{ph} \cong q\mu_n n \quad (\Omega cm)^{-1} \qquad (2.2)$$

where n is the free electron carrier density obtained from the generation rate of the monochromatic light as follows,

$$n = G\tau_n \qquad (cm)^{-1} \tag{2.3}$$

where G is the generation rate of electron-hole pairs across the bandgap and τ_n is the lifetime of free electrons. The generation rate, G, can be calculated as a function of flux of incident light, thickness of the sample, absorption coefficient at excitation energy, and the reflectivity of the material.

$$G = \frac{F(1-R)[1-\exp(\alpha t)]}{t} \qquad \left(cm^{-3}s^{-1}\right) \tag{2.4}$$

where α is the absorption coefficient, t is the thickness of the sample, R is the reflectivity of the material, and F is the incident flux. Flux is calculated using the calibrated p-i-n photodiode as

$$F(h\nu) = \frac{I_{ph}(h\nu)}{AQE(h\nu)q} \qquad \left(cm^{-3}s^{-1}\right) \tag{2.5}$$

where QE (hν) is the quantum efficiency of photodiode at a given wavelength, A is the area of the detector, I_{ph} is the measured photocurrent using the p-i-n photodiode at the photon energy hν.

Using equations (2.2) and (2.3), the mobility-time product, $\mu_n\tau_n$, also called photosensitivity of the material, can be obtained. Photosensitivity is important information about the photoconductivity material.

$$\mu\tau = \frac{\sigma_{ph}}{qG} \qquad \left(cm^2V^{-1}\right) \tag{2.6}$$

For steady state condition, the photoconductivity, σ_{ph} , is calculated from the experimental parameters using the Ohm's law.

$$\sigma_{ph} = \frac{I_{ph} d}{Vtl} \qquad (\Omega cm)^{-1} \tag{2.7}$$

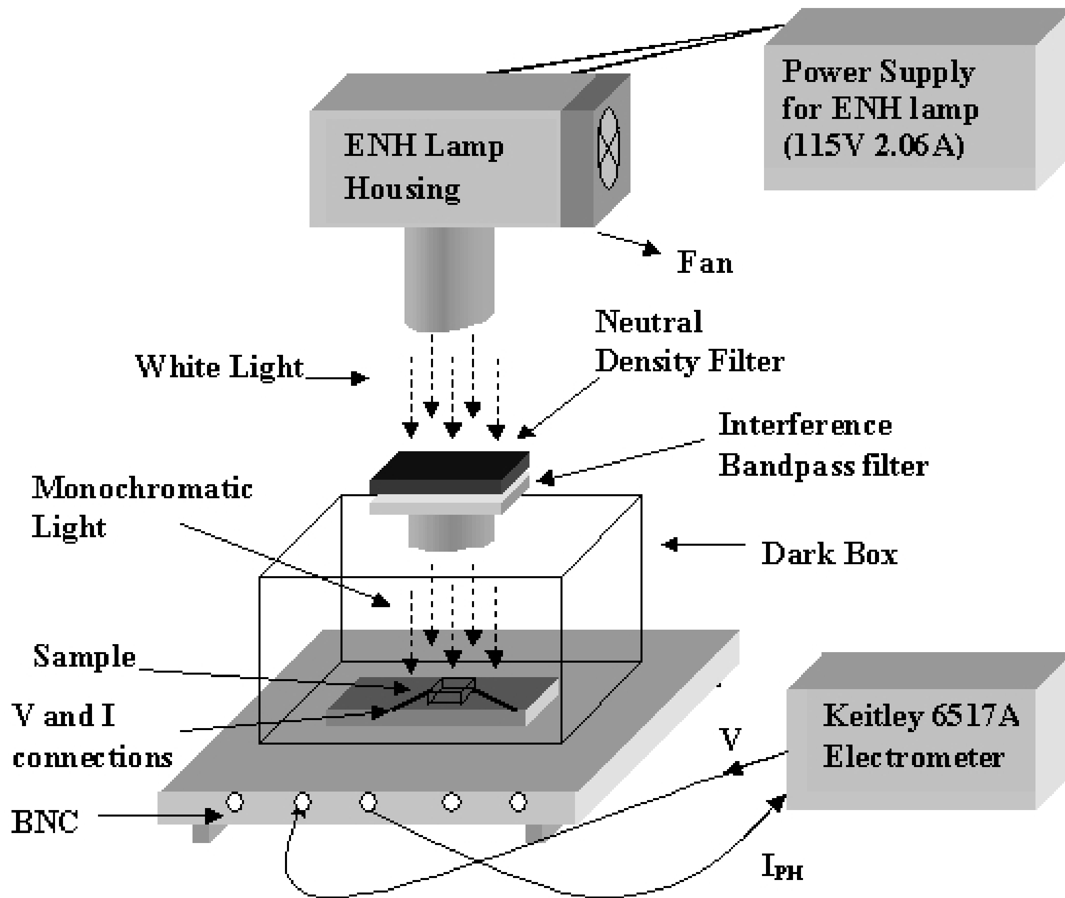

Figure 2.2 The steady state photoconductivity measurements system. (Source: Akdas 2002)

where I_{ph} is photocurrent, d is separation of electrodes, t is the thickness of the sample, l is the length of the electrodes, and V is applied voltage as shown in Figure 2.1.

Steady state photoconductivity shows a non- integer law dependence on the light intensity F or generation rate G. Also it can be expressed as follows,

$$\sigma_{ph} \propto G^{\gamma} \qquad (\Omega cm)^{-1} \tag{2.8}$$

and $\mu\tau$ product can also be written as ,

$$\mu\tau \propto G^{\gamma-1} \quad \left(cm^2V^{-1}\right)$$

where γ is the exponent and related to recombination kinetics in the photoconductive thin films. For defective amorphous and microcrystalline silicon semiconductor thin films, the value of γ is lower than unity and changes between 0.5 and 1.0 and there is no direct relation to the distribution of defect states present in the bandgap of the semiconductor.

For the photoconductivity measurements, a homemade steel box was used. The system is shown in Figure 2.2. In the steel box, an Osram 250 W ENH lamp is used as a white light source and a fan was used to cool the lamp. To obtain high intensity monochromatic light, 800-750-690 nm interference filters and RG-610 bandpass filter were used. To adjust the monochromatic light intensity to lower flux values, neutral density filters transmitting 0.1%, 1%, 10%, and 50% of incoming light, were used. Constant voltage was applied, dark and photo currents were measured by using Keitley 6517 A Electrometer. For respective photon energies, the incident white light was calibrated using a p-i-n photodiode having a 14.5 mm^2 active area and known quantum efficiency values. Using the measured flux value and film geometries, generation rate of excitation light is calculated at each light intensity. Finally, measured σ_{ph} and $\mu_n\tau_n$– product results were presented as a function of generation rate for comparison of different μc-Si: H thin films.

2.2.2 Dual Beam Photoconductivity Spectroscopy

The dual beam photoconductivity method (DBP) (Wronski et. al 1982, Lee et. al 1998, Gunes and Wronski 1992a, Gunes et. al 2003b) is generally used to measure ac photoconductivity of the sample as a function of incident monochromatic light energy. DBP technique involves the use of two light beams, a dc bias light beam and a monochromatic chopped ac light beam with 13 MHz. The generation rate of the modulated monochromatic ac light is lower than that of the dc light beam. The main idea of using high generation rate dc bias light is to keep the free carrier lifetime

constant during the measurements. This means that dc bias light keeps the electron and hole quasi Fermi levels constant during the measurement. This provides a constant distribution of occupied defect states in the bandgap. On the other hand, low generation rate monochromatic ac light beam does not affect the quasi Fermi levels. Thus, a.c photoconductivity linearly depends on monochromatic ac light intensity. This implies that no changes can be observed in the mobility lifetime product of dc light due to additional ac monochromatic light coming on the sample. Therefore, the statistics of occupied defect states will be unchanged during the measurements. Then, the monochromatic a.c light plays a role to excite the electrons from occupied defect states into conduction band. The excited electrons in the conduction band are detected as ac photocurrent. As a result, the photoconductivity spectrum is a reflection of the occupied defect states in the bandgap of the material.

The photoconductivity is derived previously as a function of the free majority carrier density and electron mobility as,

$$\sigma_{ph} = q\mu_n n \tag{2.9}$$

As mentioned in equation 2.3, the number of electrons equals to product of lifetime and generation rate. Thus, the sub-bandgap photoconductivity arising from the monochromatic beam can be written as follows,

$$\sigma_{ph}(ac) = q\mu_n\tau_n g(h\nu) \tag{2.10}$$

To obtain photoconductivity in the low absorption region, the product of absorption coefficient and thickness of the film, (αt), must be smaller than unity. For this reason, the exponential term can be neglected in equation for generation rate. Then, the generation rate can be derived as,

$$g(h\nu) = F(h\nu)(1-R)\left(1-e^{-\alpha t}\right)/t \tag{2.11}$$

for $\alpha t \ll 1$

$$g(h\nu) = F_{ac}(h\nu)(1-R(h\nu))\alpha(h\nu) \tag{2.12}$$

As a result, using the equation 2.10 the photoconductivity can be written as,

$$\sigma_{ph}(ac) = q\mu_n \tau_n F_{ac}(h\nu)(1 - R(h\nu))\alpha(h\nu) \quad (2.13)$$

The DBP yield spectrum explained as photoconductivity divided by the incident flux, Y_{DBP}, is

$$Y_{DBP} = \frac{\sigma_{ph}(ac)}{F_{ac}(h\nu)} = [q\mu\tau(1-R)\alpha(h\nu)] \quad (2.14)$$

if

$$[q\mu\tau(1-R)] = C$$

where C is a constant. α (hν) is obtained by multiplying the Y_{DBP} by a constant C which is carried out by normalizing DBP yield spectrum to absolute absorption coefficient spectrum obtained by other techniques such as, PDS or Transmission / Reflection measurements. Therefore, DBP yield is

$$Y_{DBP} \propto \alpha(h\nu) \quad (2.15)$$

or

$$\alpha(h\nu) = CY_{DBP} \quad (2.16)$$

As seen in the equation 2.15 or equation 2.16, DBP yield is proportional to the absorption coefficient of the material. Since DBP is a relative measurement method thus the obtained spectrums are in relative scale, the absolute absorption coefficients can not be directly obtained by DBP method. Generally, to acquire absolute absorption coefficient spectrum of the sample at low energies, DBP spectrum is normalized to the absolute absorption coefficient spectrum obtained from transmission and reflection (Cody et. al 1980) or from PDS (Gunes et. al 2003b). The interference fringes in DBP

spectrum are generally removed using fast Fourier transform (FFT) (Wiedeman et. al 1987), but a significant error can be introduced in this procedure for acquiring the fringe free absorption coefficient spectrum. In this thesis, absolute absorption coefficient spectrum is calculated from the Y_{DBP} and transmission spectra of the same sample using the detailed optical equations defined by Ritter and Weiser (Ritter and Weiser 1986), which was applied by Goktas in his thesis. This procedure is explained in detail in the following section.

Experimental dual beam photoconductivity (DBP) system is shown in the Figure 2.3. In DBP system, a Quartz Tungsten Halogen (QTH) lamp controlled by 300 W Radiometric power supply is used as a white light source. The lamp is located in an Oriel 66182 model lamp housing. A 0.2 nm sensitivity Oriel monochromator with a 600-lines/mm grating controlled by an Oriel monochromator driver was used in this system. As a dc bias light source, red light emitting diodes (LED) combination was used. Generally, 13 Hz was used as a chopping frequency during the DBP measurements. To chop monochromatic white light, a chopper controlled by a chopper controller was used. At the exit slit of the monochromator, a filter driver containing three long pass filters of 500 nm, 700 nm, 900 nm, and a single crystalline silicon with wavelength of 1100 nm was located to cut-off second and higher order wavelengths. In order to change filters during the measurements, Oriel filter driver controller was used. A homemade sample holder was used with BNC connection to hold samples and pyroelectric detector. In order to calibrate the flux of monochromatic white light, a pyroelectric detector was used. A Keithley 6517A Electrometer was used to apply external d.c bias voltage between two coplanar electrodes during the measurements and to measure dark and photo currents. To detect the ac signals coming from the sample, a SR830 lock-in amplifier was used. All system was located on the Oriel optical table in a closed box to provide a dark room to prevent from unwanted signals.

To control the DBP system a computer program written using Objectbench software was used. SR830 Lock-in amplifier, monochromator and filter drivers are connected to Keitley IEEE 488 card in order to provide General Purpose Interface Bus (GPIB) protocol. After initializing devices, putting the sample on the sample holder, and adjusting

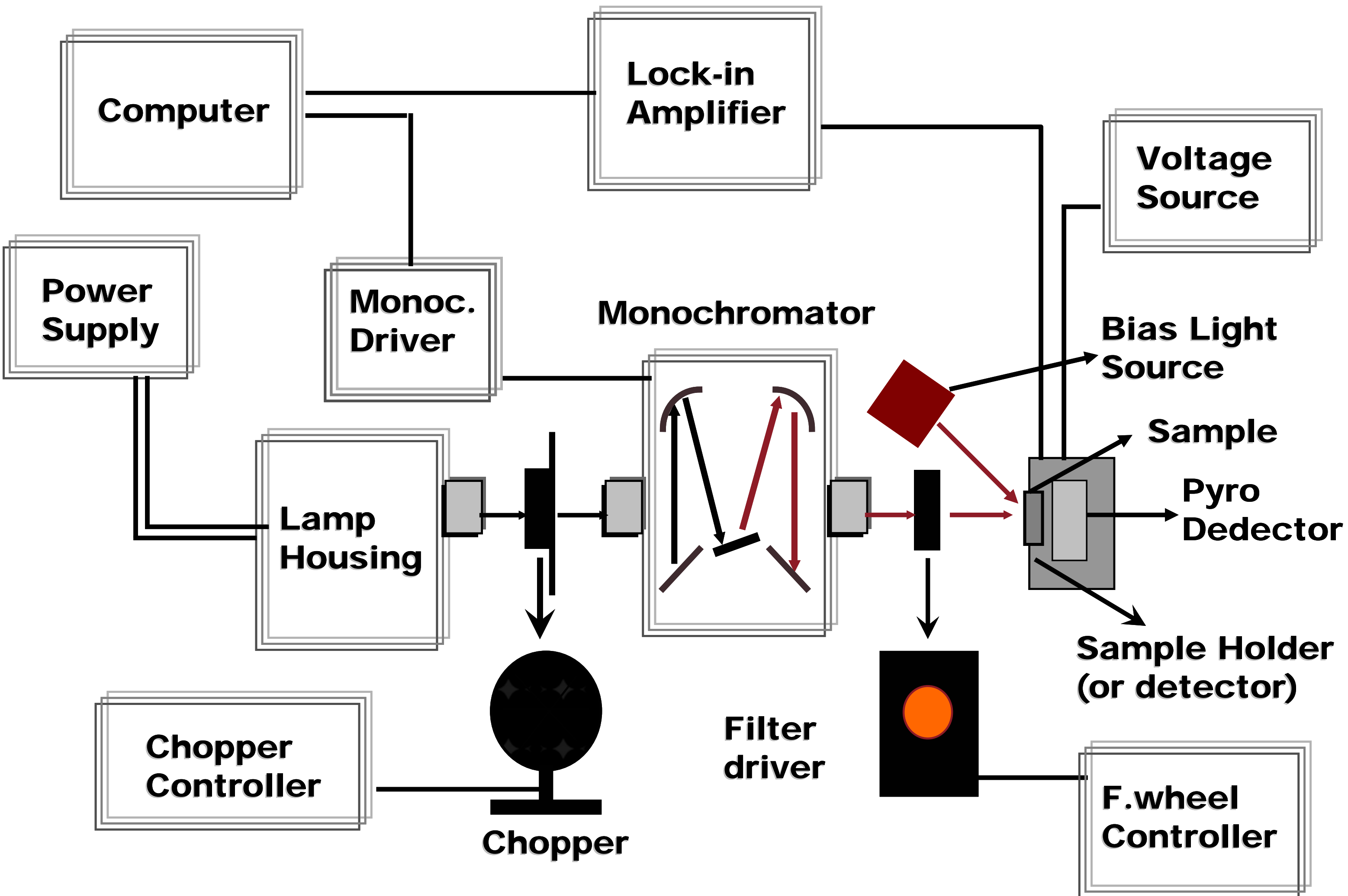

Figure 2.3 Dual beam photoconductivity (DBP) measurements system.

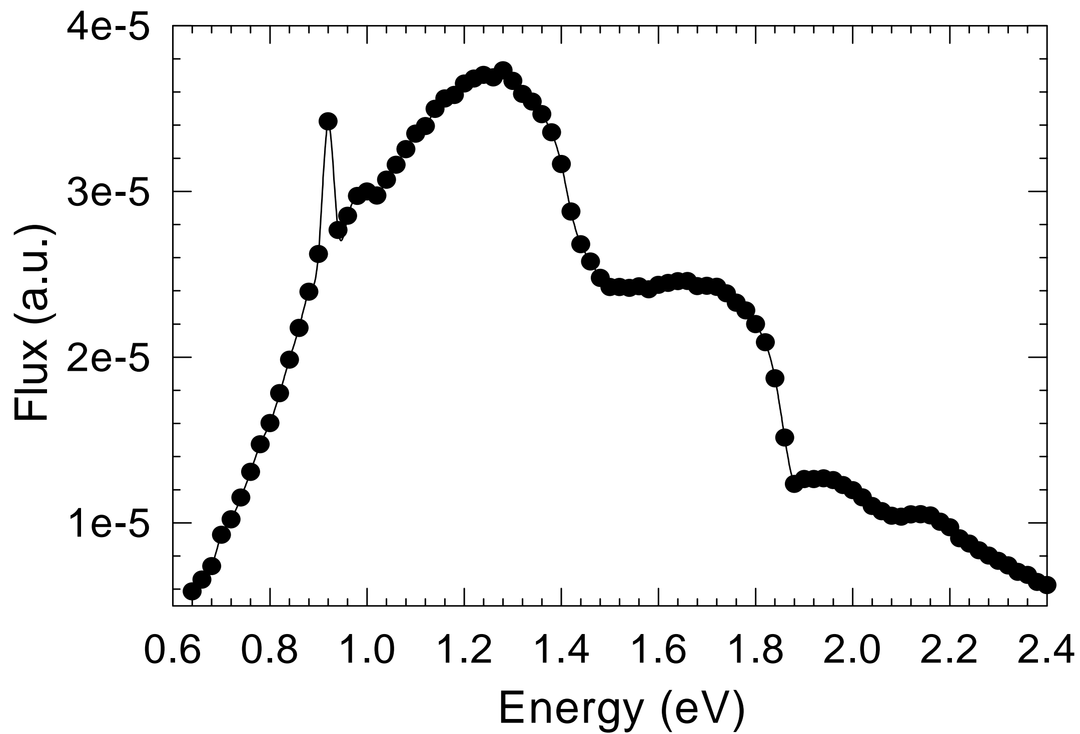

Figure 2.4 Flux spectrum of white light obtained using pyroelectric detector.

some parameters such as number of measurements for each energy, initial energy and energy step, the program is started to run the DBP measurements. The long pass filters are altered at certain energy values by the program or manual. The raw current and phase of signal were measured by lock-in amplifier. The average current values were divided by the corresponding flux data to normalize the spectrum and recorded to data file.

2.2.2.1 Flux Calibration

A Quartz Tungsten Halogen lamp used as a white light source in the system does not have a flat flux spectrum. For carrying out the flux calibration, a pyroelectric detector was used in the system. Pyroelectric detectors are thermal type infrared detectors and it is sensitive to a wide range (0.1μm-100μm) of the optical spectrum. Flux calibration is necessary because it is a very important step in order to obtain the DBP measurements. It is used to normalize raw current and transmission data.

As an example of the flux spectrum monochromatic white light source, Quartz Tungsten Halogen lamp, measured using a photodetector is shown in Figure 2.4. To

eliminate possible flux change of the lamp with time, flux calibration was carried out before the performing each measurements.

2.2.2.2 Transmission Spectrum

Transmission spectrum plays important role in the DBP system. Transmission data were used to calculate thickness of the film using two energy values corresponding to two maximum or minimum peaks in the transmission spectrum in the low energy region and the refraction index of silicon. Moreover, transmission spectrum was used to calculate the fringe free absolute absorption coefficient spectrum of the material. Transmission spectrum was measured using the pyroelectric detector. The film is placed just in front of the pyroelectric detector.

In Figure 2.5 the transmission spectrum of μc-Si: H thin films were exhibited. Because of the high absorption in the high energy region, transmission goes to zero. With decreasing energy the absorption of the sample decreases. Therefore, transmission gradually increases and the interference fringes are observed in the low energy regions due to multiple reflections at film-substrate interface.

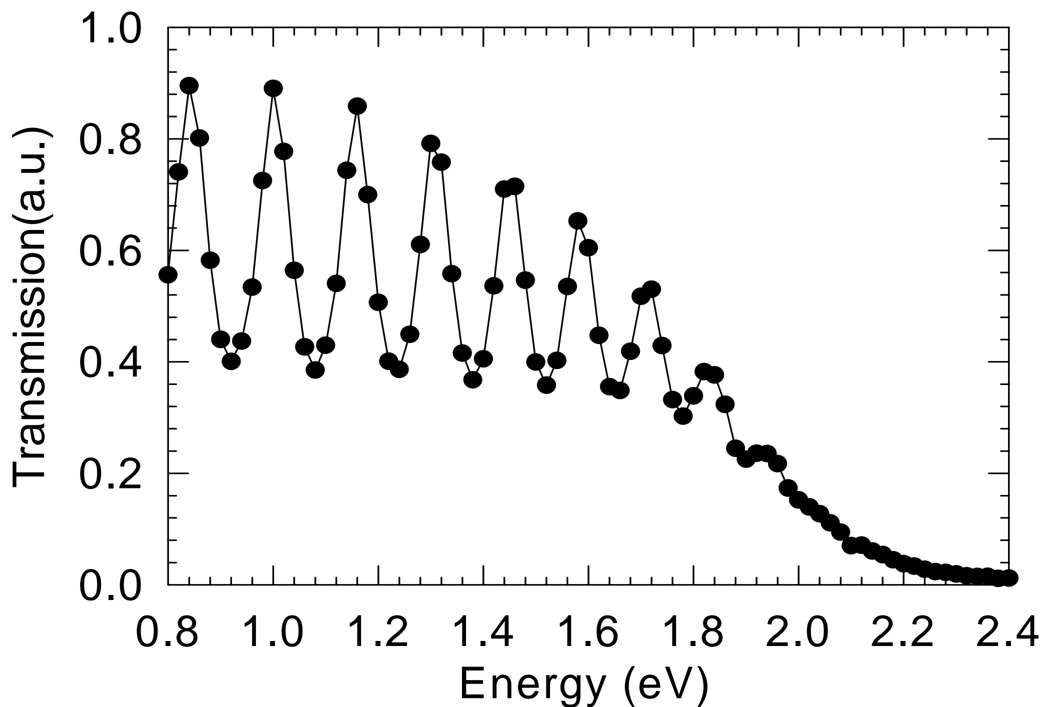

Figure 2.5 A typical transmission spectra of a μc-Si: H thin film.

2.2.2.3 Dual Beam Photoconductivity Yield Spectrum, Y_{DBP}

Dual beam photoconductivity (DBP) is a relative measurement technique therefore the absolute absorption coefficient spectrum can not be obtained using this method. In Figure 2.6, a typical raw and normalized photocurrent spectrum for a μc-Si: H thin film is shown. By changing the energy of the incoming light, the raw photocurrent spectrum is obtained. To acquire normalized photocurrent spectrum, the raw photocurrent spectrum is divided by the relative flux data since the incoming light does not give a flat flux spectrum. The resulting spectrum is called DBP yield spectrum, Y_{DBP} and it is proportional to the absolute absorption coefficient spectrum of μc-Si: H thin films as explain in the previous section. Consequently, if the required conditions are satisfied in DBP system, the absolute absorption coefficient spectrum can be obtained using the photocurrent spectrum. One of the requirements of the obtaining absorption spectrum using DBP method is to satisfy the constant μτ product of the majority carrier during the measurements.

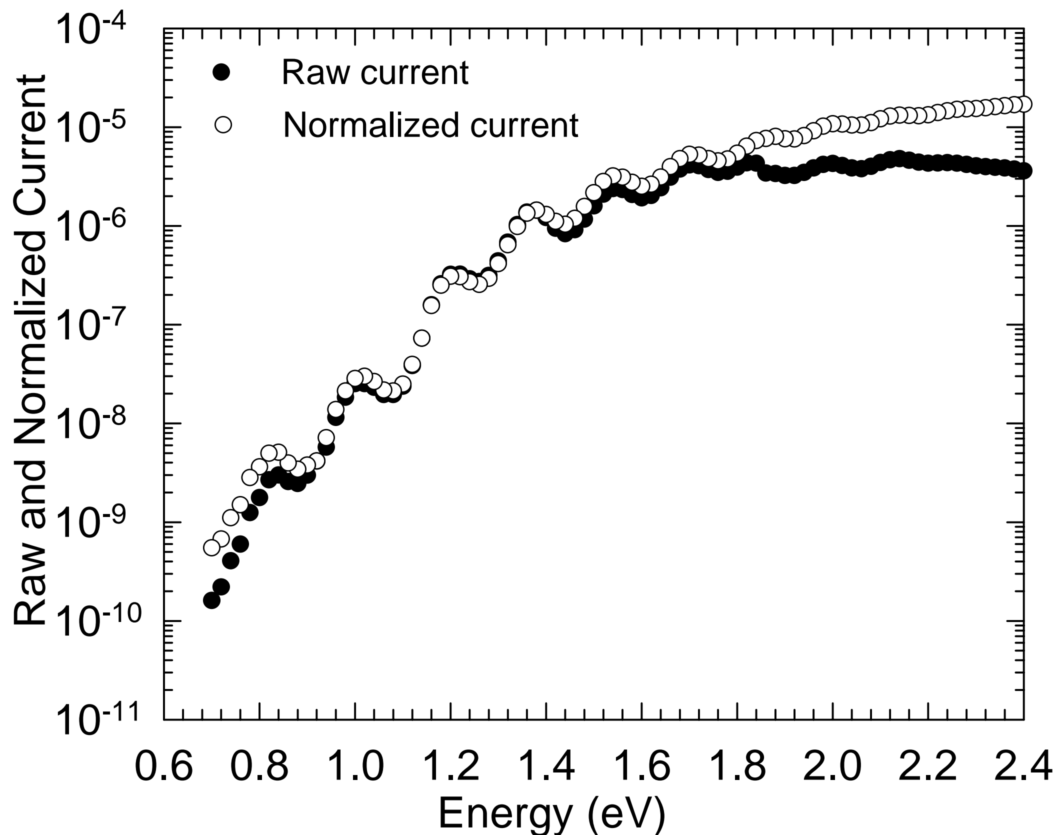

Figure 2.6 Normalized photocurrent and raw spectra of μc-Si: H thin films measured by DBP method.

As mentioned before, because of high generation of dc bias light than that of ac monochromatic light, the quasi Fermi levels are fixed by the dc bias light in DBP. Thus, I_{dc}/ I_{ac} ratio, where I_{dc} is dc photocurrent arising from applied dc bias light and I_{ac} is ac photocurrent measured by lock-in amplifier, is much higher than unity ($I_{dc} / I_{ac} >> 1$) due to the high generation rate of dc bias light. This result shows that $\mu\tau$ product of the majority carrier does not change during the measurements. On the other hand, for low generation rate of dc bias light this condition is not satisfied at all energies. To get ride of this situation, the section of photocurrent satisfying $I_{dc} / I_{ac} >> 10$ were taken as the reliable photocurrent spectrum.

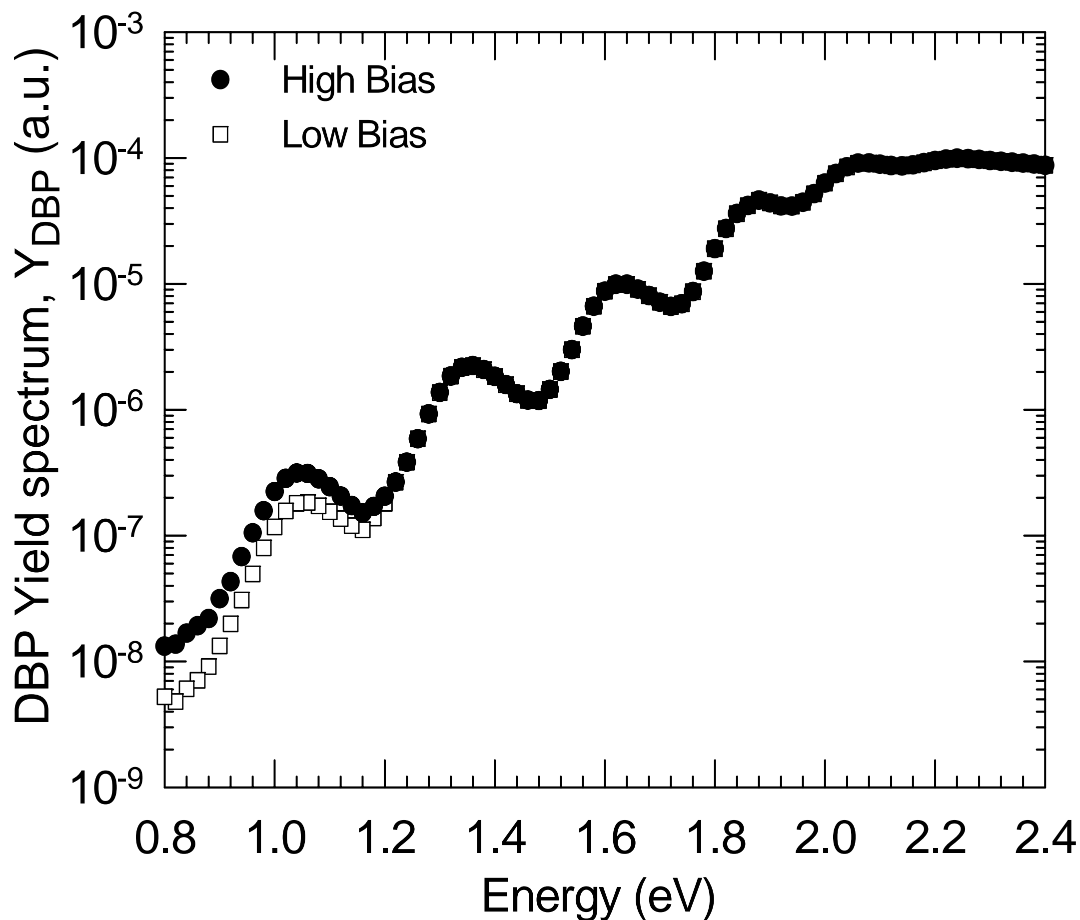

Figure 2.7 DBP yield spectra of a μc-Si: H thin film deposited HWCVD method for high and low dc bias light intensities.

The other condition which must be satisfied in DBP system to obtain absorption spectrum is uniform absorption of light. The absorption coefficient of μc-Si: H thin film is in the order of 10^3 cm^{-1} and thickness of μc-Si: H thin films are generally 0.5-0.9 μm. The absorption and thickness (αt) product is smaller than unity for μc-Si: H thin films. As a result, the condition is satisfied for DBP system.

In DBP, the bias light controls the quasi Fermi levels and changes the occupation of defect states. Because of increasing bias light intensity, more defect states above the Fermi level are occupied by electrons. Therefore, the transitions from these occupied states into conduction band exist. In Figure 2.7, typical DBP yield spectrum of μc-Si: H thin films measured at high and low bias light intensities are shown. In high energy region there is no differences between two spectra because bias light intensity does not affect the DBP yield spectrum in this energy region however deviation of the spectra begins at the bandgap energy. Changing intensity of bias light is seen as a deviation of the spectra below the bandgap, which is associated with the increased occupation of defect states in the midgap. Thus, the DBP spectra will be used to control the occupied defect distribution manually and information about the defect states present in the bandgap of the μc-Si: H thin films can be obtained.

2.2.3 Fringe Free Optical Absorption Coefficients Spectrum from DBP Yield Spectrum

The optical absorption coefficient, α (hν), of microcrystalline silicon (μc-Si: H) thin films is important, because it primarily determines the spectral response of solar cells and other opto-electric devices. In addition, the α (hν) values at sub-bandgap energies are related to the defect states present in the material which act as recombination center for free carriers. In order to obtain accurate absorption coefficient spectrum of the film, a number of studies were done. Usually, interferences fringes in the absorption and transmission spectrum were averaged to obtain the real spectrum (Cody 1984b). Firstly, Ritter and Weiser (Ritter and Weiser 1986) reported that the interference fringes are eliminated using the normalization of the absorbance (A) and transmission (T) spectrum, A/T, of the films (Vanecek et. al 1995b). For homogenous films the maxima and minima of transmission and the absorbance take place approximately in the same energy of the spectrum. Therefore, the obtained spectrum is

free of fringes. A/T was used for "absolute" CPM method to calculate the absorption coefficient spectrum of samples and it gives more accurate results than that of averaging procedure (Vanacek et. al 1995b).

For the first time, the procedure to obtain fringe free absolute absorption coefficient spectrum using A/T was presented for DBP (Goktas 2004a). As mentioned before, DBP is a relative ac photoconductivity measurement thus obtained absorbance and transmission spectrums are in relative scale. To obtain real absolute absorption coefficient, absorbance and transmission spectrum must be in absolute scale. For setting A/T in absolute scale, first step is setting the transmission spectrum in absolute scale. The transmittance maximum is written as a function of the optical refraction index, $n_{s,}$ (Swanepoel 1983).

$$T_{\max} = \frac{2n_s}{n^2{}_s + 1} \qquad (2.17)$$

For the Corning glass 7059, T_{max} is approximately 0.92. T_{max} in the transmission spectrum is set to this value. Therefore, the absolute transmission spectrum is obtained. The second step is setting A/T in absolute scale. In order to obtain absolute A/T, one reference energy point E_x is chosen in high energy region of the transmission spectrum where T is free from the interference fringes. A good transmission value T_X is taken as 0.05 at this energy point E_x. Reflectance values, R_x= 0.41 and R_x= 0.26 when film is illuminated from film and substrate side, are also free from interference fringes. These reflectance values are taken for amorphous silicon but the results which are in agreement with those of PDS will show that these values can be used for microcrystalline silicon as well as. The sum of the absorbance, reflectance, and transmittance is unity (A+R+T=1). Using the reflectance value and transmittance value in relation A+R+T=1, the absorbance value, A_x, can be calculated at this reference energy point. After finding A_x, the relative absorbance values set to this value at the reference energy, therefore whole absorbance spectrum is obtained in absolute scale.

In DBP system, the absorbance of the films can not be obtained. Therefore, to obtain the optical absorption coefficient spectrum from DBP measurements, Y_{DBP} can be used. Since the photoconductivity can be written as a function of absorbance,

$$\sigma_{ph}(ac) = \left[\frac{q\mu_n\tau_n F(h\nu)}{t}\right]\eta(h\nu)A(t,E) \qquad (2.18)$$

where, η(hν) is generation efficiency, t is the thickness of the films, and A(t, E) is the absorbance. Therefore the Y_{DBP} is obtained by dividing photoconductivity to incident flux;

$$Y_{DBP} = \frac{\sigma_{ph}(h\nu)}{F(h\nu)} = \left[\frac{q\mu_n\tau_n}{t}\right]\eta(h\nu)A(t,E) \qquad (2.19)$$

where,

$$\left(\frac{q\mu_n\tau_n}{t}\right)\eta = C$$

Therefore, Y_{DBP} is proportional to the absorbance given as follows,

$$Y_{DBP} = CA(t,E) \qquad (2.20)$$

Therefore, the absolute optical absorption coefficient, α (hν), spectrum in absolute scale calculated from the absolute A/T spectrum using the Ritter and Weiser formula is given by,

$$\alpha t = \ln 0.5\{(1-R_2)(1+A/T) + \left[(1-R_2)(1+A/T)^2 + 4R_2\right]^{1/2}\Big) \qquad (2.21)$$

where t is the film thickness, R_2 is the reflectance, T is transmission and A is the absorbance of the film. Since Y_{DBP} is proportional to the absorbance of the films, the Ritter and Weiser formula can be written in terms of Y_{DBP}. Therefore, the rearranged formula which can be used to obtain absolute absorption coefficient from DBP measurements is given as,

$$\alpha t = \ln 0.5\big((1-R_2)(1+Y_{DBP}(ab)/T_{ab}(h\nu)) + \left[(1-R_2)(1+Y_{DBP}(ab)/T_{ab}(h\nu)) + 4R_2\right]^{1/2}\Big\}$$

$$(2.22)$$

The results obtained using the Ritter and Weiser formula given in equation 2.22 are in agreement with those of PDS and CPM. In Figure 2.8, the absolute absorption coefficient spectrum, α (hν), obtained using PDS, CPM, and DBP method are shown. It is obviously seen that the absolute α (hν) spectra overlaps above the bandgap. On the other hand, the deviation among three spectra below the bandgap energy will be explained in detail in next section.

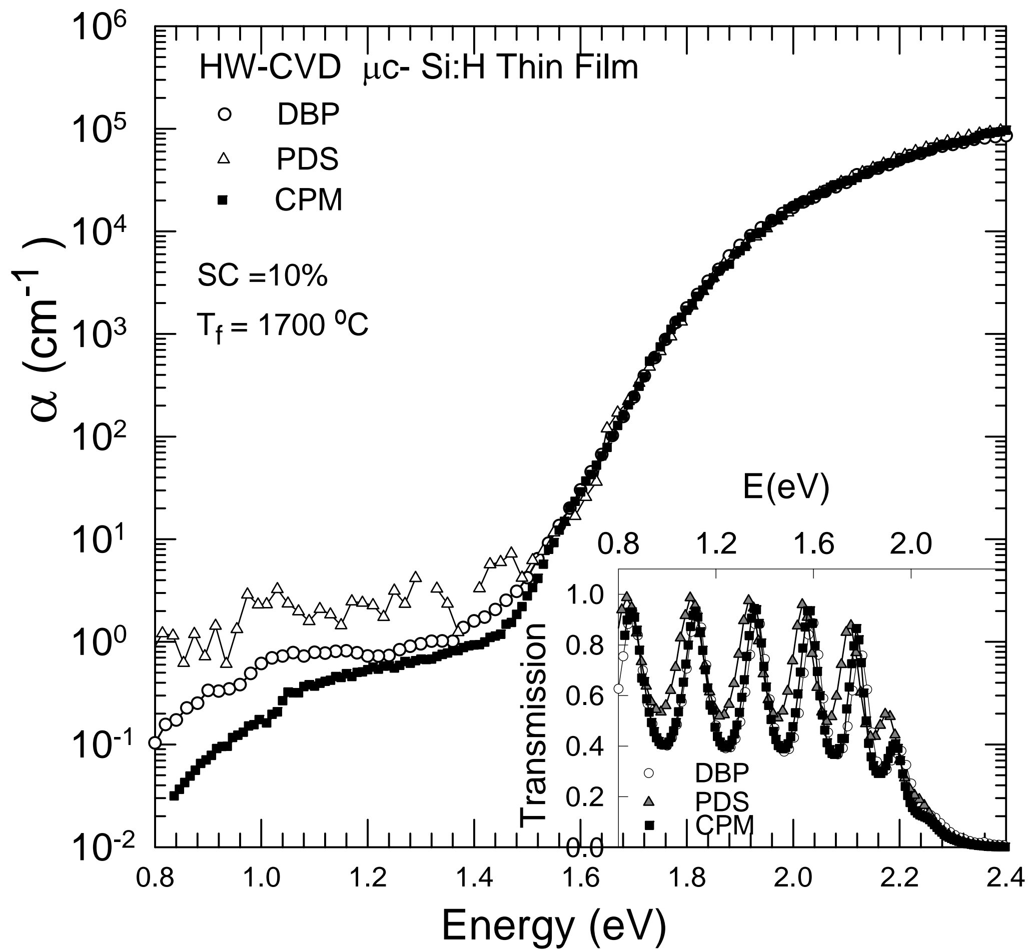

Figure 2.8 The calculated absolute α (hν) spectra of a μc-Si: H thin film deposited by HW-CVD method obtained from PDS, CPM, and DBP measurements. In the inset the corresponding transmission spectra of three methods are shown.

2.2.4 Photothermal Deflection Spectroscopy

Photothermal deflection spectroscopy (PDS) was first invented by Jackson et. al in 1982 to measure low-energy absorption coefficient spectrum of hydrogenated amorphous silicon thin films (Jackson et. al 1981a, Jackson and Amer 1982b). This technique is very powerful for measuring absorption coefficient spectrum of conductive and non-conductive thin films deposited on transparent substrates.

In this technique, sample is placed in CCl_4, good thermal conductivity and transparent medium. Monochromatic ac light chopped at a certain frequency is absorbed by the sample and causing a periodic heating of the sample due to excitation of electrons from occupied states into empty states of the band structure. Generated heat is transferred to the thermally good conducting CCl_4 medium. The refractive index of the medium at the sample surface is modulated with the frequency of the monochromatic light. As second light beam, a laser light focused on the sample surface is sent at a grazing angle on the sample surface and dropped on a position detector. When absorption of ac monochromatic light changes, the resulting deflection of laser beam is directly proportional to the absorption of the monochromatic ac light beam. By using the PDS deflection signal and transmitted light spectrum , the absolute absorption coefficient spectrum of the conducting or non-conducting thin films deposited on transparent substrate is obtained reliably. It is a routine technique for qualitative and quantitative investigation of electronic quality thin films deposited under various preparation conditions.

Experimental setup of PDS is shown in Figure 2.9. Because of having a low absorption and not changing the properties of μc-Si: H thin films, carbon tetrachloride (CCl_4) used as a deflection medium (Jackson and Amer 1982b). The PDS measurements should be performed on the optical table in order to avoid the vibration effects. The laser beam should be just above the sample surface and well focused on the sample. The effect of air currents should be eliminated. In PDS setup, a 20 mW HeN laser was used as laser beam. In order to attenuate laser beam intensity %1 neutral density filter is located in front of the laser. Two convex lenses having a focal length of 5 cm and 10 cm were used. One of them was centered in front of the monochromatic light beam so as to focus light beam on the sample. The other one is placed in way of the laser beam to graze the sample surface

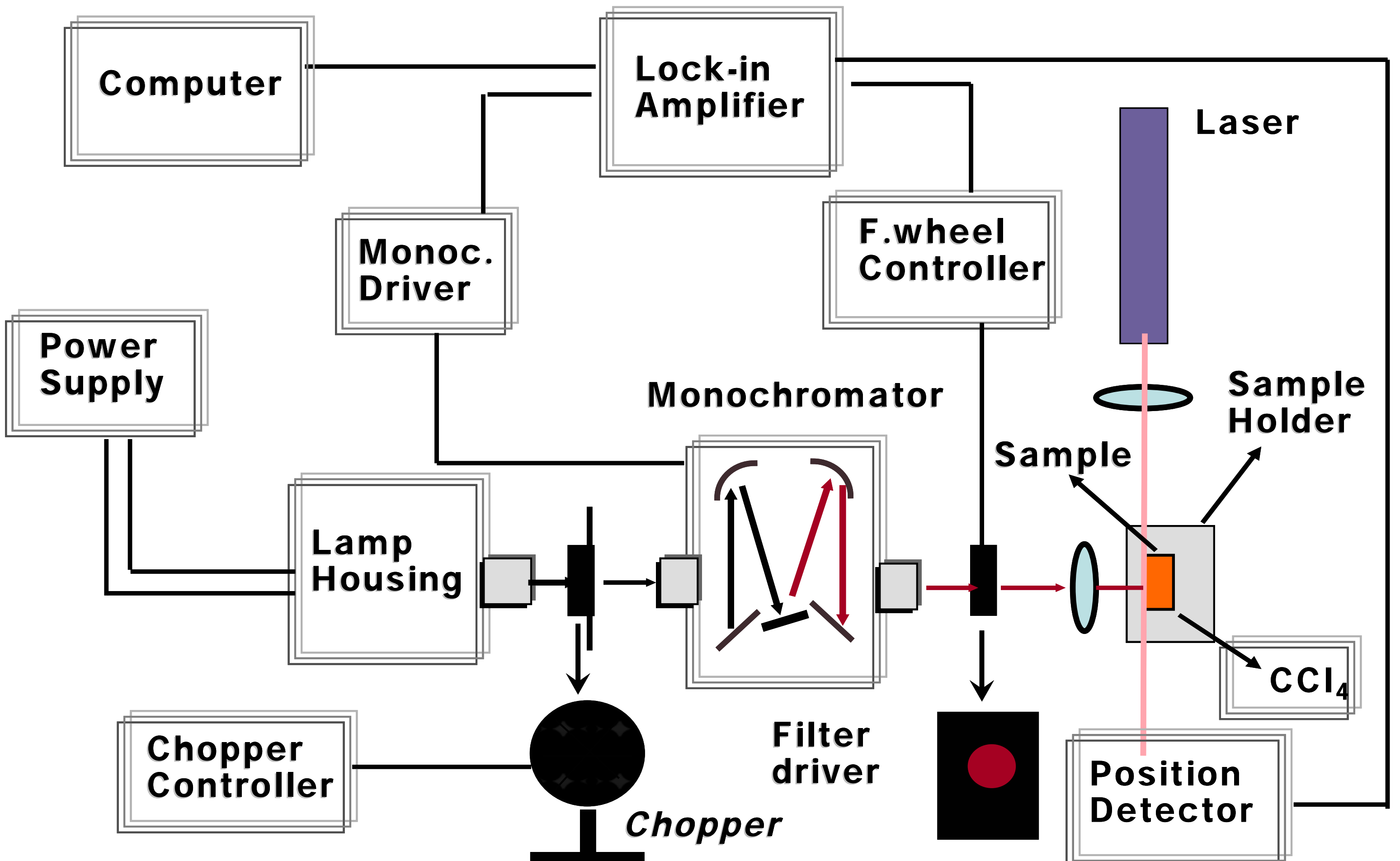

Figure 2.9 Photothermal deflection spectroscopy (PDS) measurement system.

where monochromatic light focused. To detect deflecting laser beam a position sensitive detector is connected to a lock-in amplifier and all parts of the system is controlled by a computer. A computer program written in Objectbench was used for data collection and acquisition. That system is tested for a few samples in IYTE, but mainly PDS measurements done in Jülich Research Center are used for comparison of spectra.

2.2.5 Constant Photocurrent Method

Constant photocurrent method has been widely used to derive absorption coefficient spectrum of photoconducting thin films deposited on transparent substrate from the ac photoconductivity spectrum. The optical absorption coefficient at low energies gives information about the defect states present in the material.

In CPM method, the ac photoconductivity due to photoexcitation of electrons from defects states to the conduction band is proportional to the absorption coefficient, α. The photoconductivity can be written in the simple form as follows,

$$\sigma_{ph}(ac) = nq\mu_n \qquad (2.23)$$

where n is the density of photoexcited electrons and μ_n is the mobility of electrons. As mentioned in equation 2.3, generation rate of photoexcitation G and electron lifetime τ product is equal to the photoexcited electron density $(n = G\tau_n)$. The generation rate of photoexcited electrons can also be written as follows,

$$G = F(h\nu)(1-R)(1-e^{-\alpha t})/t \qquad (2.24)$$

where F is the flux, R is the refractive index, t is the thickness of the films. Using this equation photoconductivity can be written as

$$\sigma_{ph} = q\mu_n\tau_n G = q\mu_n\tau_n F(h\nu)(1-R)(1-e^{-\alpha t})/t \qquad (2.25)$$

The equation can also be rewritten as for αt<<1

$$\sigma_{ph}(ac) = q\mu_n\tau_n[(1-R)\alpha(h\nu)F(h\nu)] \qquad (2.26)$$

and this equation also can be written in another form

$$\frac{\sigma_{ph}}{F(h\nu)} = [q\mu_n\tau_n(1-R)]\alpha(h\nu) \qquad (2.27)$$

If σ_{ph} = constant for each E= hν. Then, $[q\mu_n\tau_n(1-R)]$ is maintained as a constant. For the our purpose F(hν) is adjusted to keep σ_{ph} (hν) constant at every energy. Then resulting 1/ F(hν) spectrum is proportional to α (hν) given in equation 2.14 .

$$\alpha(h\nu) \propto \frac{1}{F(h\nu)} \qquad (2.28)$$

In literature, there are a few approaches to obtain absolute α (hν) spectrum from CPM measurements. One of the most important approaches to obtain α (hν) spectrum is CPM measurements are normalized to optical absorption coefficient obtained from transmission. However, a number of methods are used to calculate the absolute α (hν) spectrum from CPM measurements without any normalization (Wyrsch et. al 1991b, Vanecek et. al 1995b, Jensen 1990). In this technique, to keep the photocurrent constant during the measurements; a number of photon is measured using detector. This measurement gives a spectrum, which is proportional to the absorptance A. The obtained A spectrum is also in relative scale. As some approximations are considered in Beer's law $\left(A = (1-R_1)(1-e^{-\alpha d})\right)$, α (hν) spectrum can be obtained as proportional to the absorptance spectrum. The measured absorptance spectrum exhibits the interference fringes. The interference fringes must be removed in the CPM spectrum. To do this, transmission spectrum obtained using photon detector behind the sample is used, since as noted for the first time by Ritter and Weiser, the maxima and minima occur at the same energy in both spectra. This means that the absorptance to transmission ratio A/T is free of interference fringes. However, the calculated A/T is still in relative scale.

Therefore, transmission and absorptance must be set in absolute scale because the real absorption coefficient spectrum is in absolute scale. First of all, to set transmission spectrum in absolute scale, simple procedure is used. Basically, the transmittance maximum is written as a function of the optical refraction index, $n_{s,}$ (Swanepoel 1983).

$$T_{max} = \frac{2n_s}{n_s^2 + 1} \tag{2.29}$$

Using the refraction the Corning glass 7059 is 1.5, the found T_{max} is approximately 0.92. Therefore, the T_{max} value of transmission spectrum sets to 0.92 then the obtained transmission spectrum is in absolute scale. After setting transmission spectrum in absolute scale, the absorbance can be set in absolute scale. To do this, a reference energy E_x in the high photon energy of the calculated absolute transmission spectrum is chosen. T_x =0.05 is a good choice since transmission spectrum is free of fringes at this point. Also as the reflectance values R_x= 0.41 and R_x= 0.26 are used, which are also taken for calculating the absorption spectrum of amorphous silicon. The sum of transmission, reflectance and absorptance is equal 1. Using absolute transmission and reflectance value, the absolute absorptance value at the reference energy can be obtained. Then, the whole spectrum can be set in absolute scale. After obtaining absorptance spectrum in absolute scale, the Ritter and Weiser formula is used to calculate the absolute absorbance spectrum of the sample from CPM method. The formula was given in section 2.3, in the details of calculation of absolute absorption spectrum from DBP.

CHAPTER 3

EXPERIMENTAL RESULTS IN HYDROGENATED MICROCRYSTALLINE SILICON THIN FILMS DEPOSITED BY HWCVD METHOD

3.1 Introduction

Hydrogenated microcrystalline silicon (μc-Si: H) is a promising material for device application such as solar cell and large area electronics. The relationship between its electronic and microstructure properties has been the subject of research activities in recent years. In order to improve deposition rate, the stability and quality of μc-Si: H thin film, hot wire chemical vapor deposition (HW-CVD) has attracted attention for the last decade. In this study, the optical and electronic properties of hydrogenated microcrystalline silicon thin films deposited by HW-CVD method are investigated using steady state photoconductivity (SSPC), dual beam photoconductivity (DBP), and optical transmission methods to understand the effects of deposition parameters such as silane concentration (SC) and filament temperature (T_F) on absorption coefficient spectrum. Finally, optical absorption coefficient spectrum obtained from the detailed optical calculations using the relative DBP yield spectrum and optical transmission spectra are compared with that independently measured on the same samples using photothermal deflection spectroscopy (PDS) and constant photocurrent method (CPM).

3.2 The Effects of Silane Concentration

Deposition of microcrystalline silicon thin films strongly depends on the silane concentration in gas mixture of silane-hydrogen gas in HW-CVD deposition process. The ratio of crystalline phase to amorphous phase present between the crystalline grains increases with decreasing silane concentration. Therefore, properties of resulting films show strong dependence on the changing microstructure.

In this section, steady state photoconductivity (SSPC), DBP and optical transmission measurements were used to investigate the effects of silane concentration on the microstructure of microcrystalline silicon thin films deposited by HWCVD methods at 1700 ºC filament temperature with varying silane concentrations. In SSPC, majority carrier electron mobility-lifetime product ($\mu_n\tau_n$) is obtained quantitatively. Absolute absorption coefficient spectrum is obtained from the relative DBP and optical transmission spectra. The effect of silane concentration on low energy absorption coefficient is taken as a comparison criteria among the films.

3.2.1 Steady State Photoconductivity Results

Photoconductivity is an important property used in solar cells application. Steady state photoconductivity is a complex mechanism divided into three parts, generation of free electron-hole pairs, recombination of excess free carriers through the defect states, and transport of mobile carriers at the conduction band mobility edge. Therefore, absorption coefficient α (hν), density and nature of recombination centers in the bandgap and free carrier mobility at the extended states are involved in steady state photoconductivity mechanism. Thus, the direct quantitative information about the material can be obtained using steady state photoconductivity. It exhibits a non integer power-law dependence on light intensity ($\sigma_{ph} \propto G^{\gamma}$), which is important physical feature to obtain information about recombination kinetics between photogenerated electrons and holes. Using steady state photoconductivity measurements quantitative information about the mobility-lifetime product ($\mu_n\tau_n$) of majority carriers is obtained, which is called as "photosensitivity" and one of required parameter for photoactive semiconductor thin films.

Experimental steady state photoconductivity results are shown in Fig 3.1a as a function of generation rate for intrinsic microcrystalline silicon thin films deposited at filament temperature of 1700 ºC with different silane concentrations. Majority carrier $\mu_n\tau_{n-}$ products calculated from the results in Figure 3.1a are presented in Figure 3.1b as a

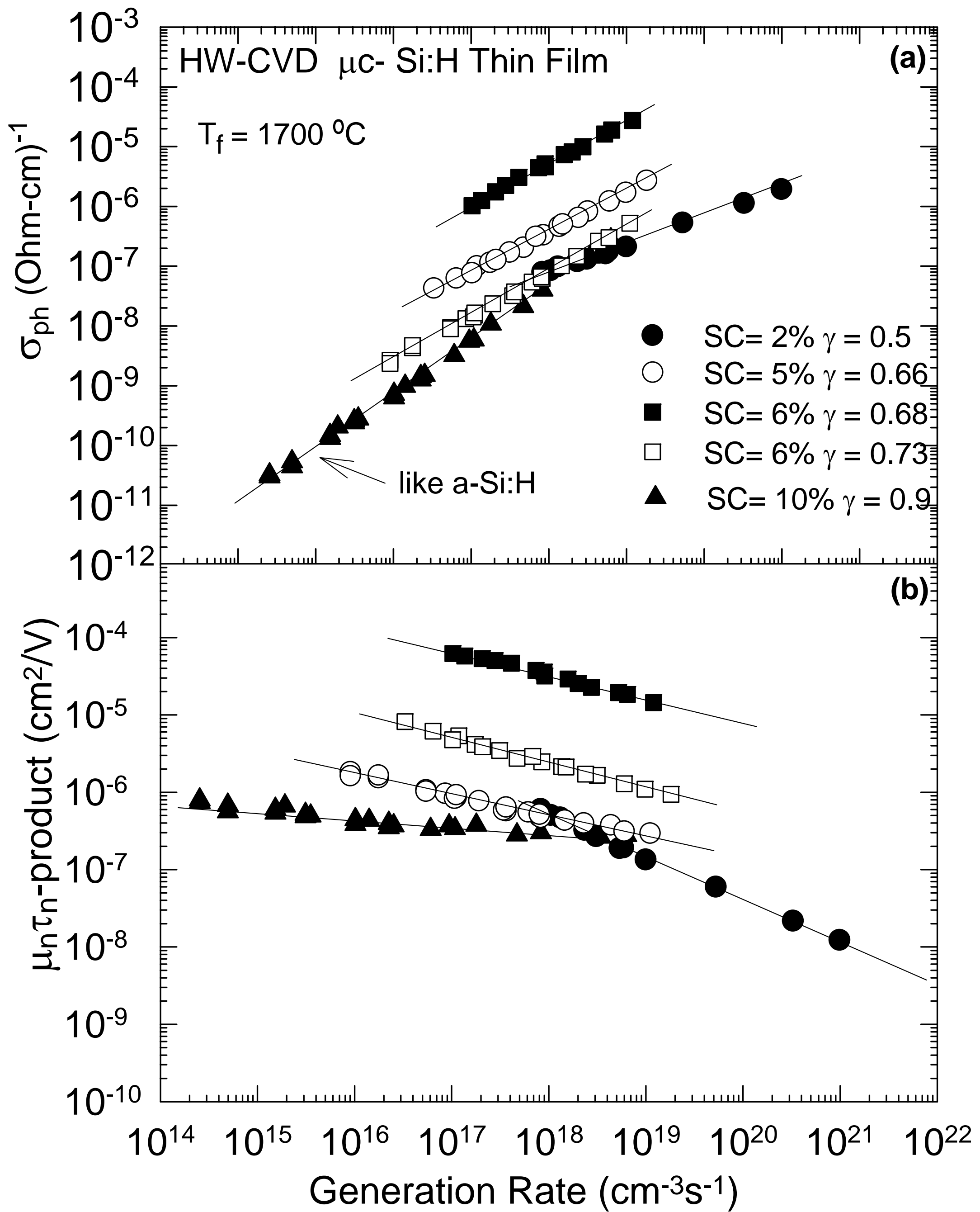

Figure 3.1 a) σ_{ph} versus generation rate for μc-Si: H thin films deposited by HWCVD method at filament temperature 1700 ºC. b) $\mu_n\tau_n$ - product versus generation rate of the same μc-Si: H thin films.

function of generation rate. A linear dependence of photoconductivity on generation rate can be seen for all the samples. However, a difference exists in the slope as a major change in the microstructure exists. Photoconductivity versus generation rate obeys the expected non-integer power dependence rule $\sigma_{ph} \propto G^{\gamma}$. For high silane concentration, SC= 10%, the microstructure is mainly dominated by amorphous phase and very small crystalline regions occur in the matrix. Therefore, the slope γ is equal to 0.9, which is close to unity, observed for most amorphous silicon thin films in the literature. As the SC decreases, the slope γ decreases towards 0.7 of which generally observed for undoped microcrystalline silicon thin films (Gunes et al. 2005c). For lowest SC=2% film, the slope reaches to 0.5, which is the value seen for crystalline Si. The meaning of the γ=0.5 is that photogenerated electrons in the conduction band extended state recombine directly with holes in the valence band extended states. However, for amorphous like film with SC=10% and other films with γ value around 0.7, photogenerated free electrons in the conduction band extended states recombine with holes in the valance band through the defect states present in the bandgap of microcrystalline silicon.

In addition, magnitude of σ_{ph} is also affected by the SC as seen in Figure 3.1a. For the highest SC=10%, amorphous phase with high defects dominates in the bandgap reduces the electron lifetime. Thus, the lowest values of σ_{ph} are obtained for amorphous like film. As SC decreases, the crystalline regions increases and σ_{ph} values increases and highest σ_{ph} values are obtained for the films prepared with SC around 5-6% film. However, as the SC=2%, for the highly crystalline film, σ_{ph} decreases again due to increasing defects on the walls of grain boundaries. Thus, $\mu_n\tau_{n-}$ product becomes strongly dependent on the generation rate as shown in figure 3.1b.

3.2.2 Sub-Bandgap Absorption Spectrum

The optical absorption coefficient, α (hν), of hydrogenated microcrystalline silicon (μc-Si: H) thin films is important to obtain information about spectral response of optoelectronic devices. This means that the optical and electronic properties of the materials can be characterize using α (hν) of material. In this section, the effect of silane concentration on the absorption coefficient spectrum in wide energy region, especially at low energies was investigated using DBP and optical transmission techniques.

Absolute α (hν) spectrum was calculated from the relative DBP and optical transmission spectra and finally compared with those independently measured by PDS and CPM.

An example of DBP yield spectra for high and low bias light intensities is shown for a μc-Si: H thin film deposited using HW-CVD method at T_f= 1700 ºC with SC=10%. At this silane concentration, sample exhibits amorphous-like characteristic since band edge extends to higher energies and exponential tail absorption is clearly observed. In these spectra, the interference fringes are observed because of the multiple reflection of incoming light at film-substrate interface. It is also clearly seen that in low energy region, the DBP spectrum is affected by the bias light used during the measurements. The deviation between two spectra can be explained with the changes in the occupation of defect states in the bandgap. With increasing bias light intensity the occupation of defect states above the dark Fermi level increases. This means that transition of excited electrons from these occupied defect states to the conduction band increases. Therefore, only an increase in DBP yield spectrum is obtained for high bias light intensity in low energies. In Figure 3.2b, optical transmission spectrum for the same sample is shown. The maxima and minima of the transmission and DBP yield spectra take place at the same energies, indicating that a uniform absorption of light throughout the material. Using the transmission fringes at lower energies, the exact thickness of the sample is calculated using the interference fringe equation. This thickness value was used for accurate calculation of the steady state photoconductivity and $\mu_n\tau_{n\text{-}}$ products of majority carriers presented in previous section.

As mentioned in chapter 2, when certain required conditions are satisfied, the DBP yield spectrum becomes proportional to the absorption coefficient spectrum. This means that the absorption coefficient spectrum can be obtained from the DBP yield spectrum. However, in DBP yield spectrum, there are interference fringes which must be removed to acquire fringe free absorption coefficient spectrum. The fast Fourier transforms method (Wiedeman et al. 1987) is commonly used to eliminate these fringes in DBP yield spectrum. In order to achieve this, fringe removed DBP yield spectrum is normalized to absolute values obtained from T&R or PDS measurements (Wronski et al. 1982, Gunes and Wronski 1992a). However a large error into shape and magnitude of the spectrum can be introduced for the thin films less than 1μm. Therefore, some

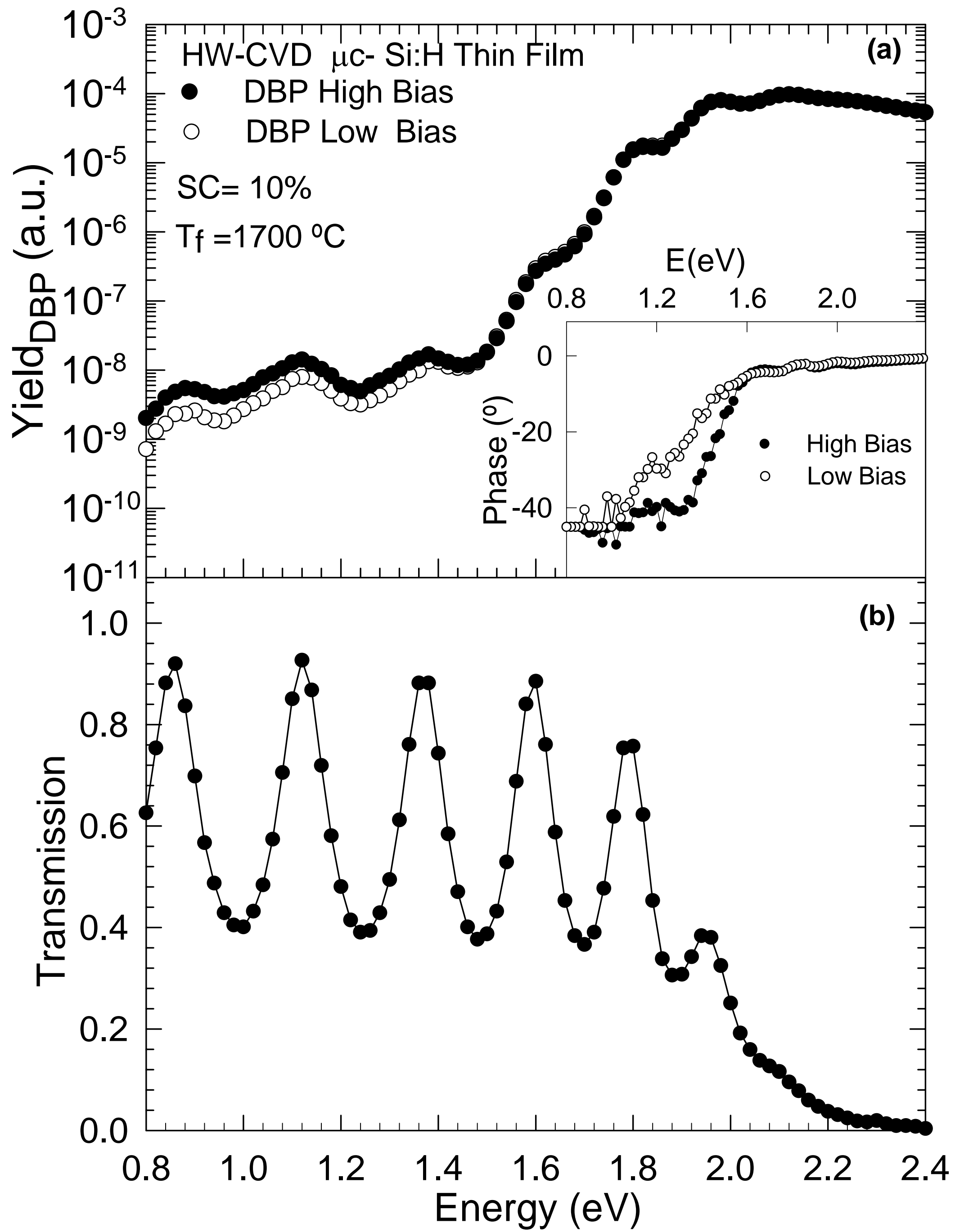

Figure 3.2 a) DBP yield spectrum for high and low bias light intensities for μc-Si: H thin films deposited by HW-CVD method with SC=10% and 1700 ºC. The phases of both measurements are shown. b) Corresponding transmission spectrum is exhibited.

important information can be lost during the fringe removing Fourier transform procedure. On the other hand, in this thesis, fringe free absorption coefficient spectrum is calculated from DBP yield and transmission spectra given in Figure 3.2a and Figure 3.2b using the detailed optical equations given by Ritter and Weiser (Ritter and Weiser 1986).

Fringe free absolute α (hν) spectrum obtained for high and low bias light DBP measurements are shown in Figure 3.3. A good overlap exists in the absolute α (hν) spectrum obtained for both bias light DBP measurements at higher energies, down to the exponential valance band tail state observed in amorphous silicon thin films. On the other hand, in low energy region high bias light α (hν) spectrum gives higher values than low bias light α (hν) spectrum. The physical reason for the increase is that higher bias light intensity increases the separation of quasi Fermi levels in the bandgap, the electron quasi Fermi level moves closer to the conduction band edge and hole quasi Fermi level moves closer to the valance band edge. Therefore, the density of electron occupied defect states above the dark Fermi level increases. Monochromatic probe beam of DBP excites more electrons from the occupied states into conduction band at lower energies. This results in an increase only in the α (hν) spectrum at lower energies since there is no change in the occupation of states at higher energies.

Accuracy of the absolute α (hν) spectrum obtained from detailed calculation of DBP and optical transmission spectra has been carried out by comparing the α (hν) spectrum of the sample measured independently using the PDS method carried out in Research Center Jülich, Germany. In Figure 3.4, the absolute α (hν) spectrum of DBP low bias light and that of PDS measurement are shown for the same sample. It is clearly seen that, a perfect overlap in the absolute α (hν) spectra independently obtained from PDS and DBP low bias light measurements is seen at energies above the 1.4 eV. On the other hand, at low energy regions, there is a difference between PDS and DBP spectra. Generally, the PDS measurements give noisy signal at lower energies; however in that region DBP spectrum is a smooth curve that it is relatively noise free. At energies below the 1.4 eV, the absolute α (hν) spectrum of PDS is higher than those of low bias DBP measurements, which can be attributed to the substrate absorption and that of highly defective surface layer. The effects of substrate absorption can also be seen in the phase of PDS given in the inset of the Figure 3.4. Conversely, the shift

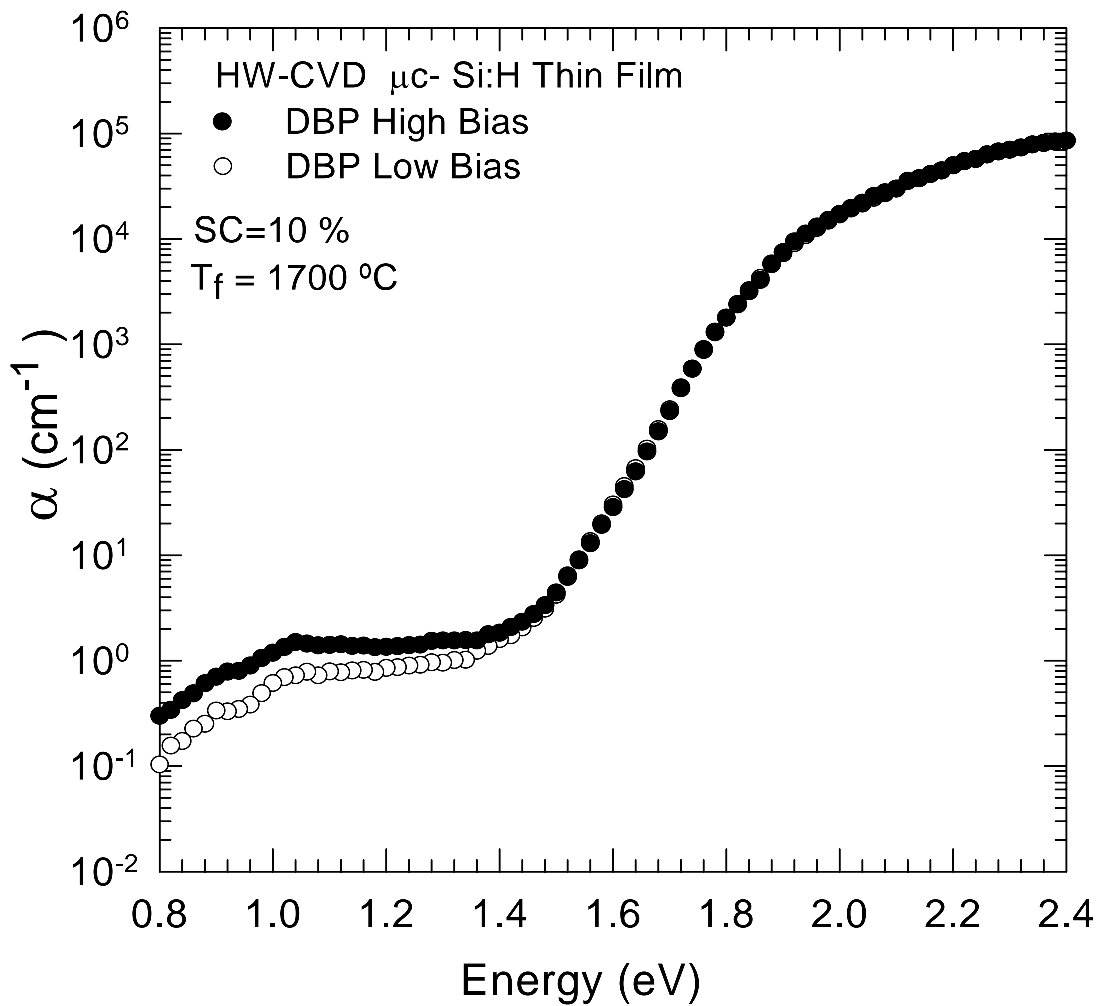

Figure 3.3 The calculated absolute α (hν) spectra of DBP for high and low bias light measurements of μc-Si: H thin films deposited by HW-CVD method with SC=10%.

in phase signal of DBP can be explained by changing the recombination kinetics of defect states present in the bandgap. In addition, modulation in the phase signals of DBP is seen in the inset of Figure 3.4. This modulation is due to the degree of inhomogeneous absorption of light because of inhomogeneity present in the μc-Si: H thin films. The results in the Figure 3.4 indicate that reliable and accurate absorption coefficient spectrum at lower energies can be obtained using the low bias light DBP measurement together with optical transmission spectrum. Even though PDS is a routine technique to obtain qualitative information on the deposited thin films, it overestimates the absolute α (hν) values of bulk sample due to highly defective surface

layer absorption and substrate absorption. At higher energy part of spectrum, both method probe the same distribution of defect states and give exactly the same α (hν) values. In this thesis, the absolute α (hν) values at low energy region are called sub-bandgap absorption coefficient and used to compare the samples deposited under different conditions.

The effect of SC on the sub-bandgap absorption of μc-Si: H thin films have been investigated for films deposited at silane concentrations lower than 10%. In the growth of microcrystalline silicon, microcrystalline phase becomes dominating as the SC decreases. The results of DBP and optical transmission measurements presented in Figure 3.5 for μc-Si: H film deposited with the SC=7% at filament temperature of 1700 ºC. In Figure 3.5a, raw DBP yield spectrum measured with high and low bias light intensities are shown. In the inset, the phases of both spectra are illustrated. Modulations on the both spectra are clearly observed. Corresponding transmission spectrum of the sample is shown in the Figure 3.5b. Similarly, fringe free absolute α (hν) spectrum is calculated using the DBP and optical transmission spectra as carried out in the previous section. The resulting calculated α (hν) spectrum for high and low bias light measurements are shown in Figure 3.5c. Even though, fringe free calculation of α (hν) spectrum has been used, there are observable fringes left on the α (hν) spectrum. Physical reason of the left fringes on the spectrum is the nonuniform absorption of monochromatic light due to inhomogeneous structure of μc-Si: H thin film. Another main differences of the α (hν) spectrum from that of SC=10% sample is the shape of α (hν) spectrum, which is shifted to lower energies and becomes more like that of crystalline silicon. Comparison of the absolute α (hν) spectrum of SC=10% and SC=7% samples are given in Figure 3.5d. It clearly indicates that microcrystalline phase becomes dominating the microstructure and substantially changes the absolute α (hν) spectrum. At high energy region, α (hν) has lower values like that of c-Si: H. For this sample, independently measured α (hν) spectrum using the PDS method is not available for direct comparison.

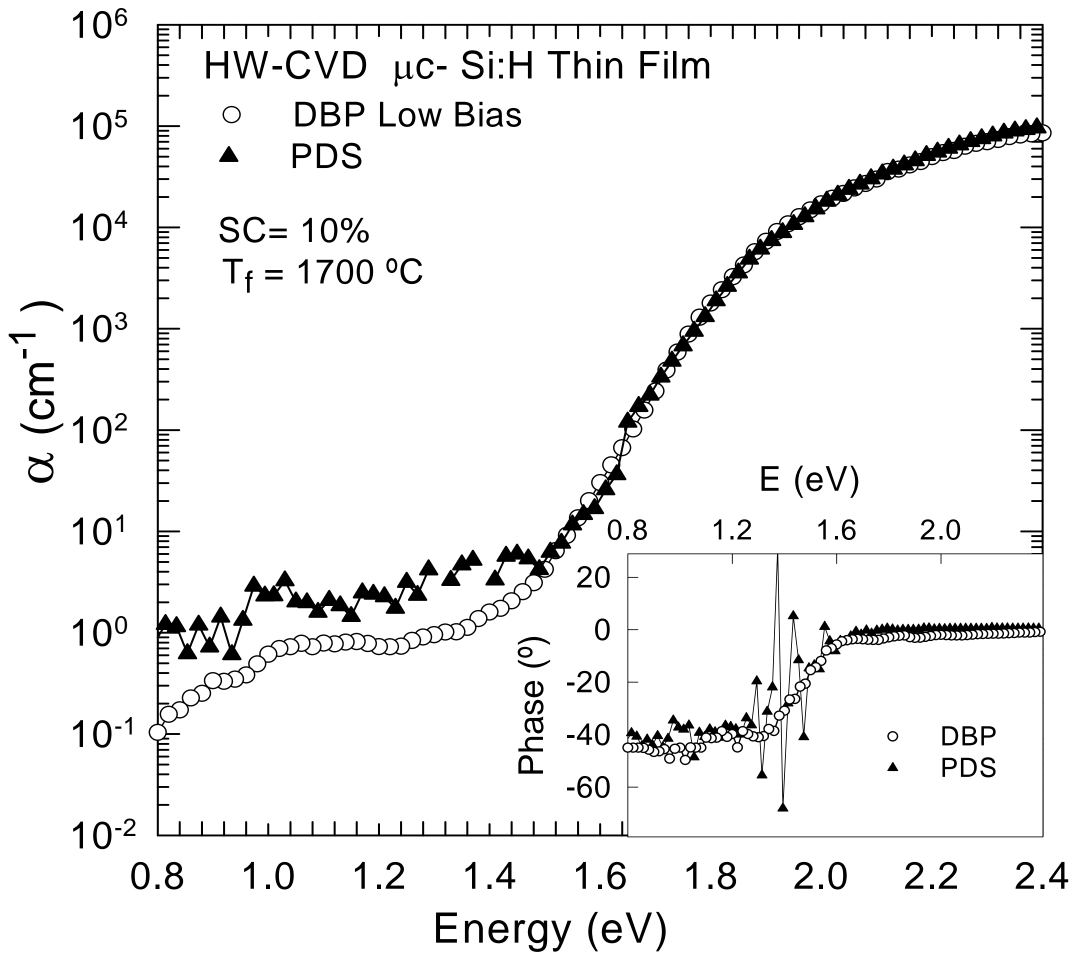

Figure 3.4 The calculated absolute α (hν) spectra of PDS and DBP for high and low bias light measurements of μc-Si: H thin films deposited by HW-CVD method with SC= 10%. In the inset, the phase of PDS, DBP are presented.

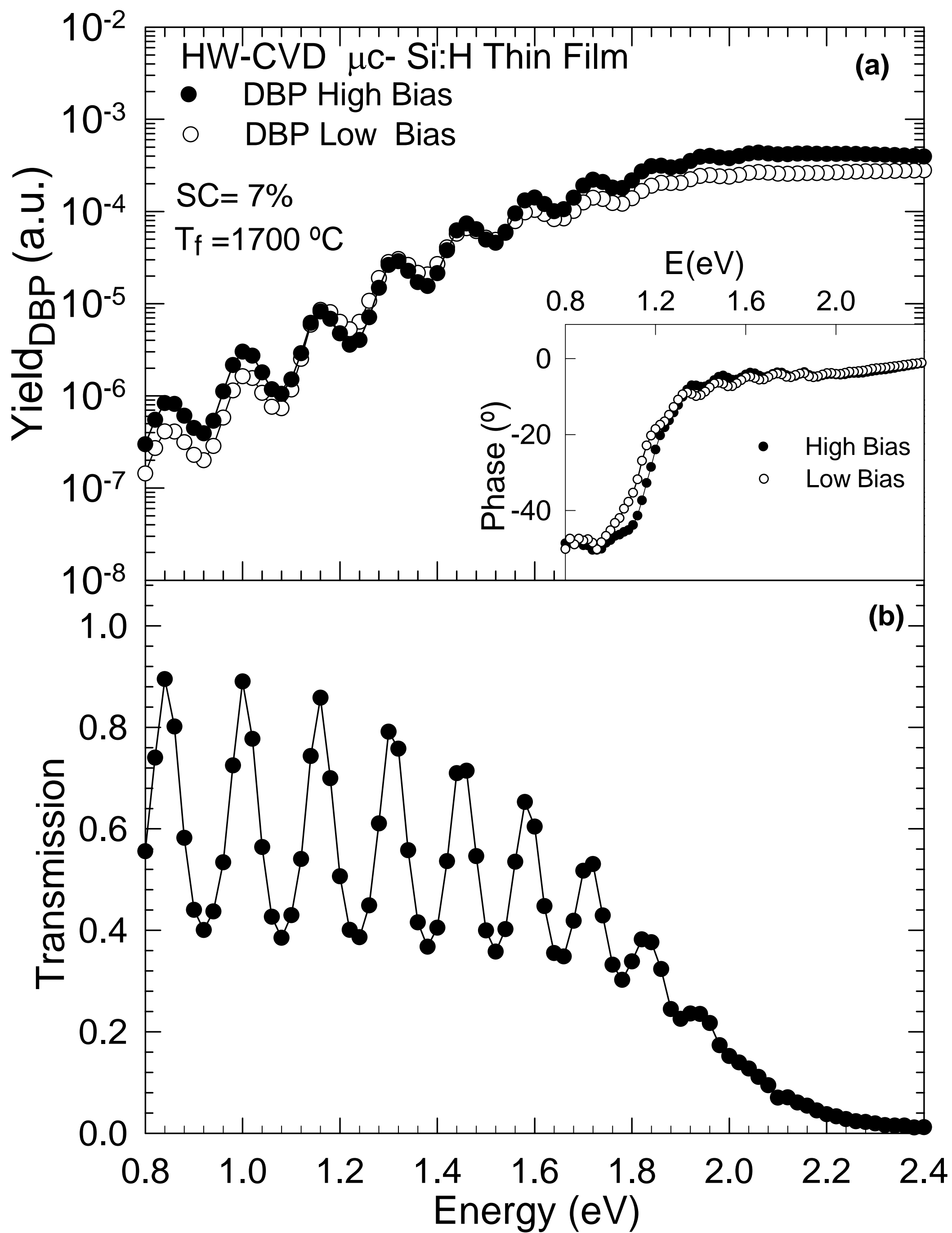

Figure 3.5 a) Yield DBP signals measured at two different dc bias light intensities are shown. In the inset the phase of DBP signals are shown. b) The corresponding transmission spectrum is given for a μc-Si: H thin film deposited with SC=7%.

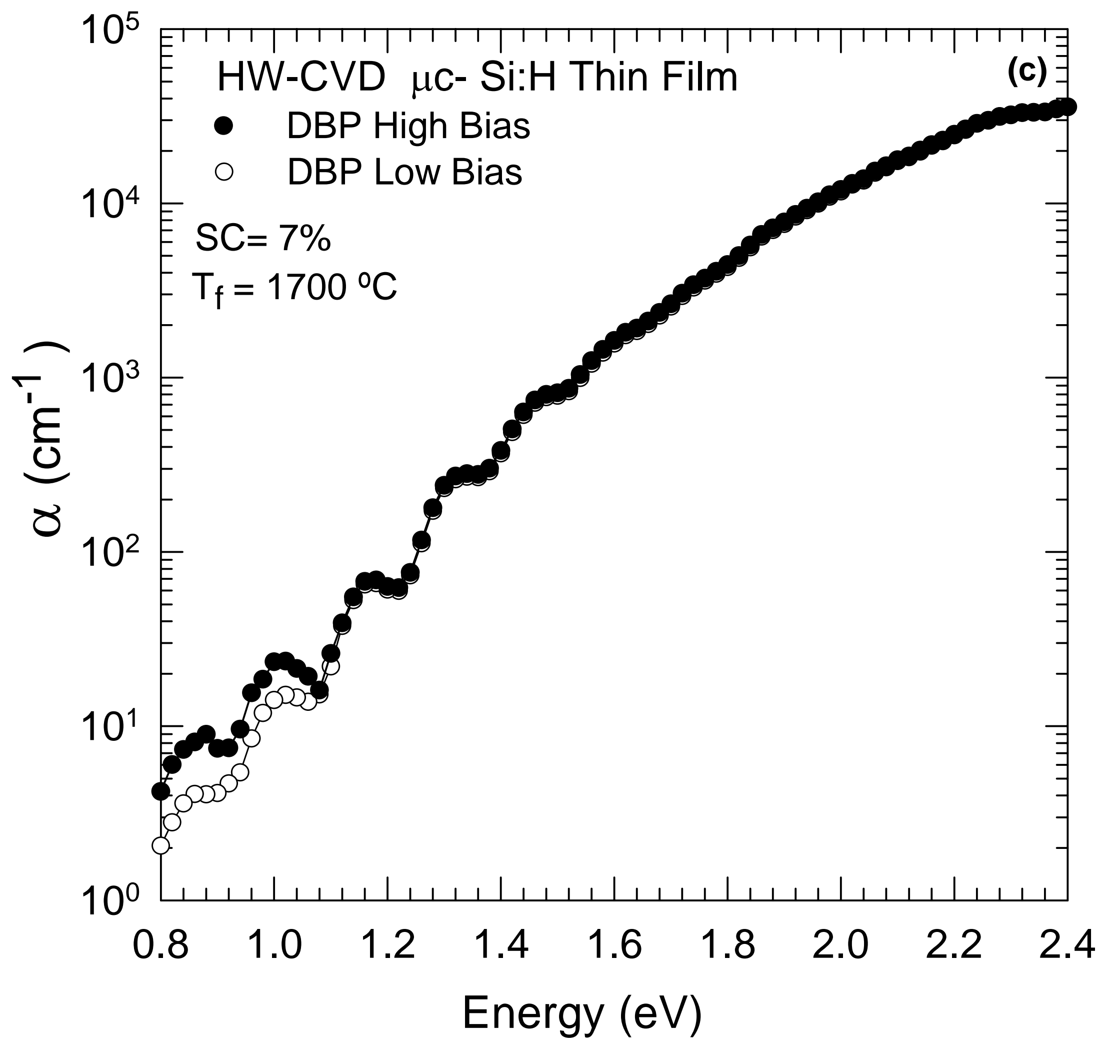

Figure 3.5 c) The calculated absolute α (hν) spectra of DBP for high and low bias light measurements of μc-Si: H thin films deposited by HW-CVD method with SC=7%.

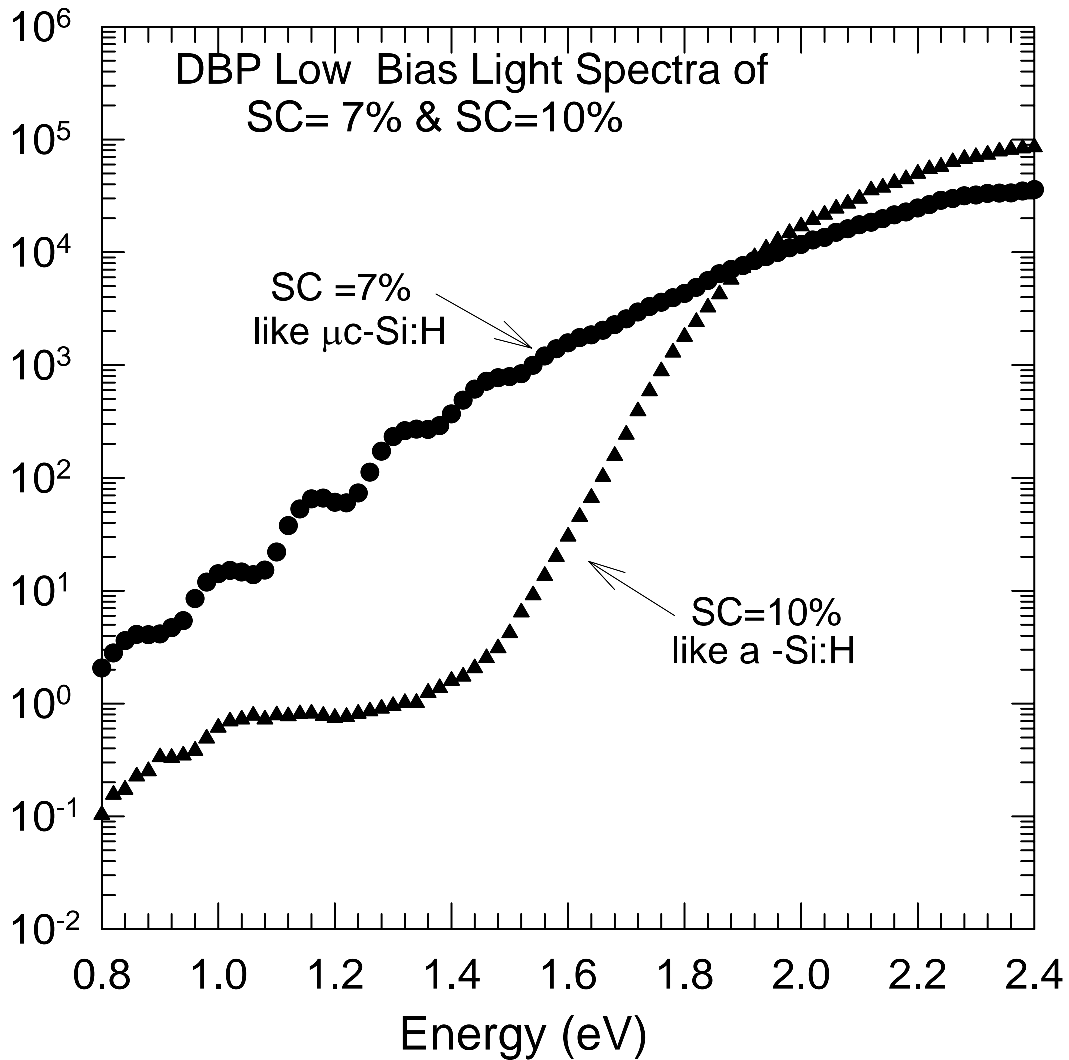

Figure 3.5 d) The calculated absorption coefficient spectra obtained from DBP low bias light intensity for two μc-Si: H thin films deposited by HW-CVD with SC=10% and SC=7%.

As the SC is decreased further, the crystalline volume fraction in the sample increases as reported in the literature (Carius 2001b). The samples deposited at lower SC's are also investigated using same procedures. The results of the other samples are shown in Figure 3.6, Figure 3.7, and in Figure 3.8, for the films deposited with SC=6%, 5%, and 2%, respectively. In each figure, in (a), raw DBP results, in (b), optical transmission spectrum, in (c), calculated absolute α (hν) spectra, and in (d), comparison of α (hν) spectrum obtained from DBP and PDS methods are shown for each sample. It is clearly seen that all of these sample exhibit similar α (hν) spectrum, which is

microcrystalline like in nature. However, some of samples have left fringes after fringe free calculation of the absolute α (hν) spectrum such as SC=6% and SC=2% films. The samples with SC=5% has still very small fringes left on the spectrum. These results indicate that in the growth of microcrystalline silicon, inhomogeneous microstructure grows on the substrate, an initial more defective layer and rough surface layer at the top can also form for some of the samples. In these measurements, these effects are clearly observed in both DBP and PDS measurements.

To investigate the effects of the SC on the sub-bandgap absorption coefficient, the α (hν) values at lower energies has been generally taken as a comparison criteria for different samples. Because the absolute α (hν) values at the low energies are due only to the defect states present in the bulk of the thin film material. In this thesis, the α (hν) values at 0.8 eV measured with low bias light DBP is taken as a comparison criteria for μc-Si: H thin film deposited with different SC's. For some samples, those values at 0.8 eV are also represented to show how two different methods estimate the α (hν) values due to defect states presented in the material. The effects of the SC's on the α (0.8 eV) is shown in Figure 3.9 for both PDS and DBP measurements. It is seen that PDS values are always higher than those of DBP results. For SC=10% sample, amorphous silicon with very small crystallites show amorphous like spectrum. It has different result. However, at SC=7%, the α (hν) is higher and decreases as SC decreases. It reaches to a minimum around SC=5%. As the SC is decreased further, the α (0.8 eV) values starts to increase again even though more crystalline phase grows in the film. This indicates that film becomes more defective in highly crystalline films. For these films, it is claimed that defects occur on the grain boundary walls of the crystalline regions, which is also confirmed by the electron spin resonance (ESR) experiments (Finger et al. 2004c). As a result, these results indicate that lowest defect density films can be deposited with the SC's of around 5% at 1700 ºC filament temperature. These results are also consistent with our previous study reported by Goktas on HW-CVD films deposited at lower filament temperatures (Goktas et al. 2005b).

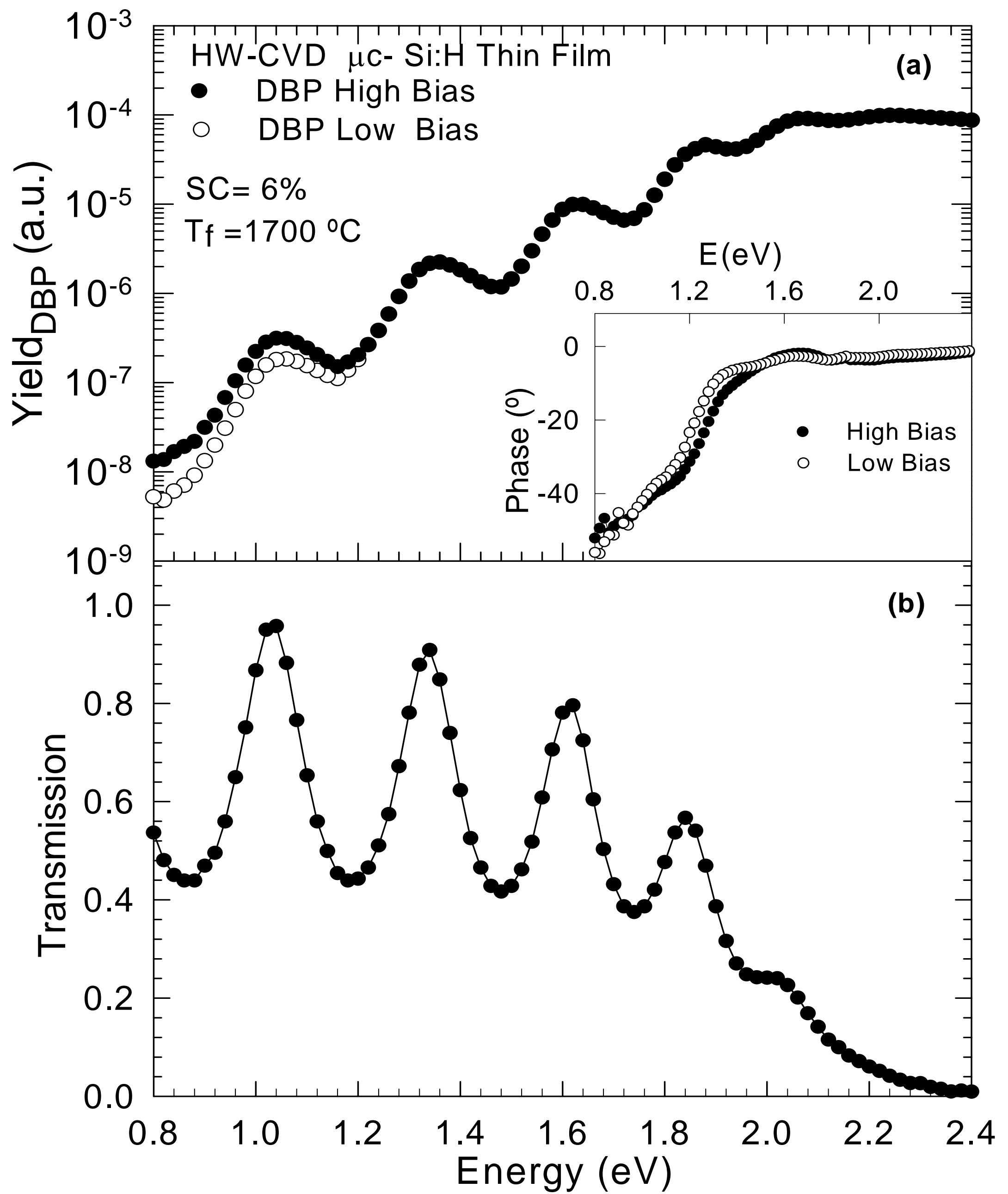

Figure 3.6 a) Yield DBP signals measured at two different dc bias light intensities are shown. In the inset the phase of DBP signals are shown. b) The corresponding transmission spectrum is given for a μc-Si: H thin film deposited with SC=6%.

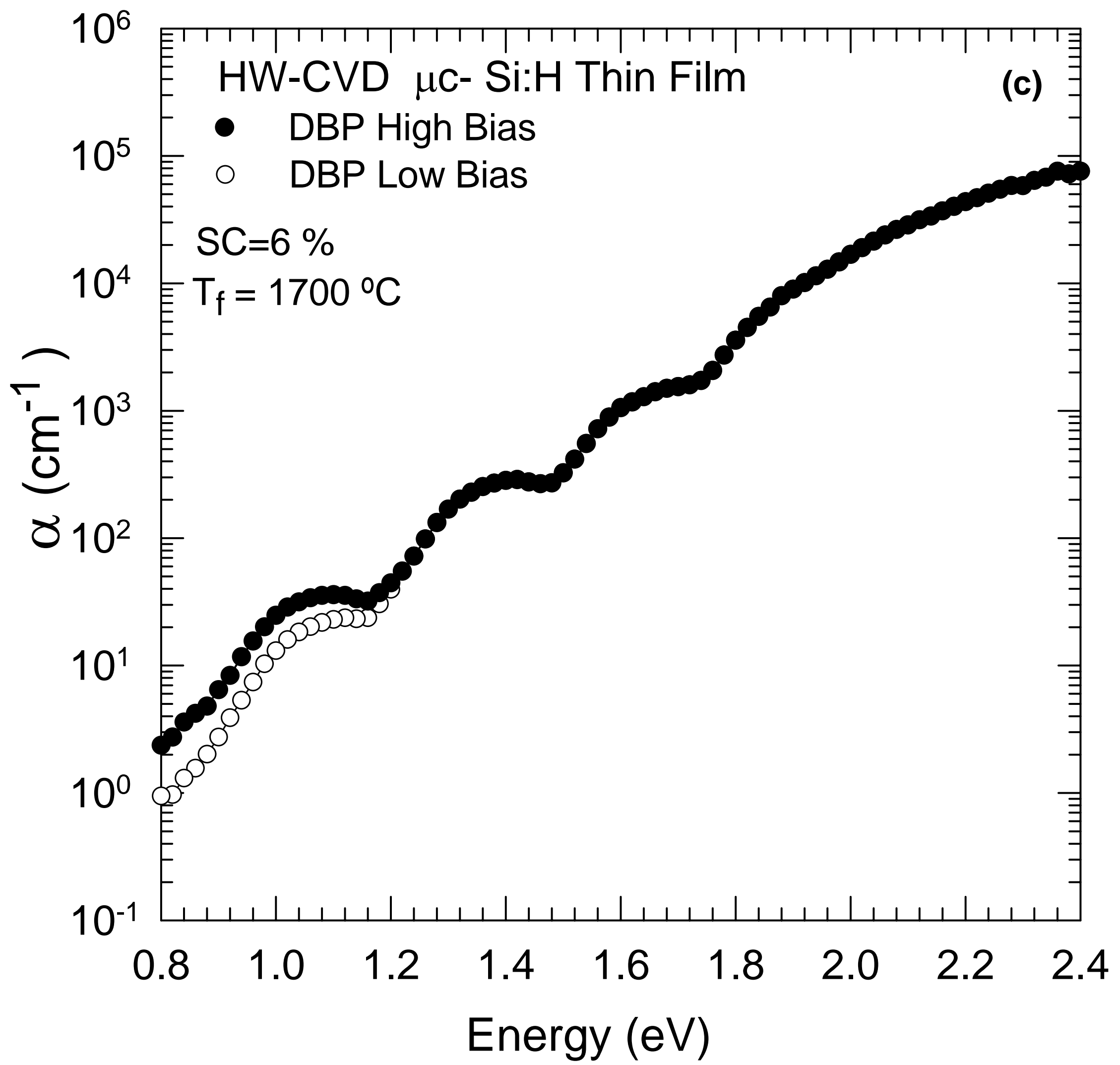

Figure 3.6 c) The calculated absolute α (hν) spectra of DBP for high and low bias light measurements of μc-Si: H thin films deposited by HW-CVD method with SC=6%.

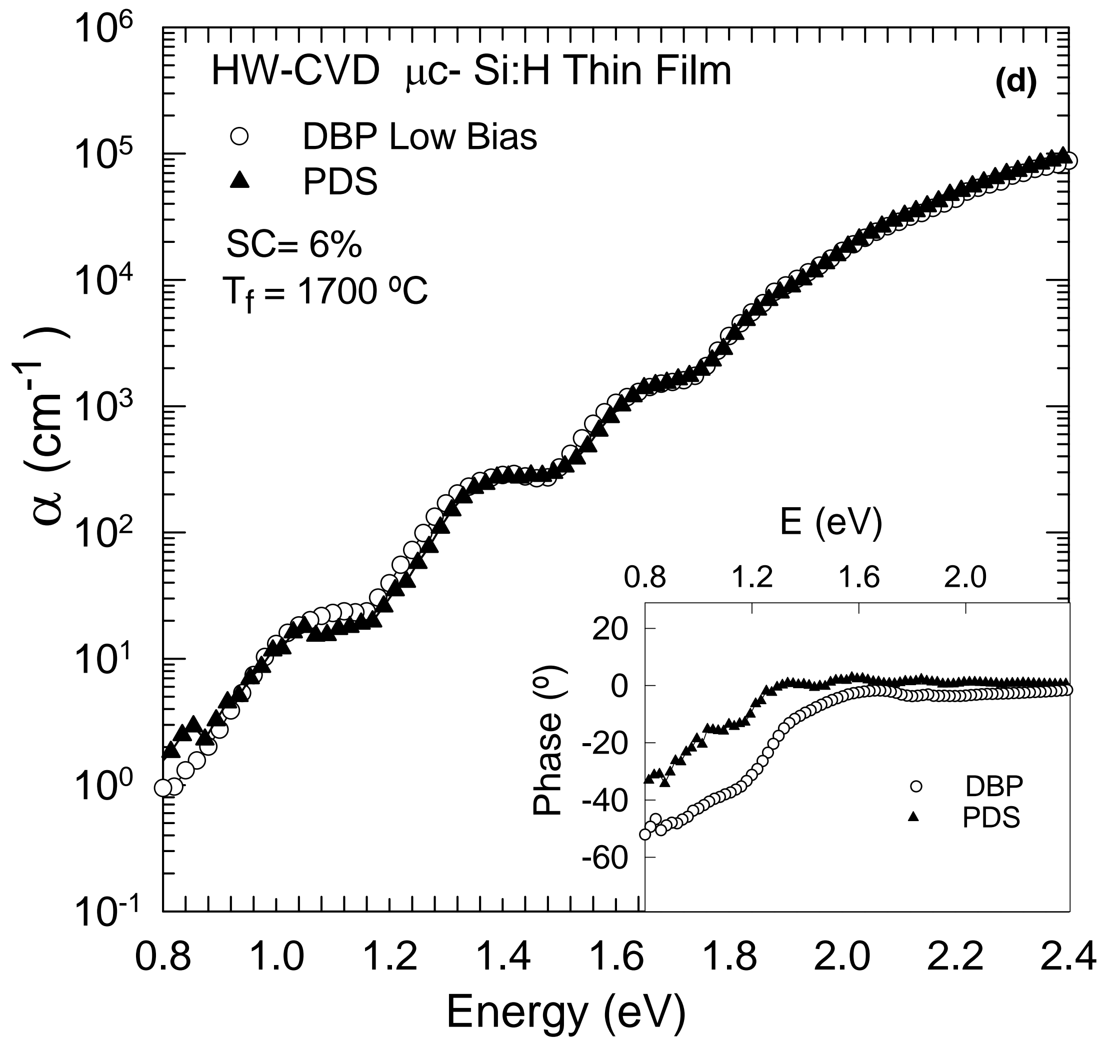

Figure 3.6 d) The calculated absolute α (hν) spectra of PDS and DBP for low bias light measurements of μc-Si: H thin films deposited by HW-CVD method with SC=6%. In the inset, the phase of PDS, DBP are presented.

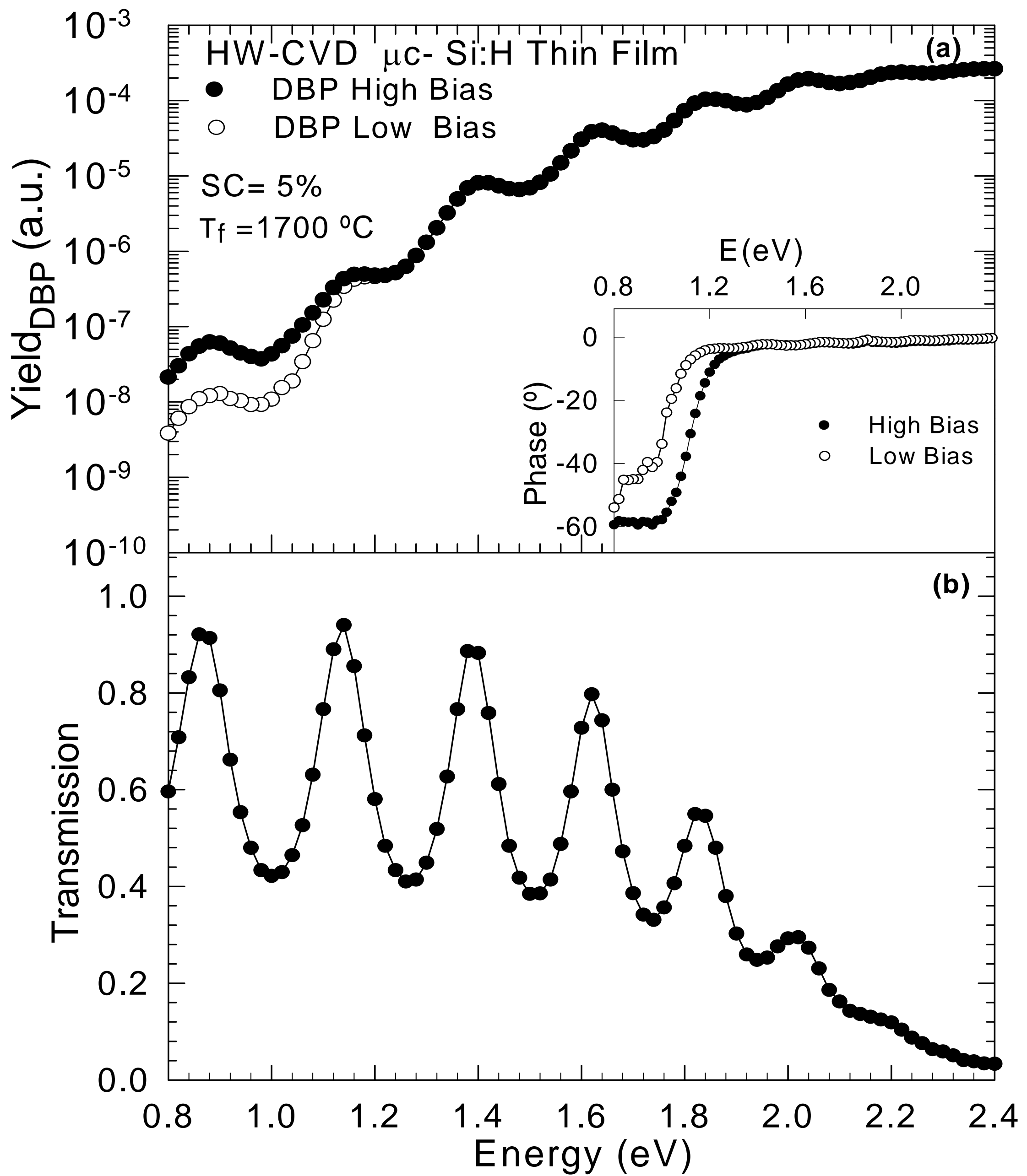

Figure 3.7 a) Yield DBP signals measured at two different dc bias light intensities are shown. In the inset the phase of DBP signals are shown. b) The corresponding transmission spectrum is given for a μc-Si: H thin film deposited with SC=5%.

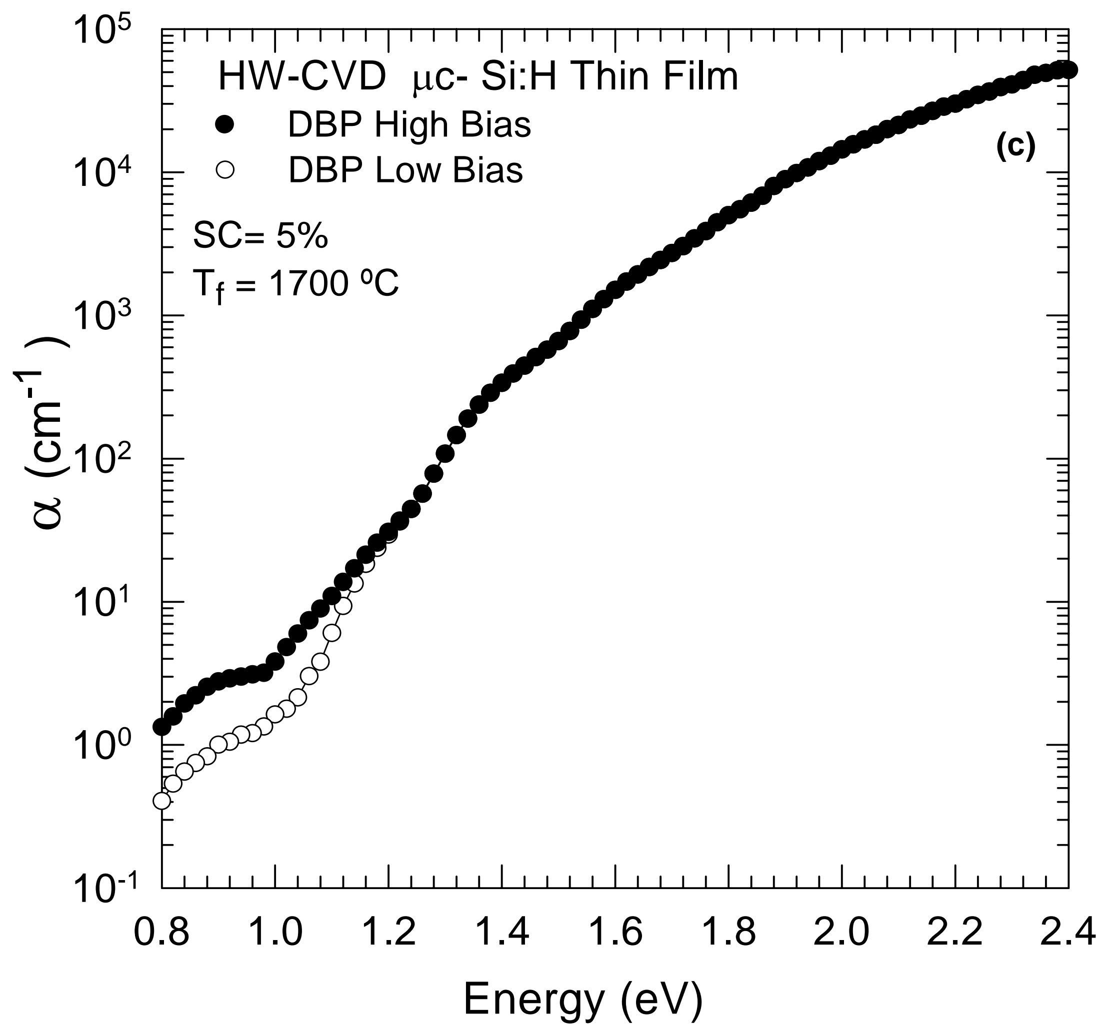

Figure 3.7 c) The calculated absolute α (hν) spectra of DBP for high and low bias light measurements of μc-Si: H thin films deposited by HWCVD method with SC=5%.

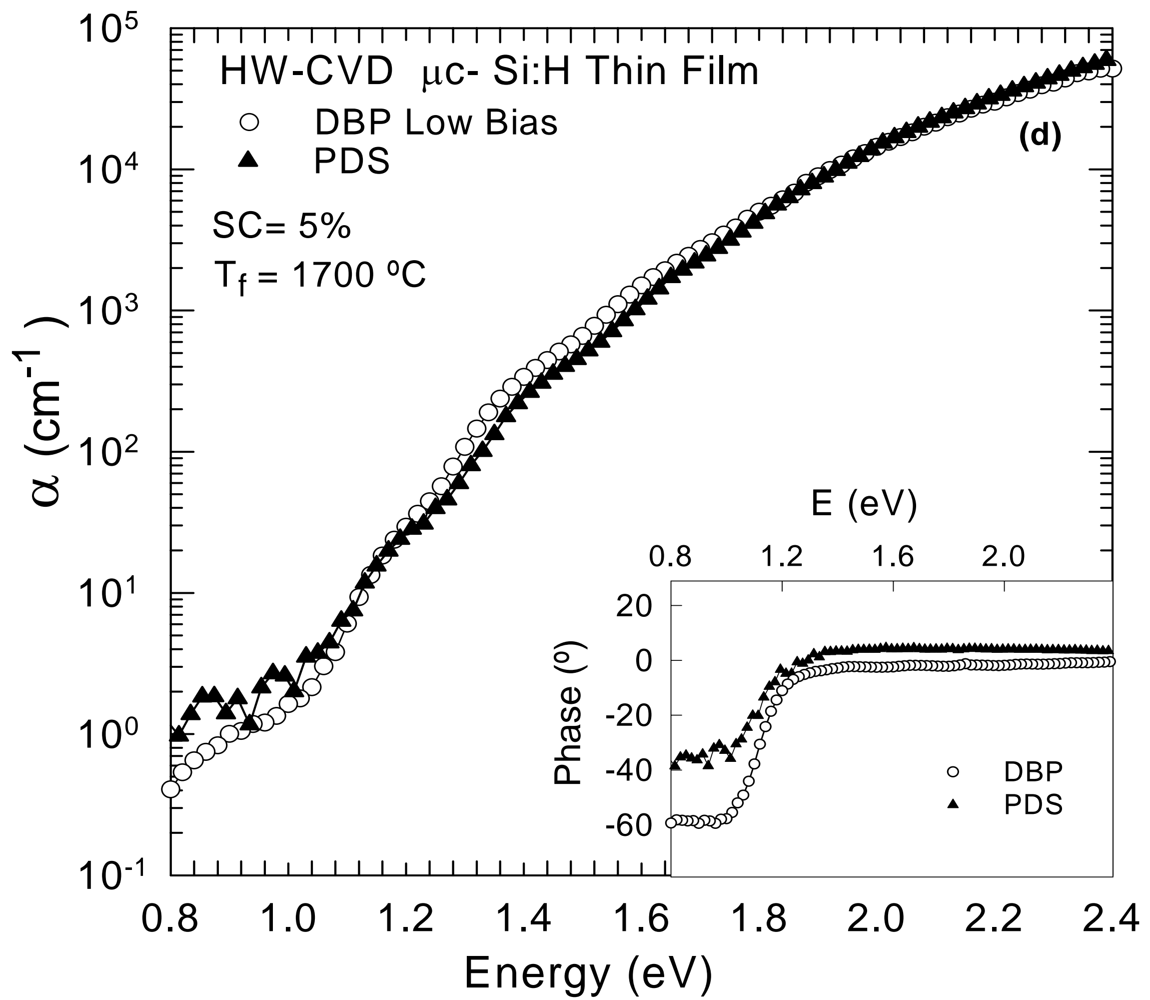

Figure 3.7 d) The calculated absolute α (hν) spectra of PDS and DBP for low bias light measurements of μc-Si: H thin films deposited by HWCVD method with SC=5%. In the inset, the phase of PDS, DBP are presented.

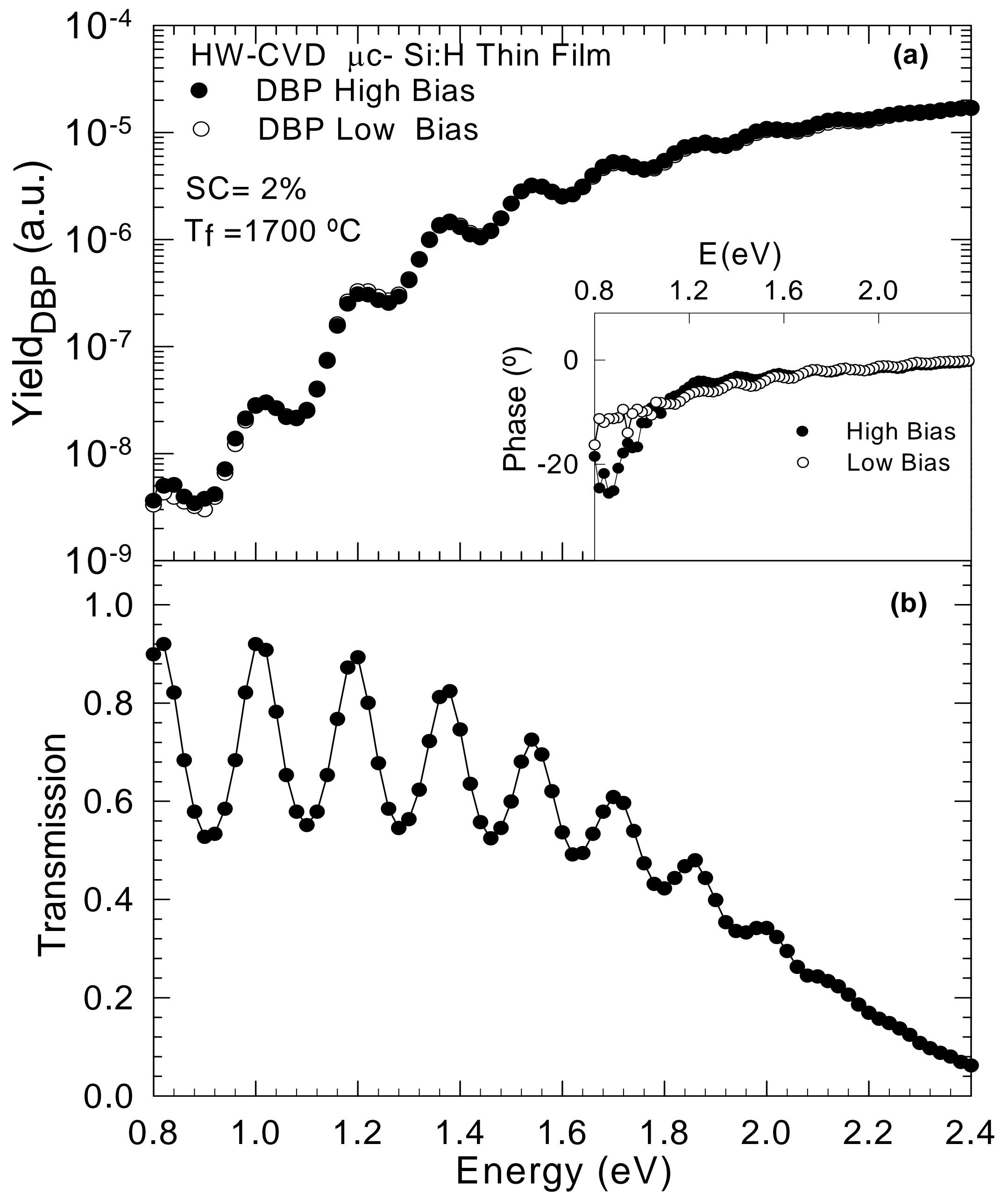

Figure 3.8 a) Yield DBP signals measured at two different dc bias light intensities are shown. In the inset the phase of DBP signals are shown. b) The corresponding transmission spectrum is given for a μc-Si: H thin film deposited with SC=2%.

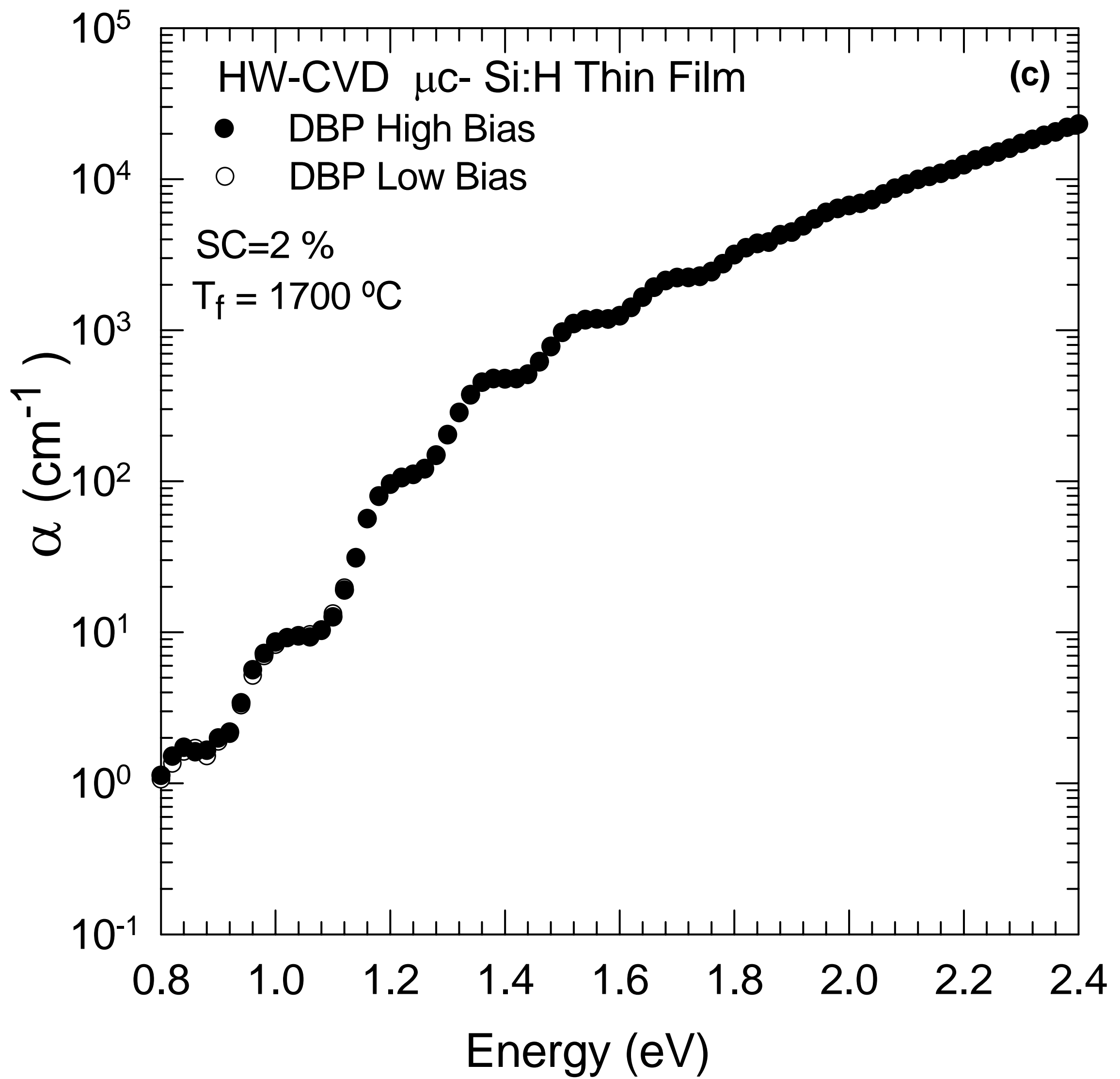

Figure 3.8 c) The calculated absolute α (hν) spectra of DBP for high and low bias light measurements of μc-Si: H thin films deposited by HWCVD method with SC=2%.

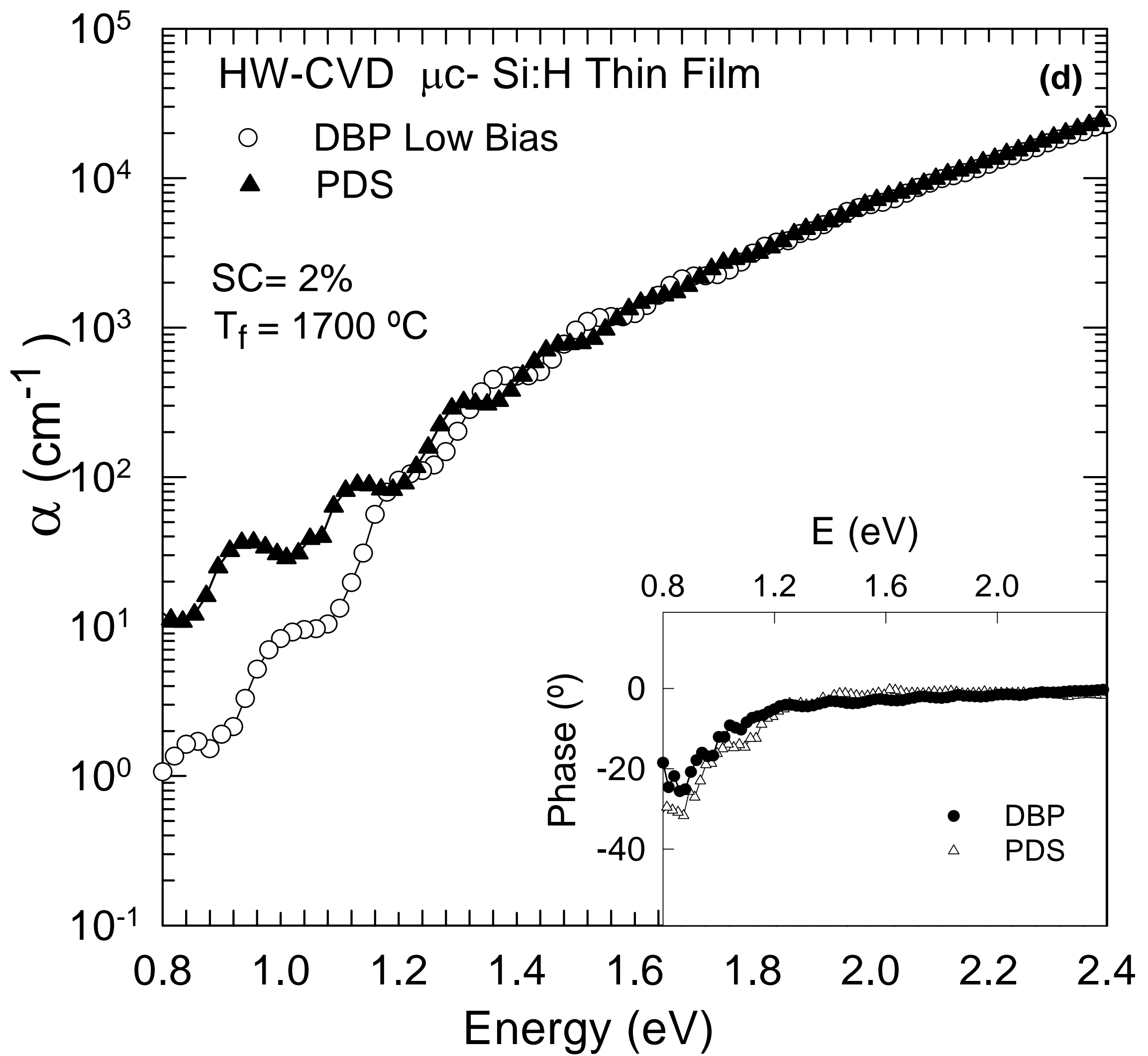

Figure 3.8 d) The calculated absolute α (hν) spectra of PDS and DBP for low bias light measurements of μc-Si: H thin films deposited by HWCVD method with SC=2%. In the inset, the phase of PDS, DBP are presented.

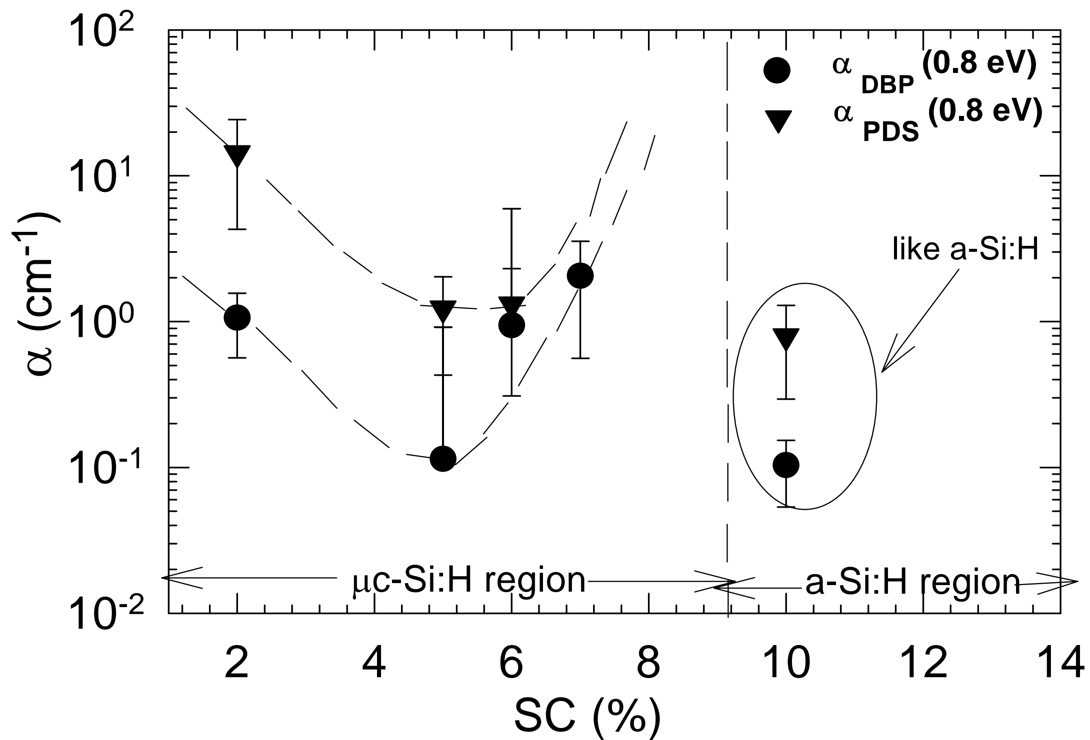

Figure 3.9 Absolute absorption coefficients versus the SC measured by PDS and DBP front ac illumination (low bias light) for μc-Si: H thin films prepared using HWCVD method at filament temperature 1700 ºC.

3.2.2.1 Comparison of PDS, DBP, and CPM absolute absorption coefficient spectra

The optical absorption spectrum of the μc-Si: H thin films is also commonly measured using the constant photocurrent method (CPM) that is also an alternative photoconductivity method to derive the α (hν) spectrum. The principle of the CPM is similar to that of DBP; however, there are major differences in measuring the photoconductivity spectrum as explained in chapter 2. The validity of the absolute α (hν) spectrum of μc-Si: H thin films are also confirmed for a few samples using the CPM measurements carried out in Research Center Jülich, Germany. In CPM, very low generation rate monochromatic light is used to excite electrons from the occupied defect states in the bandgap. Therefore, occupation of the defect states in the dark is very

slightly modified by the ac monochromatic light. There is no bias light used in CPM. However, the $\mu_n\tau_n$- product of electrons is maintained constant by keeping the photocurrent constant at each photon energy by adjusting the flux of the ac monochromatic light.

Comparison of the α (hν) spectra measured by DBP, PDS, and CPM for the samples deposited with the SC=6% and SC=10% are shown in Figure 3.10 and Figure 3.11., respectively. For SC=6% sample, three method result in α (hν) spectrum with exactly the same shape and left over fringes on the spectrum. Therefore, present inhomogeneity in the sample shows its effect in each characterization method. The α (hν) spectrum overlap very well at higher energy part of the spectrum. However, at low energy part, the CPM shows the lowest values. Even though low bias light is used in DBP measurements, it is sufficiently higher than the generation rate of CPM ac monochromatic light and results in higher α (hν) values in the lower energies. Similar effect is also observed for SC=10% sample shown in Figure 3.11. All three spectra overlap very well energies above 1.4 eV, but differences exists below 1.4 eV energies. The CPM spectrum is the lowest among the three and PDS is always much higher at lower energies. To obtain DBP spectrum closer to that of CPM spectrum, the intensity of bias light must be decreased further. For some sample, this has been successfully carried out. But for most of the samples, the signal at lower energies is very low and noise dominates the measurement. Because of this effect, the intensity of bias light has been kept as low as possible until reliable noise free measurement is obtained. The α (hν) values of low bias light DBP are slightly higher than those of measured by the CPM measurements.

Finally, the α (hν) spectrum independently obtained by three different method agrees very well at higher energy part of spectrum, differences at lower energies involve important information about the absorption of light by the defect and must be carefully evaluated for each measurement technique.

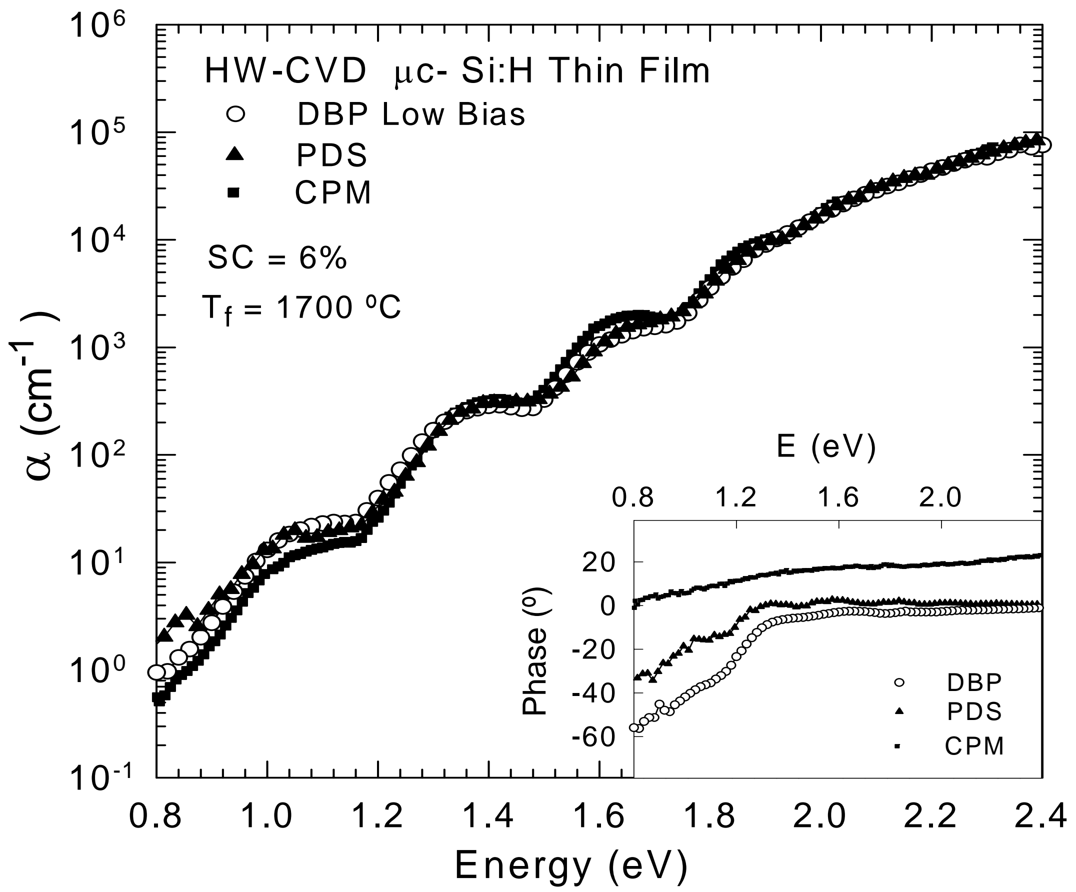

Figure 3.10 The calculated α (hν) spectra independently obtained the PDS, CPM, and low bias light DBP measurements for a μc-Si: H thin film deposited with SC=6%. In the inset the phase of PDS, CPM, and DBP low bias light signals are shown.

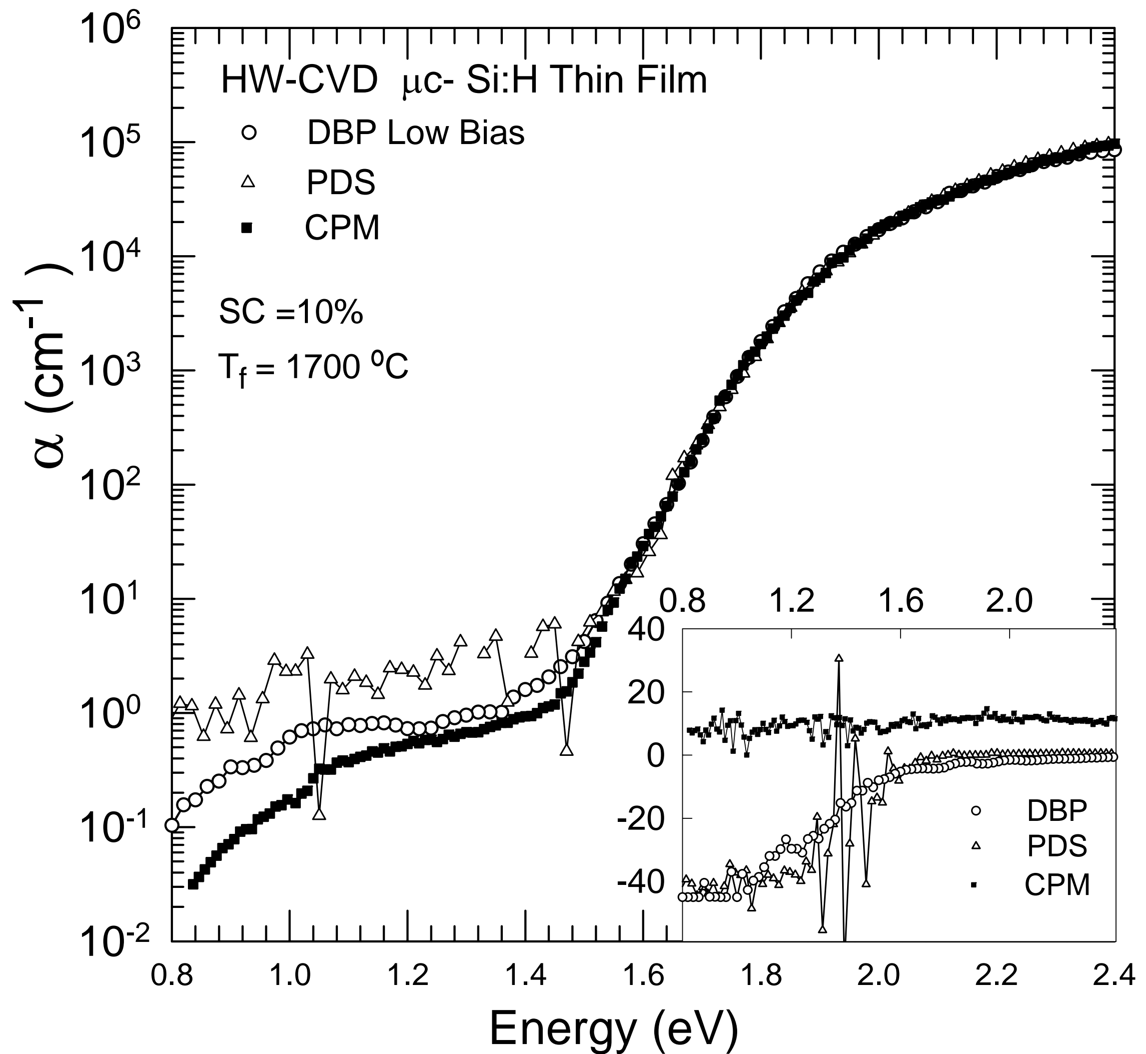

Figure 3.11 The calculated α (hν) spectra independently obtained the PDS, CPM, and low bias light DBP measurements for a μc-Si: H thin film deposited with SC=10%. In the inset the phase of PDS, CPM, and DBP low bias light signals are shown.

3.3 The Effects of Filament Temperature

The filament temperature is another important process parameter in HW-CVD process. The electronic and optical properties of μc-Si: H thin films deposited by HW-CVD method strongly depend on the filament temperature, which affects the deposition rate and microstructure of the materials. The effect of filament temperature exists as a change in the breaking of the silane gas (SiH_4) molecules during the deposition, which

is used as a main source gas in the HW-CVD process to grow the μc-Si: H thin films. As the filament temperature increases, the efficiency of breaking of silane molecules increases. This increases the density of atomic H. The atomic hydrogen effectively etches Si atoms. Therefore, with increasing filament temperature, a transition from amorphous to microcrystalline occurs. The transition is only observed on the films deposited with higher SC and higher filament temperature.

In this section, the effects of filament temperature on microstructure of microcrystalline silicon thin films deposited by HWCVD method has been investigated with constant SC=10% by changing the filament temperatures from 1700 ºC to 1880 ºC. Steady state photoconductivity, dual beam photoconductivity, and optical transmission measurements were used to see its effect on microstructure.

3.3.1 The Effect on Steady State Photoconductivity

In order to see the effect of filament temperature on steady state photoconductivity measurements giving quantitative information about the material, the filament temperature was increased from 1700 ºC to 1880 ºC and silane concentration was kept constant at 10%.

As an example, the photoconductivity σ_{ph} versus generation rate spectra for three microcrystalline silicon thin films deposited at filament temperatures of 1700 ºC, 1800 ºC, and 1880 ºC with constant SC=10% are shown in Figure 3.12a. A linear dependence of photoconductivity on generation rate is clearly seen for three samples. In general, for the samples deposited with higher silane concentration, the amorphous phase dominants in the microstructure of material. However, with increasing filament temperature the behavior of the materials deposited with the same SC changes. For high filament temperature, T_f=1880ºC, the slope γ is equal to 0.96, which is very close to unity. In literature, this slope value is observed for most amorphous silicon materials. However, the photoconductivity versus generation rate spectrum indicates that this film shows higher σ_{ph} values than those of other samples. The increase in σ_{ph} values show that the microcrystalline region increases in the microstructure of the material. For the filament temperature, T_f=1800 ºC, the slope decreases and reaches to 0.76 which is the value generally seen for the undoped microcrystalline silicon. However, the σ_{ph} values decrease due to increasing defect states and dominating amorphous phase in the

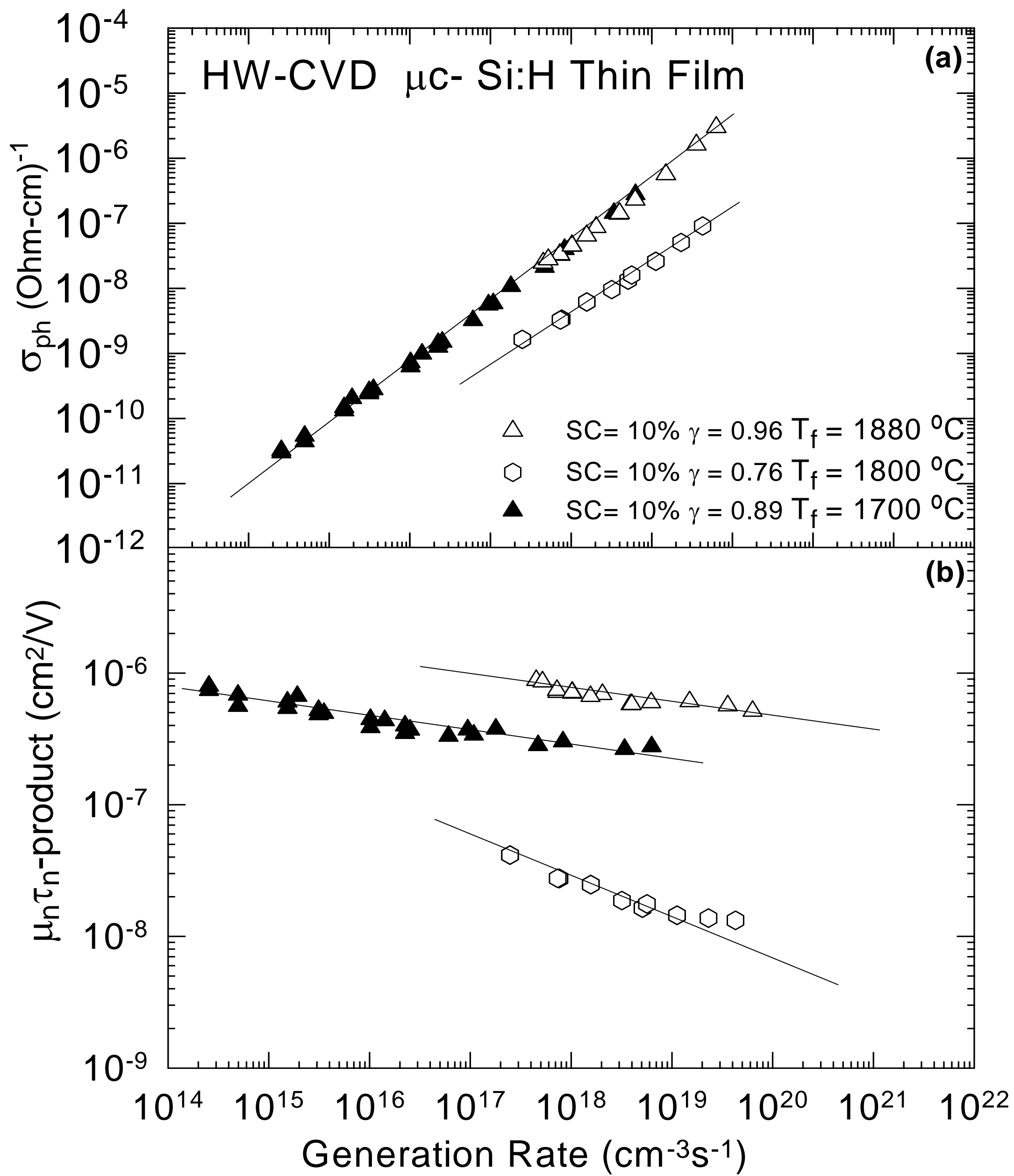

Figure 3.12 a) σ_{ph} versus generation rate for μc-Si: H thin films deposited by HWCVD method at filament temperatures 1700 ºC, 1800 ºC, and 1880 ºC with SC=10%. b) $\mu_n\tau_n$ -product versus generation rate of the same μc-Si: H thin films.

material. For the lowest T_f=1700 ºC film, the slope γ increases again, which reaches to 0.9 which is close to unity and also observed for amorphous silicon. The σ_{ph} values indicate that this film exhibits amorphous like characteristic as expected. In addition, the majority carrier $\mu_n\tau_n$ products calculated using the σ_{ph} values given in Figure 3.12a are presented as a function of generation rate in Figure 3.12b.

3.3.2 The Effect on the Sub-Bandgap Absorption Spectrum

The effects of filament temperature (T_f) on the electrical, optical and structural properties of μc-Si: H thin films deposited by HWCVD technique at filament temperatures of 1700 ºC, 1800 ºC, and 1880 ºC with SC=10% were investigated using the sub-bandgap absorption coefficient spectrum. The filament temperature affects the microstructure of the material. The films deposited at higher filament temperature exhibits a transition from amorphous to fully microcrystalline growth (Jadkar et al 2003). The transition only is observed for the films deposited with higher silane concentration.

DBP yield spectrums for high and low bias light intensities are shown for μc-Si: H thin films deposited by HWCVD method at filament temperature T_f=1700 ºC with SC=10% in Figure 3.13. The DBP yield spectra for high and low bias light intensities exhibit amorphous like characteristics. The effect of bias light intensity is seen in the low energy region. The spectrum obtained from high bias light intensity shows higher values than those of low bias light intensity in the low energy region. The corresponding transmission spectrum is shown in Figure 3.13b. Generally, with increasing filament temperature, the microcrystalline region increases in the microstructure of the material. For the filament temperature T_f=1800 ºC, the obtained DBP yield spectra for high and low bias light intensities are exhibited in Figure 3.14. Even though the investigated film deposited at higher filament temperature similar to that of presented in Figure 3.13, the film exhibits amorphous like characteristics. On the other hand, for higher filament temperature T_f=1880 ºC, the obtained DBP yield spectrums for high and low bias light intensities given in Figure 3.15a indicate that the film shows microcrystalline silicon like characteristics. There is no big difference observed between the spectra for high and low bias light intensities. The optical transmission spectrum is also exhibited in Figure 3.15b.

The absorption coefficient spectra calculated using DBP yield spectra for low bias light intensity obtained for the same μc-Si: H thin films illustrated in Figure 3.16. As mentioned before the amorphous phase dominants in the microstructure of the thin films deposited at lower filament temperatures. This result is also observed in the absorption coefficient spectrums obtained for the filament temperatures T_f=1700 ºC and T_f=1800 ºC. The filament temperature effect on the microstructure of the material is not observed between two spectrums. However, the absolute absorption coefficient spectrum for T_f=1800 ºC exhibits some remaining fringes attributed to the inhomogeneity present in the bulk of the film. On the other hand, for the filament temperature T_f=1880 ºC, the microcrystalline like characteristics is observed in the absolute absorption coefficient spectrum. Even though both films deposited with filament temperatures of T_f=1700 ºC and T_f=1800 ºC exhibit amorphous like characteristics, microcrystalline like characteristic is observed in the films deposited with T_f=1880 ºC. This means that the films deposited at higher filament temperature shows a transition from amorphous to fully microcrystalline growth.

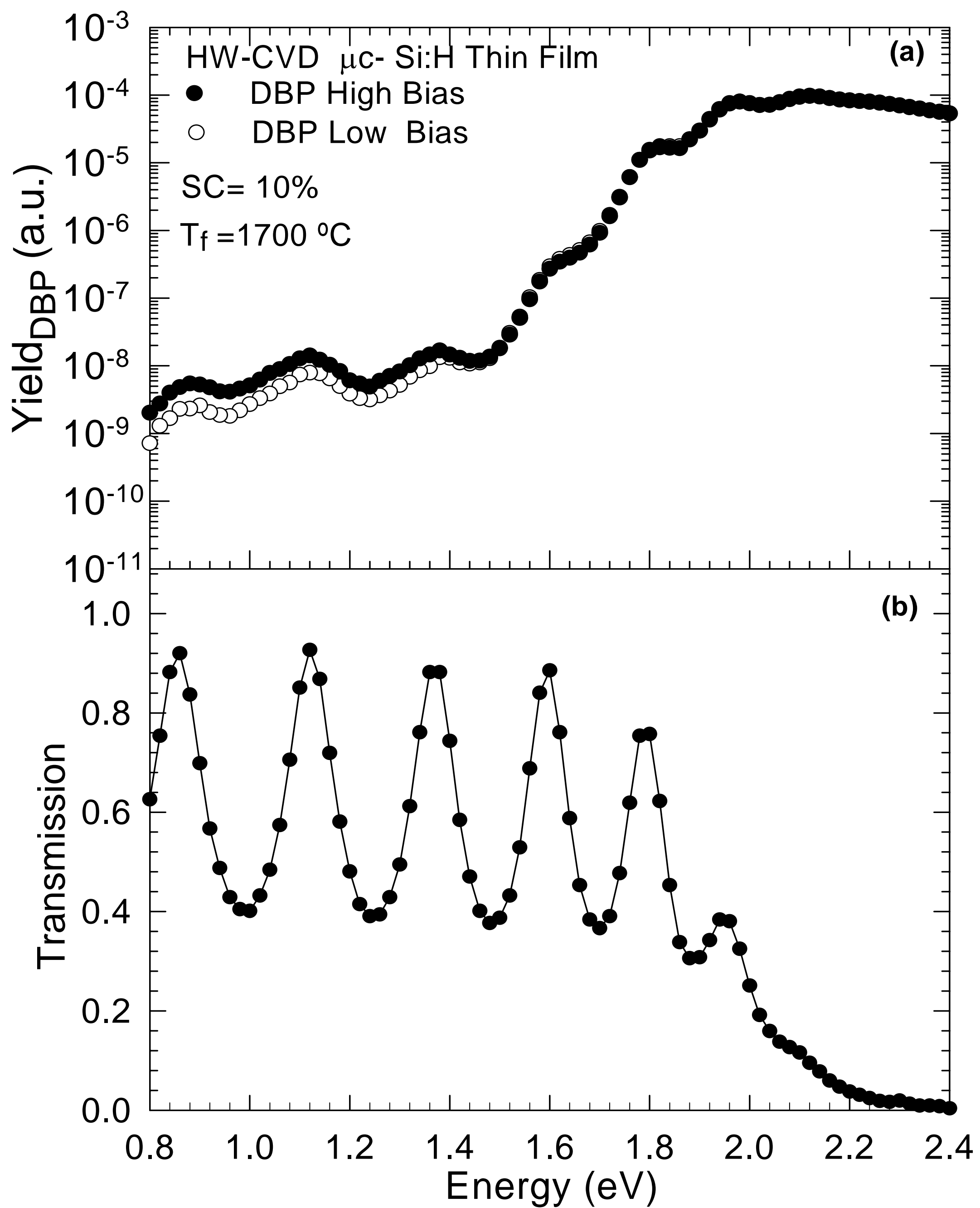

Figure 3.13 a) DBP yield spectrum for high and low bias light intensities for μc-Si: H thin films deposited by HWCVD method with SC= 10% and filament temperature of 1700 ºC. b) Corresponding transmission spectrum is exhibited.

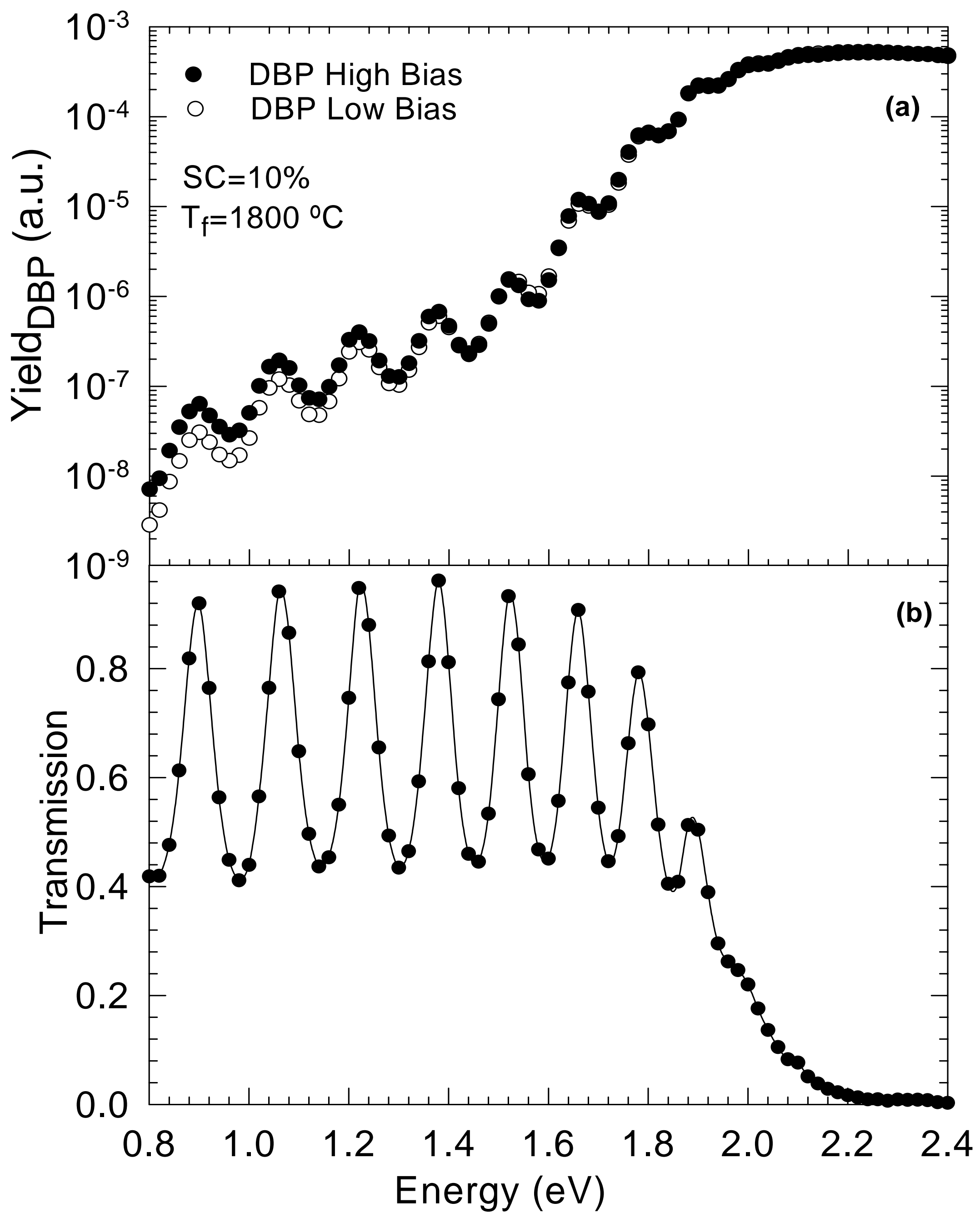

Figure 3.14 a) DBP yield spectrum for high and low bias light intensities for μc-Si: H thin films deposited by HW-CVD method with SC=10% and filament temperature of 1800ºC. b) Corresponding transmission spectrum is exhibited.

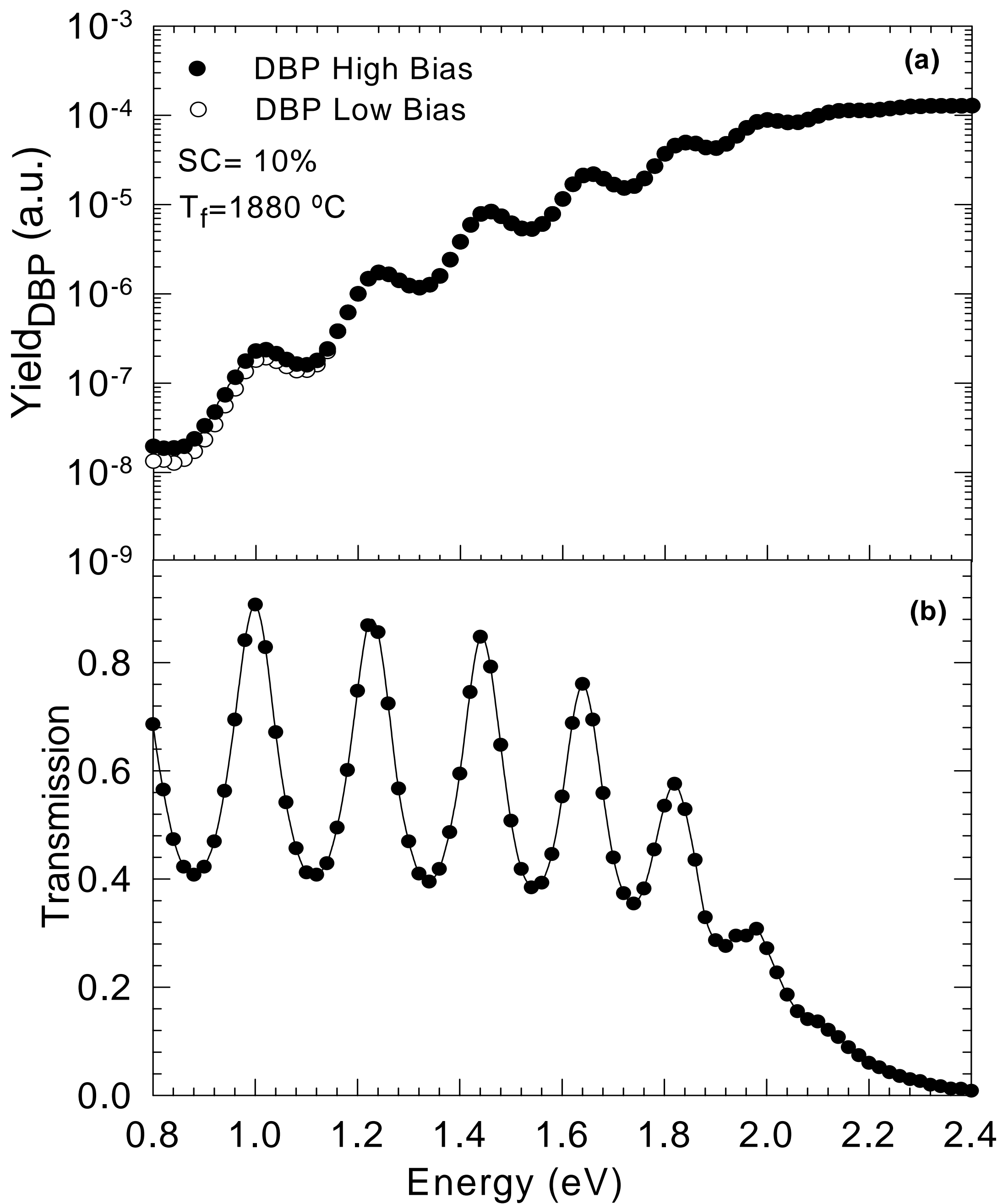

Figure 3.15 a) DBP yield spectrum for high and low bias light intensities for μc-Si: H thin films deposited by HWCVD method with SC= 10% and filament temperature of 1880 ºC. b) Corresponding transmission spectrum is exhibited.

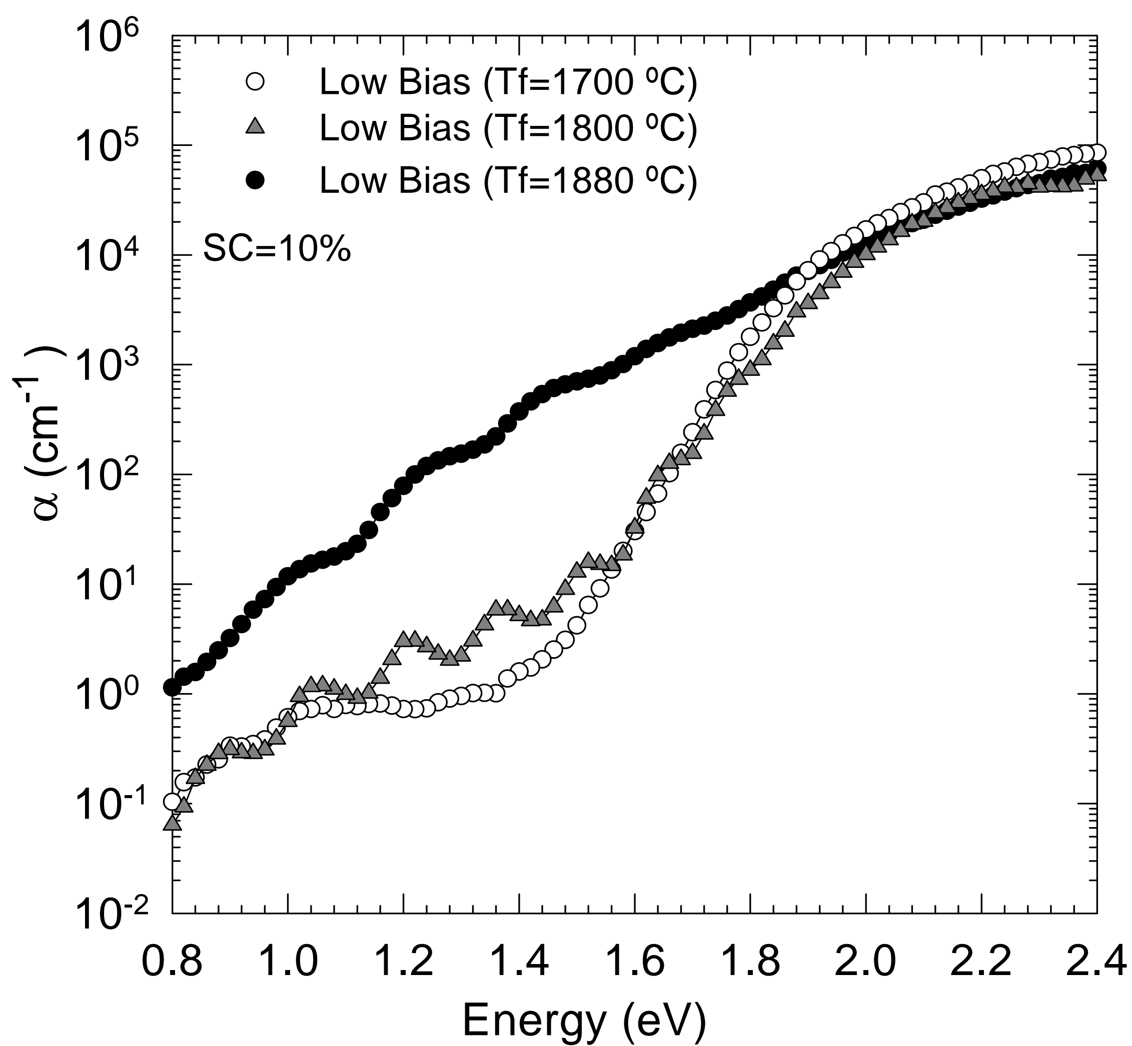

Figure 3.16 The calculated absolute α (hν) spectra obtained from DBP low bias intensities for three thin films deposited at filament temperatures of 1700 ºC, 1800 ºC, and 1880 ºC.

3.4 The Effects of Microstructure on Dual Beam Photoconductivity Method

In the analysis of the DBP and optical transmission spectra, for the some films, there was interference fringes left on the absolute α (hν) spectrum after carrying out the fringe free calculation of α (hν) spectrum. That was an indication of inhomogeneous absorption of monochromatic light in the material. In order to investigate the effects of inhomogeneity present in μc-Si: H thin films, DBP measurements were carried out by illuminated ac monochromatic light through film side (front) and substrate side (back) at the same dc bias light intensity. An example of DBP yield spectra obtained for front and back ac illuminations are shown for sample with SC=10% and filament temperature of 1700 ºC in Figure 3.17. The measurements conditions are the same for both front and back ac illuminations but only the direction of the ac light is different. As clearly seen, in high energy region (above 1.2eV) the interference fringes of both spectrums are at the same energy values; however the shift begins in back ac illumination below 1.2 eV. This indicates that light is not uniformly absorbed throughout the material. The optical transmission spectrums obtained for both front and back ac illumination was found to be identical as shown inset of Figure 3.17. The resulting α (hν) spectra calculated for front and back ac illumination are presented in Figure 3.17b. It is clearly seen that the interference fringes remain on absolute absorption spectrum from back ac illumination. The reason of remaining fringes in α (hν) spectrum is the non-uniform absorption of the monochromatic light due to inhomogeneous structure of μc-Si: H thin film. This indicates that there exists a defective interfacial layer which affects the optical and electric properties of samples. The defective layer observed in this sample is closer to the substrate of material. The phase signals of front and back ac illuminations measurements are also shown inset of Figure 3.17b.

In Figure 3.18, another results of the DBP measurements obtained for front and back ac illuminations are shown for sample with SC=6% and filament temperature of 1700 ºC. It is clearly seen that the interference fringes take place at the same energy values in both DBP yield spectrums for front and back ac illumination. However, the depth of fringes observed for front ac illumination is higher than that of back ac illumination.

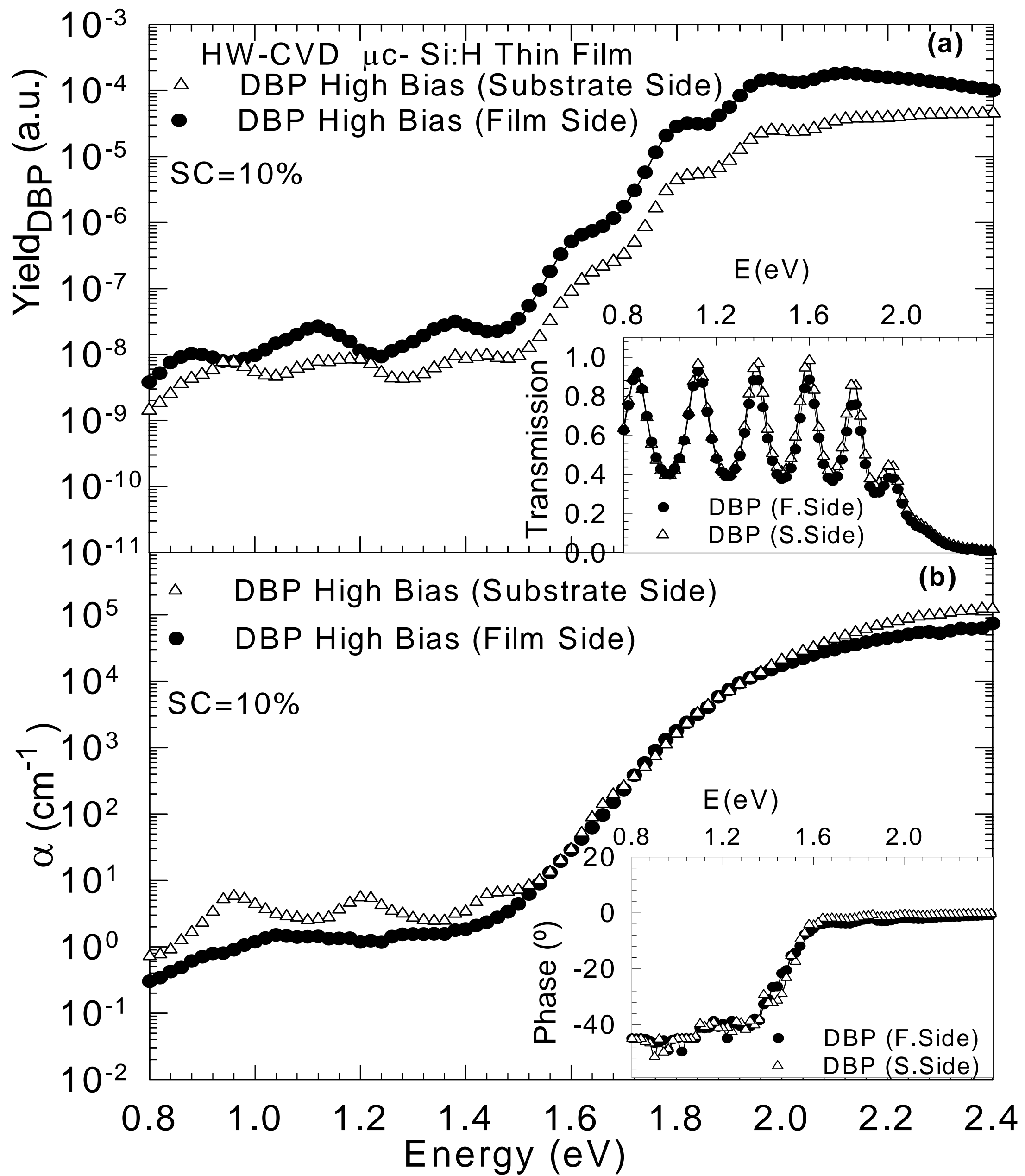

Figure 3.17 a) DBP yield spectra for μc-Si: H thin film with SC=10% for ac light incident from film side and substrate side. Inset of the figure, transmission spectrums of both measurements are shown. b) The calculated absolute α (hν) spectrum of both measurements are shown. In the inset, the phases of both measurements signals are presented.

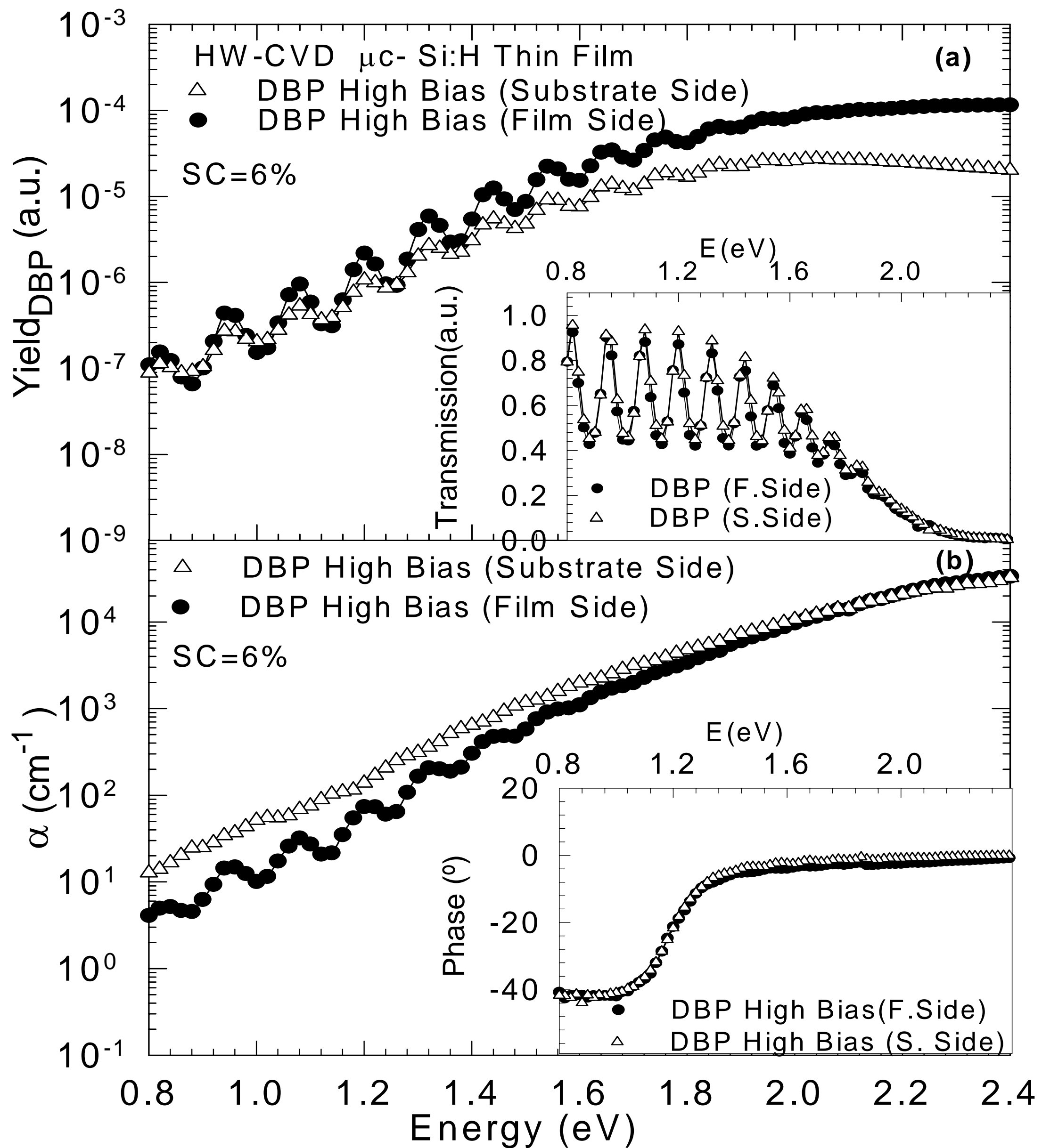

Figure 3.18 a) DBP yield spectra for μc-Si: H thin film with SC= 6% and filament temperature 1700 ºC for ac light incident from film side and substrate side. Inset of the figure, transmission spectrum of the sample is shown. b) The calculated absolute α (hν) spectrum of both measurements are shown. In the inset, the phases of both measurements signals are presented.

The corresponding transmission spectra obtained for both measurements agree with each other given in the inset of Figure 3.18a. Using measured optical transmission and DBP yield spectra, the calculated absorption coefficient spectra were presented in Figure 3.18b. The calculated absolute α (hν) spectrum for back ac illumination is almost free of fringes and has higher α (hν) values at energies below the 1.8 eV. However, some interference fringes are observed in the calculated absolute α (hν) spectrum for front ac illumination. The remaining fringes indicate that the inhomogeneous defective layer can exist through the bulk of the material. On the other hand, at lower energies, the absolute α (hν) spectrum for back ac illumination gives higher values. This indicates that DBP back illumination probes slightly higher defective layer. Therefore, there is no clear information about where the defective layer takes place.

The similar effect about the inhomogeneity is presented in Figure 3.19 for highly crystalline film with SC=2%. The differences between DBP yield spectra for front and back ac illuminations are presented in the Figure 3.19a. The interference fringes take place at the same energies in both spectra. On the other hand, the modulation depth is smaller for back illumination. It is clearly seen in the calculated absolute α (hν) spectra for both measurements; some interference fringes remain in the absolute α (hν) spectra of front and back ac illumination measurements which can be attributed to the inhomogeneous absorption of light during the measurements. However, the depth of fringes is higher for front ac illumination. The calculated α (hν) spectrum for front ac illumination indicates that the inhomogeneous defective layer can exist closer to the bulk of the material.

As a result, this kind of structural inhomogenities can exist on the surface or through the bulk, at the film- substrate interface or combination of all as inferred from the calculated absolute α (hν) spectrum for front and back ac illuminations.

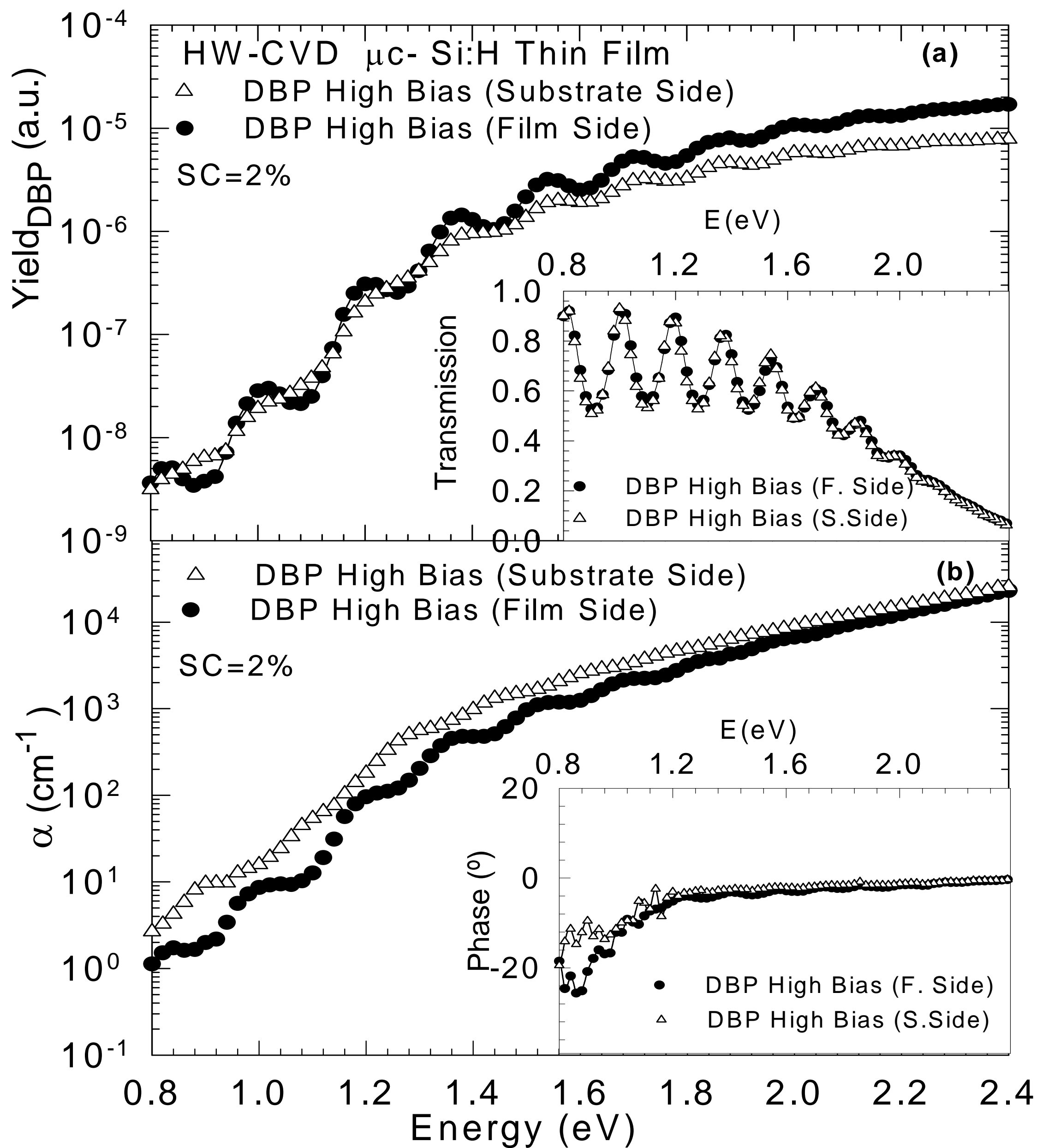

Figure 3.19 a) DBP yield spectra for μc-Si: H thin film with SC=2% and filament temperature 1700 ºC for ac light incident from film side and substrate side. Inset of the figure, transmission spectrum of the sample is shown. b) The calculated absolute α (hν) spectrum of both measurements are shown. In the inset, the phases of both measurements signals are presented.

3.5 Conclusions

In this thesis, the effect of silane concentration and filament temperature of the hot wire CVD deposited microcrystalline silicon thin films on the optical and electronic properties have been investigated. Majority carrier electron $\mu_n\tau_n$ products and sub-bandgap absorption coefficient spectrum are used for the comparison of different μc-Si: H thin films deposited under different conditions. Sub-bandgap absorption coefficient spectrum is calculated from DBP yield and optical transmission spectra and finally compared with those independently measured using PDS and CPM methods.

The effect of silane concentration on steady state photoconductivity indicates that amorphous silicon films are deposited at SC=10%. They have lower photoconductivity and have exponent γ close to unity as reported for a-Si: H films. As the silane concentration decreases, σ_{ph} increases in magnitude and its exponent decreases to values around 0.7, which is an indication of recombination process of electrons and holes through defect states in the bandgap of thin film silicon. For the lowest silane concentration of SC=2%, highly crystalline film is prepared. Magnitude of photoconductivity decreases substantially and its exponent becomes 0.5. The exponent γ=0.5 is generally observed in crystalline silicon meaning that photogenerated electrons recombine directly with holes, no defect states in the bandgap is involved in the recombination process.

The effect of the silane concentration on the sub-bandgap absorption coefficient spectrum as determined from the DBP and optical transmission measurements indicate that at the SC=10% amorphous structure dominates the characteristics. The α (hν) spectrum similar to that of a-Si: H is measured for SC=10% (Klein et al. 2004a). As SC decreases, the ratio of the crystalline region to that of amorphous region increases, the shape of the α (hν) spectrum becomes similar to that of crystalline silicon. But at lower energies, the α (hν) due to defect states present show a variation among the films. The degree of defect states present is represented by the α (hν) at 0.8 eV and compared as a function of silane concentration. In the microcrystalline growth regime, the α (hν) decreases as silane concentration decreases down to 5% value. Further decrease of the SC produce highly crystalline in μc-Si: H thin films but the α (hν) starts increasing again. The lowest α (hν) values are obtained for films deposited under the SC around 5%.

The α (hν) spectrum of the samples were also compared with those independently measured by PDS and CPM measurements. At higher energy region, three methods give consistent absorption coefficient spectrum. However, the differences in the lower energies are due to differences in the principle of three methods. In addition, for some sample there exist interference fringes left on the fringe free calculated α (hν) spectrum. These fringes are the indication of inhomogeneous growth of μc-Si: H thin film which results in inhomogeneous absorption of light in the sample and affects the experimental results of different methods, these effects can be used as a probe for the inhomogeneity of sample growth.

Another deposition condition of the μc-Si: H growth was investigated by changing the filament temperature in the HW-CVD deposition process. To see the effect of T_f, the highest silane concentration is considered. For SC=10%, T_f is changed from 1700 ºC to 1880 ºC. For 1700 ºC and 1800 ºC, still an amorphous structure dominates the α (hν) spectrum. However, microcrystalline phase becomes dominant at 1880 ºC and α (hν) shows a shift to microcrystalline silicon spectrum.

Finally, the effect of inhomogeneous microstructure in the sample was investigated using front and back ac illumination of DBP measurements and absolute α (hν) spectra were calculated. It is clearly seen that, for some samples, front and back α (hν) spectra show substantial differences due to different absorption path of light in the material. A careful evaluation of the results must be carried out for such situations.

CHAPTER 4

DISCUSSIONS AND CONCLUSIONS

Hydrogenated microcrystalline silicon (μc-Si: H) is a promising thin film material for technological applications such as solar cells, flat panel, and optical sensors. Its unique properties can be shown as reasons of this popularity. As compared with its amorphous and single crystalline from, it has higher optical absorption coefficient spectrum in the visible region than single crystalline silicon and it has higher optical absorption coefficient spectrum in the infrared region than amorphous silicon. In addition, it has higher free carrier mobility values than those of amorphous silicon. Furthermore, μc-Si: H does not suffer from the light-induced degradation (known as Staebler-Wronski effect), which is a main problem for hydrogenated amorphous silicon (a-Si: H) in PV applications. However, its electronic and optical properties strongly depend on its microstructure. Therefore, the microstructure is one of the most considered properties of μc-Si: H because of showing varying properties under the different deposition conditions especially silane concentration and filament temperature for HW-CVD prepared thin films. For such kind of candidates for the photovoltaic applications, photosensitivity and the level of defect states present in the material are two of the most important fundamental properties of photovoltaic materials. Photosensitivity, $\mu_n\tau_n$–product, was obtained form the steady state photoconductivity and the level of defect states are generally estimated from the optical absorption coefficient values at lower energies. In this thesis, to understand the optical and electronic properties of μc-Si: H thin films deposited by HW-CVD method as a function of silane concentration and filament temperature, steady state photoconductivity (SSPC), dual beam photoconductivity (DBP), and optical transmission methods were used. Absolute absorption coefficient α (hν), spectrum was calculated from DBP and optical transmission spectra to see the effect of microstructure on the low energy sub-bandgap absorption coefficient values. Finally, the absolute α (hν) results are compared with those of photothermal deflection spectroscopy (PDS), constant photocurrent method (CPM).

Steady state photoconductivity measurements were carried out in order to investigate the photosensitivity of μc-Si: H thin films due to changing silane concentration during the deposition process of HW-CVD method. Log-log plot of photoconductivity, σ_{ph}, versus generation rate results show a linear dependence on the generation rate, G, meaning that σ_{ph} versus generation rate obeys the non-integer power law, $\sigma_{ph} \propto G^{\gamma}$ .The exponent γ gives direct information about recombination kinetics between photogenerated electrons and holes. The value of exponent γ was found to be between 0.5-1.0. The obtained exponent values indicate that for higher silane concentration, photogenerated free electrons in the conduction band recombine with holes in the valence band through the defect states present in the bandgap of μc-Si: H thin films, however, for highly crystalline films deposited with lowest silane concentration, photogenerated electrons in the conduction band recombine directly with holes in the valence band extended states for which the exponent is equal to 0.5. In addition, the quantitative information about the mobility lifetime product, $\mu_n\tau_n$ –product, of majority carriers is obtained using steady state photoconductivity measurements. The obtained results indicate that the $\mu_n\tau_n$–product decreases with increasing G. For higher SC=10%, the lowest $\mu_n\tau_n$ –product values around 10^{-6} was obtained indicating that amorphous phase with highest defects dominates in the bandgap which reduces the electron lifetime. Thus, the lowest values of $\mu_n\tau_n$ –product are generally obtained for amorphous like film. As SC decreases, $\mu_n\tau_n$ –product increases and show maximum values for films deposited at SC=6%. This region is called as a transition from microcrystalline to amorphous structure (Vetterl et. al 2000a, Klein et. al 2004a, Goktas et. al 2005b). Further decrease of the SC does not improve the $\mu_n\tau_n$ –products but a decrease in photosensitivity is observed for highly crystalline film deposited at SC=2%. This indicates that life time of free carriers is reduced due to increased recombination centers present on the walls of the crystalline grain boundaries. Such increases in defect states are also reported by ESR measurements (Finger et. al 1998b).

The optical absorption coefficient, α (hν), spectrum of μc-Si: H thin film is important to obtaining the information about the electronic and optical properties of the material. In addition, at lower energies, the absolute α (hν) values has been taken as a comparison criteria for different samples, since it gives information about the level of defect states present in the bandgap of the material. Therefore, the sub-bandgap

absorption coefficient spectrum is used to compare different materials prepared under different deposition conditions.

Since DBP is a relative photoconductivity measurement technique, the absolute absorption coefficient is not directly obtained from DBP measurements. In literature, the obtained DBP yield spectrum has been normalized to T&R or PDS spectrum in order to obtain the optical α (hν) spectrum in absolute scale. In addition, DBP yield spectrum has interference fringes. The fringes in the spectrum must be eliminated using fast Fourier Transform, since the absolute absorption coefficient spectrum is free of fringes. On the other hand, some important information can be lost during this process since these fringes are not only due to interference of light but also due to inhomogeneity of the material (Amato et. al 1990). However, in this thesis, to get ride of these interference fringes on DBP yield spectrum and the fringe free absolute α (hν) spectrum from DBP and optical transmission spectra, a procedure based on Ritter and Weiser formula (Ritter and Weiser 1986) was used as explained chapter 2. Using this procedure, no information about the inhomogeneity of material lost. Therefore, it gives information about the structure of the material as well. The resulting absolute α (hν) spectrum are compared with those independently measured by PDS method. In high energy region, a perfect overlap was observed in the absolute α (hν) spectra of PDS and DBP; however some differences were observed among three spectra for μc-Si: H thin films at the lower energy region. It is found that the absolute α (hν) spectrum calculated from the raw PDS spectrum is higher than those of DBP, also very noisy at sub-bandgap energies. This higher absorption of PDS can be attributed to the substrate absorption and higher defective surface layer. On the other hand, the absolute α (hν) spectrum of DBP is noisy free and reflects the defect of bulk material. The absolute α (hν) values of DBP spectrum in the sub-bandgap energies does not results in absolute absorption coefficient. However it reflects the occupied defect states present in the material. This situation can be attributed to DBP measurement dependence on the bias light intensities. The DBP measurements obtained using low bias light intensity probes the distribution of occupied defect states which are very close to that in dark condition. With increasing bias light intensity, the density of occupied defect states above the Fermi level increases. Therefore, more transitions form these occupied defect states to conduction band at bandgap energies occur. As a result of these transitions, the absolute α (hν) values show an increase in the spectrum at low energies.

At lower energies, the absolute α (hν) values measured by low bias light DBP are lower than those obtained from PDS measurements. These differences between PDS and DBP spectrums can be attributed to the nature of both methods. This means that PDS probes all transition from occupied states to empty states, on the other hand only the transition from occupied defect states into empty conduction band extended states can be probe by the low bias light DBP measurement. For this reason, the absorption coefficient values in the sub-bandgap region are used as a comparison of different materials. The obtained results from DBP method were also compared with those of constant photocurrent method (CPM). Even though in high energy region, the absolute α (hν) spectrums obtained from both methods are in agreement with each other, at low energies below the 1.4 eV, some differences between two absolute α (hν) spectrums are observed. Since only low generation rate ac monochromatic light used in CPM, which is significantly lower than the low bias dc light intensity used in DBP, the obtained CPM spectrum shows lower values than low bias light DBP. In order to obtain DBP spectrum closer to that CPM spectrum, the intensity of the bias light must be decreased further. This has been carried out successfully for some samples. As a result, the absolute absorption coefficient spectra obtained from two methods agree very well at all energies. Finally, absolute α (hν) spectrum obtained by three different methods are agree very well at higher energies for all the samples indicating that three methods probe the same distribution of states. However, at lower energies, sub-bandgap absorption results must be carefully evaluated to understand the effects of deposition conditions.

The absolute α (hν) values at 0.8 eV measured by both PDS, and DBP low bias light intensity were used to investigate the defect states present in the material. As PDS and low bias light DBP methods compared, PDS always results in higher sub-bandgap absorption coefficients. However, both methods indicate the similar functional dependence on the SC as shown in Figure 3.9. It is found that the μc-Si: H thin films deposited at lower silane concentration show higher absorption α (hν) values at 0.8 eV. It can be inferred that highly crystalline μc-Si: H thin films contain high defect density. As silane concentration increases the absolute α (hν) values at 0.8 eV decrease and give minima at around 5% of SC. At this critical value of silane concentration (SC=5%), a transition from microcrystalline to fully amorphous phase has been observed. The absolute α (hν) values at 0.8 eV tend to increase as silane concentration further increases. These results show that the μc-Si: H thin films deposited in the transition

region have lowest defect density and will result in a better performance in solar cells. As we have discussed in previous section, these films show the highest photosensitivity consistent with α (hν) results.

Moreover, the defect states inferred from absolute α (hν) values at 0.8 eV obtained from PDS and low bias DBP measurements is also consistent with the defect density measured by ESR method (Yamamoto et. al 2002, Vetterl et. al 2002, Shah et. al 2000b, Mai et. al 2004, Klein et. al 2003c, Gross et. al 2001). Higher defect densities are measured by the ESR measurements for highly crystalline μc-Si: H thin film. On the other hand, ESR measurements give information about only three paramagnetic defects in undoped μc-Si: H, which gives resonance at g= 2.0052, g= 2.0043. These two defects represent the majority of deep defects in the gap of μc-Si: H and in addition, defects with g= 1.996-1.998 are also observed. The resonance at 2.0052 is attributed to Si dangling bonds (db's). The resonance at 2.0043 is still unclear, but the speculations in the literature show that this resonance is caused by Si db's in oxygen rich regions. The last measured resonance at 1.996-1.998 is attributed to conduction electrons (CEs) in the crystalline regions of the material. Although ESR senses only the paramagnetic defects, DBP can probe not only paramagnetic defect states but also non-paramagnetic (charged) defect states. The non-paramagnetic defect states consist of doubly occupied Si dangling bonds (negatively charged) and unoccupied Si dangling bonds (positively charged). These defect states are most common defects in a-Si: H films and affect high and low bias DBP measurements. Therefore, it is impossible to identify which defects cause the sub-bandgap absorption coefficient measured at lower energies.

The effect of silane concentration on the absolute absorption coefficient spectrum calculated using DBP and optical transmission spectra were investigated for μc-Si: H deposited by HW-CVD with filament temperature of 1700 ºC. For higher silane concentration SC=10% film, the obtained absolute α (hν) spectrum is similar to that of a-Si: H films. This means that the film exhibits amorphous like characteristics. As SC decreases, the crystalline region increases and the shape of the absolute α (hν) spectrum becomes similar to that of crystalline silicon. For SC=7%, it is clearly seen that the shape of the absolute α (hν) spectrum becomes more like that of crystalline silicon due to dominating microcrystalline phase in microstructure. As crystalline phase increases with decreasing SC, the microstructure substantially changes the absolute α (hν) spectrum. The α (hν) decreases as SC decreases and given a minimum around SC=5%. As SC decreases further, highly crystalline microcrystalline silicon thin film is

produced. However, the absolute α (hν) values starts increasing again. It indicates that the defect density present in the material increases. Therefore, the lowest α (hν) values are obtained for film deposited under the SC around 5%. These observations are consistent with photosensitivity results of the same samples, where highest $\mu_n\tau_n$ –products are obtained for sample SC=5-6% and lowest $\mu_n\tau_n$ –products values are obtained for highly crystalline and amorphous sample. These results indicate that solar cells prepared with absorber layers in the SC=5-6% region will exhibit the band solar cell characteristics. Such results have already reported for the μc-Si: H solar cells by several groups (Vetterl et. al 2000a, Klein et. al 2004a, Goktas et. al 2005b).

The microstructure of μc-Si: H deposited by HWCVD method strongly depends on another deposition condition, filament temperature. Therefore, the effect of filament temperature on the microstructure of μc-Si: H deposited using HWCVD method at filament temperature between 1700 ºC-1880 ºC with constant silane concentration SC=10% was investigated. Steady state photoconductivity measurements indicate that for higher filament temperature T_f=1880 ºC, the slope γ is equal to 0.96, which is very close to unity and generally observed for amorphous silicon. However, the results indicate that the film deposited at T_f=1880 ºC shows higher photoconductivity values which is related to the increasing microcrystalline region in material. With decreasing filament temperature, the amorphous phase dominates in the microstructure. Therefore, the growths of films at lower filament temperature exhibit amorphous like characteristics.

The effects of filament temperature on the absolute α (hν) spectrum obtained were investigated for μc-Si: H thin films deposited at constant SC=10% with changing filament temperature between 1700-1880 ºC. For filament temperature of 1700 ºC, the obtained absorption coefficient spectrum exhibits amorphous like characteristics. As filament temperature increases to 1880 ºC, the α (hν) spectrum is similar to that measured for T_f=1700 ºC, i.e. microstructure is still amorphous in nature. When filament temperature increases to 1880 ºC, there exists a substantial change in the α (hν) spectrum and it becomes similar to that of crystalline silicon. This indicates that growth of microcrystalline phase becomes dominant and absorption edge shifts to lower energies (Jadkar et. al 2003).

The effect of filament temperature in microcrystalline growth regime is also interesting note. However, a complete set for silane concentration from each filament

temperature was not available. Therefore, there is no comparison can be done for such series of μc-Si: H films.

Finally, it was found that for most film, obtained calculation of absorption coefficient spectrum exhibited interference fringes left on the fringe free calculated α (hν) spectrum. There is an indication of inhomogeneous absorption of light due to defective layer on the surface, at the substrate- film interface or inhomogenities throughout the bulk (Goktas et. al 2005b). In the microcrystalline growth, it generally exists a defective amorphous layer on the glass substrate than columnar crystalline regions forms on film growth. In addition, at the top surface, rough defective surface layer also exists. In order to investigate the level of inhomogeneity and its effect on the α (hν) spectrum, DBP measurements were carried out by ac monochromatic light through film and through substrate side. It is found that there exists difference between spectra measured through film and substrate side for the same sample. The level of interference fringes left on the α (hν) spectrum changes and magnitude of α (hν) generally is higher for back ac measurements for most of the samples. A highly defective interface layer at the film substrate interface and/or inhomogeneity throughout the bulk exists. They affect optical measurements and care must be taken in evaluation of real α (hν) spectrum. This effect exists exactly same in nature for α (hν) spectrum measured by three different absorption spectroscopy methods, resulting in exactly the same shape and magnitude of interference fringes left on the fringe free calculated α (hν) spectrum. For the future study, the nature and degree of the inhomogeneity should be investigated in detailed when sample is in high vacuum environment and for different temperature regimes.

REFERENCES

Akdas, D. 2002. MSc Thesis. "Sub-bandgap absorption spectroscopy and its application to amorphous semiconductor materials" Izmir Institute of Technology, Department of Material Science and Engineering, Izmir.

Amato, G., Benedetto, G., Boarino, L., and Sagnolo, R. 1990. "Photothermal detection of surface states in amorphous silicon films" *Appl. Phys. A* Vol. 50, p. 503.

Beck, N., Meier, J., Fric, J., Remes, Z., Poruba A., Fluckiger, R., Pohl, J., Shah, A., Vanecek, M. 1996. "Enhanced optical absorption in microcrystalline silicon "*J. Non-Crys. Solids*.Vol.198-200, p. 903.

Boehme, C., Lips, K. 2004. "The nature of dangling bond recombination in c-Si: H" *Journal of Non-Crystalline Solids* Vol. 338-340, pp.434- 439.

Bube, H. R., Benatar, E. L., Grimbergen, N. M., and Redfield, D. 2004. "Corrections to the constant photoconductivity method for determining defect densities, with application to amorphous silicon" *J. Appl. Ph*ys. Vol. 72, p. 12.

Carius R., Merdzhanova T., Finger, F., Klein, S., Vetterl, O. 2002a. "A comparison of microcrystalline silicon prepared with plasma enhanced chemical vapor deposition and hot wire chemical vapor deposition: electronic and device properties "*Journal of Material Science; Materials in Electronics* Vol. 14, p.625-628.

Carius, R. 2001b."Structural and optical properties of microcrystalline silicon for solar cell applications" in Photovoltaic and Photoactive Materials-Properties, Technology and Application, NATO Science series 2 , vol. 80, p.93.

Carius, R., Finger, F., Backhousen, U., Luysberg, M., Hapke, P., Houben, L., Otte, M., Overhoff, H. 1997c. "Electronic Properties of Microcrystalline Silicon" *Mater. Res. Soc. Symp. Proc*. Vol. 467, p.283.

Cody, G. D., Wronski, C. R., Abeles, B., Stephens, R., and Broks, B. 1980a."Optical characterization of amorphous silicon hydride films " *Solar Cells*. Vol. 2, p. 227.

Cody, G. D.1984b. *in Semiconductors and semimetals*, Vol. 21B, ed. J. I. Pankove (Academic Press ,New York), p. 11.

Faraji, M., Gokhale, S., Choudhari, S. M., Takwle, M. G., Ghaisas, S. V. 1992. "High mobility hydrogenated and oxygenated microcrystalline silicon as a photosensitive material in photovoltaic applications" *Appl. Phys. Lett*. Vol. 60, p. 3289.

Feitknecht, L., Kluth, O., Ziegler, Y., Niquille, X., Torres, P., Meier, J., Wyrsch, N., Shah, A. 2001."Microcrystalline n-i-p solar cells deposited at 10 Å/s by VHF-GD "*Solar Energy Mater. Solar Cells*. Vol. 66, p.397.

Finger, F., Hapke, P., Luysberg, M., Carius, R., Wagner, H., and Scheib, M. 1994a. "Improvement of grain size and deposition rate of microcrystalline silicon by use of very high frequency glow discharge" *Appl. Phys. Lett*. Vol. 65, p. 2588.

Finger, F. Muller, J., Malten, C., and Hapke, H. 1998b. "Electronic states in hydrogenated microcrystalline silicon" *Philosophical Magazine B,* Vol. 77, No.3, pp. 805- 830.

Finger, F., Neto, A.L.B., Carius, R.,Dylla, T., and Klein, S. 2004c."Paramagnetic defects in undoped microcrystalline silicon" *Phys. Stat. Sol. C* .1, No.5, pp. 1248-1254.

Flückiger, F., Meier, J., Keppner, H., Kroll, U., Shah, A., Greim, O., Morris, M., Pohl, J., Hapke, P., Carius, R.1992. "Microcrystalline Silicon prepared with the Very High Frequency Glow Discharge Technique for p-i-n Solar Cell Application" Proc. of the 11th EC PV Solar Energy Conference, Montreux.

Goktas, O. 2004a. MSc. Thesis. "Sub-bandgap absorption spectroscopy in microcrystalline silicon thin films" Izmir Institute of Technology, Department of. Physics, Izmir.

Goktas, O., Isik, N., Okur, S., Gunes, M., Carius, R., Klomfass, J., Finger, F. 2005b. "Sub-bandgap optical absorption spectroscopy of hydrogenated microcrystalline silicon thin films prepared using hot wire CVD (Cat-CVD) process" *Thin solid Films*, Submitted.

Gross, A., Vetterl, O., Lambertz, A., Finger, F., Wagner, H., and Dasgupta, A. 2001. "N-side illuminated microcrystalline silicon solar cells" *Appl. Phys. Lett.* Vol. 79, p. 2841.

Gunes, M., and Wronski, C. R.1992a. "Differences between light induced and native midgap states in intrinsic hydrogenated amorphous silicon obtained from detailed modeling of photoconductivities and sub-bandgap absorption" *Appl. Phys. Lett.* Vol. 61, p. 678.

Gunes, M., Akdas, D., Goktas, O., Carius, R., Klomfass, J., and Finger, F. 2003b. "Photoconductivity spectroscopy in hydrogenated microcrystalline silicon thin films" *J. Mater. Sci: Mat. In Electr*. Vol. 14, p. 729.

Gunes, M., Goktas, O., Okur, S., Isik, N., Carius, R., Klomfass, J., Finger, F., 2005c "Sub-bandgap absorption spectroscopy and mınority carrier transport propertıes of hydrogenated microcrystalline silicon thin films" *J. of Opt. Elect. and Adv. Mater*. Vol. 7, No. 1, pp. 161-168.

Houben, L., Luysberg, M., Hapke, P., Carius, R., and Wagner, H. 1998."Structural properties of microcrystalline silicon in the transition from highly crystalline to amorphous growth " *Philos. Mag. A*. Vol. 77, p. 1447.

Jackson, W., Amer, N. M., Boccara, A. C., and Fournier, D. 1981a." Photothermal deflection spectroscopy and detection" Appl. Opt. Vol. 20, p. 1333.

Jackson W., and Amer, N. M. 1982b. "Direct measurement of gap-state absorption in hydrogenated amorphous silicon by photothermal deflection spectroscopy" *Phys. Rev. B.* Vol. 25, p. 5559.

Jadkar, S.R., Sali, J.V., Kshrisagar, S.T., Takwale, M.G. 2003."Deposition of hydrogenated amorphous silicon (a-Si:H) films by hot wire chemical vapor deposition: role of filament temperature" *Thin Solid Films*. Vol. 437 p. 18-24.

Jensen, P. 1990. "Deconvolution of CPM absorption spectra: A new technique " *Solid State Communications*, Vol. 76, No. 11, p. 1301-1303.

Jun, K. H., Carius, R., and Stiebig, H. 2002. "Optical characteristics of intrinsic microcrystalline silicon" *Phys. Rev. B* Vol. 66, p. 115301.

Klein, S., Repmann T., Brammer T. 2004a. "Microcrystalline silicon films and solar cells deposited by PECVD and HWCVD" *Solar Energy* Vo. 77, pp. 893-908.

Klein, S., Finger, F., Carius, R., Wagner, H., Stutzmann, M. 2001b."Intrinsic amorphous and microcrystalline silicon by hot-wire-deposition for thin film solar cell applications "*Thin Solid Films*. Vol. 395, p. 305.

Klein, S., Finger, F., Carius, R., Dylla, T., Rech, B., Grimm, L., Stutzmann, M. 2003c."Intrinsic microcrystalline silicon prepared by hot-wire chemical vapor deposition for thin film solar cells "*Thin Solid Films*. Vol. 430, p. 202.

Kondo, M. 2003."Microcrystalline materials and cells deposited by RF glow discharge" *Solar Energy Materials & Solar Cells*. Vol. 78, pp. 543-566.

Lee, S., Kumar, S., Wronski, C.R., and Maley, N.M. 1998." A critical investigation of a-Si:H photoconductivity generated by subgap absorption of light "J. *Non-Cryst, Solids.* Vol. 114, p. 316.

Lima, M. M. De., Morrison, S., LeGeune, A., Marques, F. C., and Taylor, P.C.2002. "Paramagnetic Centers in Microcrystalline Silicon" *Mat. Res. Symp. Proc*. Vol. 715.

Lips, K., Kanschat, P., Fuhs, W. 2003. "Defects and recombination in microcrystalline silicon " *Solar Energy Mat& solar Cells*. Vol. 78, p. 513.

Lucovsky, G., Wang, C., Nemanich, R. J., Williams, M. J.1991."Deposition of c-Si and c-Si---C thin films by remote plasma-enhanced chemical-vapor deposition "*Solar Cells*. Vol. 30, p. 419.

Luysberg, M., Hapke, P., Carius, R., Finger, F.1997. "Structure and growth of microcrystalline silicon: investigation by TEM and Raman spectroscopy of films grown at different plasma excitation frequencies" *Philosophical Magazine A* Vol. 75, No. 1, p. 31.

Mahan, A. H., Carapella, J., Nelson, B. P., Crandall, R. S., Balberg, I.1991. "Deposition of device quality, low H content amorphous silicon" *J. Appl. Phys. Vol.* 69, p. 6728.

Mai, Y., Klein, S., Geng, X., and Finger, F.2004. "Structure adjustment during high-deposition-rate growth of microcrystalline silicon solar cells" *Appl. Phys. Lett*. Vol. 85, pp. 2839-2841.

Matsuda, A. 1983. "Formation kinetics and control of microcrystallite in c-Si: H from glow discharge plasma" *Journal of Non- Crystalline S*olids. Vol. 59/60, pp. 767-747.

Matsumura, H.1986. "Catalytic Chemical Vapor Deposition (CTC-CVD) Method Producing High Quality Hydrogenated Amorphous Silicon "*Jap. J. Appl. Phys*. Vol. 25, p. L949.

Meier, J., Fluckiger, R., Keppner, H., Shah, A.1994a."Complete microcrystalline p-i-n solar cell—Crystalline or amorphous cell behavior?" *Appl. Phys. Lett*. Vol. 65, p. 86.

Meier, J., Torres, P., Platz, R., Dubail, S., Kroll,U., Selvan, J. A. A., Pellaton-Vaucher, N., Hof, C., Ficsher, D., Keppner, H., Shah, A., Ufert, K. D.1997b. "Towards high efficiency thin-film silicon solar cells with the "micromorph" concept" *Solar Energy Material Solar Cells.* Vol. 49, p. 35.

Nasuno, Y., Kondo, M., Matsuda, A.2000. "Microcrystalline silicon thin-film solar cells prepared at low temperature using RF-PECVD" Photovoltaic Specialists Conference Record of the Twenty-Eighth IEEE. p. 142-145.

Neto, A.L.B., Lambertz, A., Carius, R., Finger, F.2002a. "Relationships between structure, spin density and electronic transport in 'solar-grade' microcrystalline silicon films " *Journal of Non-Crystalline Solids* Vol. 299- 302, pp. 274-279.

Neto, A. L. B., Dylla, T., Klein, S., Repmann, T.2004b. Lambertz, A., Carius, R., and Finger, F., "Defects and structure of hydrogenated microcrystalline silicon films deposited by different techniques" *Journal of Non-Cryst. Solids* Vol. 338-340, p. 168.

Ossadnik, Ch., Veprek, S., and Gregora, I.1999." Applicability of Raman scattering for the characterization of nanocrystalline silicon "Thin Solid Films. Vol. 337, p.148.

Pierz, K., Mell, H., and Terukov, J. 1985. "Sub-bandgap absorption in a-Si: H from photoconductivity spectra "*J. of Non-Cryst. Sol*. Vol 77-78, p. 547.

Poruba, A., Fejfar, A., Remes, Z., Springer, J., Vanecek, M., Kocka, J., Meier, J.,Torres, P., Shah, A. 2000a."Optical absorption and light scattering in microcrystalline silicon thin films and solar cells" *J. Appl. Phys.* Vol. 88, p.148.

Poruba, A., Fejfar, A., Salyk, O., Vanevek, M., Kocka, J. 2000b." Surface and bulk light scattering in microcrystalline silicon for solar cells "*J. Non-Crys. Solids* Vol. 271, p. 152.

Proceedings of the 3rd World Conference on Photovoltaic Energy Conversion. 2003. Osaka, Japan.

Rath, J. K.2002. "Micro and poly -crystalline silicon materials for thin film photovoltaic devices "deposition process and growth mechanism" in Photovoltaic and Photoactive Materials-Properties, Technology and Application, NATO Science series 2. vol. 80 p. 157.

Ray, S., Mukhopadhyay, S., Jana, T., Carius, R.2002." Transition from amorphous to microcrystalline Si:H: effects of substrate temperature and hydrogen dilution " *Journal of Non-Cryst. Solids*. Vol. 299-302, p. 761.

Ritter, D., and Weiser, K.1986."Suppression of interference fringes in absorption measurements on thin films "*Opt. Commun*. Vol. 57, p. 336.

Schroop, R. E. I.2004. "Present status of micro- and polycrystalline silicon solar cells made by hot-wire chemical vapor deposition" *Thin Solid Films*. Vol. 451-452, pp. 455-465.

Shah, A.V., Meier, J., Vallat-Sauvain, E., Wyrsch, N., Kroll, U., Droz, C., Graf, U.2003a. "Material and solar cell research in microcrystalline silicon" *Solar Energy Materials & Solar Cells*. Vol. 78, pp. 469-491.

Shah, A., Vallat-Sauvain, E., Torres, P., Meier, J., Kroll, U., Hof, C., Droz, C., Goerlitzer, M., Wyrsch, N. and Vanecek, M.2002b."Intrinsic microcrystalline silicon (c-Si:H) deposited by VHF-GD (very high frequency-glow discharge) a new material for photovoltaics and optoelectronics" *Mater. Sci. B*. Vol. 69/70, p. 219.

Sinha, A. K., and Agarval, S. C.1998." Determination of surface states in hydrogenated amorphous silicon by subgap absorption measurements" Philosophical Magazine B. Vol. 77, No. 4, pp. 945-957.

Swanepoel, R.1983." Determination of the thickness and optical constants of amorphous silicon" *J. Phys. E*. Vol. 16, p. 1214.

Usui, S., Kikuchi, M.1979. "Properties of heavily doped GD---Si with low resistivity "*J. Non- Cryst. Solids*. Vol. 3, p. 1.

Vanecek, M., Poruba, A., Remes, Z., Beck, N., Nesladek, M.1998a." Optical properties of microcrystalline materials " *J. Non-Crys. Solids*. Vol. 227-230, p. 967.

Vanecek, M., Kocka, J., Poruba A., and Fejfar, A.1995b."Direct measurement of the deep defect density in thin amorphous silicon films with the ``absolute" constant photocurrent method" *J. Appl. Phys*. Vol. 78, p. 6203.

Vanecek, M.,Kocka, J., Stucklik, j., Kozisek,Z., Stika, O., and Triska, A.1983c. "Density of the gap states in undoped and doped glow discharge a-Si:H" *Solar Energy Materials*. Vol. 8, p. 411.

Veprek, S., Maracek, V.1986a."The preparation of thin layers of Ge and Si by chemical hydrogen plasma transport "*Solid State Electron*. Vol. 11, p. 683.

Vetterl, O., Finger, F., Carius, R., Hapke, P., Houben, L., Kluth, O., Lambertz, A., Mück, A., Rech, B., Wagner, H. 2000a. "Intrinsic microcrystalline silicon: A new material for photovoltaics" *Solar Energy Materials & Solar Cells.* Vol. 62, p. 97.

Vetterl, O., Groβ, A., Jana, T., Ray ,S., Lambertz, A., Carius, R., Finger, F.2002b." Changes in electric and optical properties of intrinsic microcrystalline silicon upon variation of the structural composition "*Journal of Non- Crys. Solids*. Vol. 299-302, p. 772.

Wiedeman, S., Bennet, M. S., and Newton, J. L.1987. *Mat. Res. Soc. Symp*. Proc. Vol. 95, p.145.

Wronski, C.R., Abeles, B., Tiedje, T., and Cody, G.D.1982."Recombination centers in phosphorous doped hydrogenated amorphous silicon " *Solid State Comm.*Vol. 44, p. 1423.

Wyrsch, N., Torres, P., Goerlitzer, M., Vallat, E., Kroll, U., Shah, A., Poruba, A., Vanecek, M, 1995a" Hydrogenated microcrystalline silicon for photovoltaic applications" *Solid State Phenomena*, Vol. 44-46, p. 525

Wyrsch, N., Finger, F., McMahon, T.J., and Vanecek, M.1991b."How to reach more precise interoretation of subgap absorption spectra in terms of deep defect density in a-Si: H" *Journal of Non-Crystalline Solids*, Vol 137-138, pp. 347-350.

Yamamoto, K., Yoshimi, M., Tawada, Y., Fukuda, S., Sawada, T., Meguro, T., Takat, H., Suezaki, T., Koi, Y., Hayashi, K., Suzuki, T., Ichikawa, M., Nakajima, A. 2002. "Large area thin film Si module" *Solar Energy Materials and Solar Cells*. Vol. 74, pp. 449-455.

APPENDIX A

COMPUTER PROGRAM USED FOR DBP MEASUREMENTS

This program used for DBP measurements was written in ObjectBench software. It was first written by D. Akdas on this system and improved during the previous and this thesis study. It used to control lock-in amplifier, monochromator driver, and filter driver and for data acquisition between computer and lock-in amplifier. The commands are written in regular fonts and explanations are written in italic fonts.

start: *the main loop*

graphcomment$="Comments about the graph "

sensflag=0:timeflag=0.3:oldflag=0.3

dir$="D: \" *Defines the directory that data willl be stored*

input "sample name",sampname$: filecomment$=sampname$

rem **********************************

input "data file name",dbs$

format #1,energy["energy=","eV"],average["average current=","A"],avgdevia["angle=",""],-

ratio["dc/ac=",""],absorp["absorp. coeff.=",""]

format #2,energy["energy=","eV"],curr[" current=","a"],avgdevia["angle=",""]

format #3,energy["energy=","eV"],Logaverage["average current=","A"],avgdevia["angle=",""],Logratio["dc/ac=",""],Logabsorp["absorp. coeff.=",""]

open #1, file= dir$+dbs$+".dat",desc$,overwrite

rem open #1, file= dbs$+".dat",desc$,overwrite

open #2, file= "v"+dbs$+".dat",desc$,overwrite

open #3, file= "graph_f.dat",desc$,overwrite

open #3, graph= "dualbeam",overwrite

open #3, screen

The files to store data and to use screen are defined

rem **********************************

```
input "first value of energy",start Initial values are defined
input "step value for energy",step
input "input number of measurements for each energy",n
input "enter dc current dueto bias light(format 1e-5 )",dcac
rem ****************************************

rem ****************************************
gosub fluxRead Flux file will be read and will be used to normalize raw current
rem*******************************************
Lock-in amplifier will be initialized
gpibwrite(8,"OUTX 1,OVRM 1"):gpibwrite(8,"*RST"):gpibwrite(8,"*CLS"):
gpibwrite(8,"FMOD 0"):gpibwrite(8,"DDEF 1,1,0"):gpibwrite(8,"DDEF 2,1,0"):
gpibwrite(8,"ICPL 0"):gpibwrite(8,"ISRC 2"):gpibwrite(8,"OFSL 3")
gpibwrite(8,"IGND 1"):rem gpibwrite(8,"SENS 23"):gpibwrite(8,"SYNC 1")
gpibwrite(8,"OFLT 9"):gpibwrite(8,"AGAN"):gosub delay4:gosub delay4
gpibwrite(8,"ARSV"):gosub delay4:gosub delay4:gpibwrite(8,"APHS")
gosub delay4:gosub delay4:gosub delay4:gpibwrite(8,"RMOD 1")
gosub delay4:gosub delay4:gosub delay4:
rem
energy=start the initial energy value is defined
wl=6200/energy: fark=(2.5-start) : fark=fark/(0.02) : bbb$=str$(fark) :
z=val(mid$(bbb$,1,2))
loop: the main loop of the measurement
sum=0: dvsum=0: r=0: z=z+1
rem ********************************
loopa:
r=r+1

The value of CH1 and CH2 will be read
gpibwrite(8,"OUTR? 1") : a$=gpibread$(8) : gpibwrite(8,"OUTR? 2") :
j$=gpibread$(8)
curr=val(mid$(a$,1)) : standdev(r)=curr : ? "current=",curr," A" : devia=val(mid$(j$,1))
angldev(r)=devia : ? devia : sum=sum+curr : dvsum=dvsum+devia
rem **************
```

```
write #2 The value of CH1 and CH2 wil be stored for temporary use
if timeflag=0.3 then gosub delay3msec Here the appropriate delay is set
if timeflag=1 then gosub delay1sec
if timeflag=3 then gosub delay3sec
if timeflag=10 then gosub delay10sec
if timeflag=30 then gosub delay30sec
rem ************************

if r<n then goto loopa For each energy value n data will be read
average=sum/n : avgdevia=dvsum/n The current and phase averaged
rem ************************************
b$=str$(wl) : wv=val(mid$(b$,1,5)) : realw=2*wv
ratio=dcac/average the value of dc current over ac current is calculated
absorp=average/y(z) the average raw current is divided to flux value to normalize it
Logabsorp=0.43429489*log(absorp) To show data on the screen in log scale
Logaverage=0.43429489*log(average) To show data on the screen in log scale
Logratio=0.43429489*log(ratio) To show data on the screen in log scale
Write #1 The raw current, phase, dc over ac ratio and normalized current is stored
write #3 The data is written on the screen in log scale
if z=94 then goto bitti
Monochromator will be set to next energy value (wavelenght)
energy=energy-step
wl=6200/energy : c$=str$(wl) : wk=val(mid$(c$,1,5)) : filterw=2*wk
kf=wk-wv : d$=str$(kf) : kw=0.5*kf : f$=str$(kw) : wt=val(mid$(f$,1,3))
i$=str$(wt) : kg=0.3*kf : g$=str$(kg) : wy=val(mid$(g$,1,3)) : h$=str$(wy)
rem ------------------------------
if energy=1.86 then gosub ttl Filters willl be changed
if energy=1.36 then gosub ttl Filters willl be changed
if energy=1.0 then gosub ttl Filters willl be changed
gosub delay2
gpibwrite(14,"C") : gpibwrite(14,"E")
if energy>=0.9 then gosub shortw
if energy<0.9 and energy>0.8 then gosub midw
if energy<=0.8 then gosub longw
```

```
gosub delay
rem *******************
The fallowing delay is used to wait for saturation of signal after monochromator
changed the next energy value
if timeflag=0.3 then gosub delay1sec : if timeflag=0.3 then gosub delay1sec
if timeflag=1 then gosub delay1sec : if timeflag=1 then gosub delay1sec
if timeflag=1 then gosub delay1sec : if timeflag=3 then gosub delay3sec
if timeflag=3 then gosub delay3sec : if timeflag=3 then gosub delay3sec
if timeflag=3 then gosub delay3sec : if timeflag=10 then gosub delay10sec
if timeflag=10 then gosub delay10sec : if timeflag=10 then gosub delay10sec
if timeflag=10 then gosub delay10sec : if timeflag=10 then gosub delay10sec
if timeflag=30 then gosub delay30sec : if timeflag=30 then gosub delay30sec
if timeflag=30 then gosub delay30sec : if timeflag=30 then gosub delay30sec
if timeflag=30 then gosub delay30sec
gosub bosoku
xxx=1 The value of ac current will be read to set lock-in amplifier to the appropriate
sensitivity and time constant
lopsens:
gpibwrite(8,"OUTR? 1") : a$=gpibread$(8)
gpibwrite(8,"OUTR? 2") : j$=gpibread$(8)
curr=val(mid$(a$,1)) : ? "current=",curr," A"
devia=val(mid$(j$,1)) : average=average+curr
xxx=xxx+1
if xxx<6 goto lopsens
average=average/5
gosub delay : gosub delay
Lock-in amplifier will be set to the appropriate sensitivity and time constant will be set
depending on the value of signal
if 4.9e-7<=average and average<1e-6 then gosub sensita :
if 1.9e-7<=average and average<4.9e-7 then gosub sensitb
if 9e-8<=average and average<1.9e-7 then gosub sensitc
if 4.5e-8<=average and average<9e-8 then gosub sensitd
if 1.5e-8<=average and average<4.5e-8 then gosub sensite
if 8e-9<=average and average<1.5e-8 then gosub sensitf
```

```
if 4e-9<=average and average<8e-9 then gosub sensith
if 1.5e-9<=average and average<4e-9 then gosub sensitk
if 7.5e-10<=average and average<1.5e-9 then gosub sensitl
if 3.5e-10<=average and average<7.5e-10 then gosub sensitm
if 1.5e-10<=average and average<3.5e-10 then gosub sensitn
if 7.5e-11<=average and average<1.5e-10 then gosub sensito
if 3.5e-11<=average and average<7.5e-11 then gosub sensitp
if 1.5e-11<=average and average<3.5e-11 then gosub sensitr
if 7.5e-12<=average and average<1.5e-11 then gosub sensits
if 3.5e-12<=average and average<7.5e-12 then gosub sensitt
if 1.5e-12<=average and average<3.5e-12 then gosub sensitab
if 6.5e-13<=average and average<1.5e-12 then gosub sensitac
if 2.5e-13<=average and average<6.5e-13 then gosub sensitad
if 8e-14<=average and average<2.5e-13 then gosub sensitae
if 1e-14<=average and average<8e-14 then gosub sensitaf
if average<=1e-14 then gosub sensitag
if sensflag>=15 then gosub tflag300msec : if sensflag=14 then gosub tflag1sec
if sensflag=13 then gosub tflag3sec : if sensflag<13 and sensflag=>10 then gosub
tflag10sec
if sensflag<10 then gosub tflag30sec
if sensflag>=15 and oldflag<>timeflag then gosub tcons300msec
if sensflag=14 and oldflag<>timeflag then gosub tcons1sec
if sensflag=13 and oldflag<>timeflag then gosub tcons3sec
if sensflag=12 and oldflag<>timeflag then gosub tcons10sec
if sensflag=11 and oldflag<>timeflag then gosub tcons10sec
if sensflag=10 and oldflag<>timeflag then gosub tcons10sec
if sensflag<10 and oldflag<>timeflag then gosub tcons30sec
rem *****************************
if timeflag=0.3 then gosub delay1sec : if timeflag=0.3 then gosub delay1sec
if timeflag=1 then gosub delay1sec : if timeflag=1 then gosub delay1sec
if timeflag=1 then gosub delay1sec : if timeflag=1 then gosub delay1sec
if timeflag=1 then gosub delay1sec
if timeflag=3 then gosub delay3sec : if timeflag=3 then gosub delay3sec
if timeflag=3 then gosub delay3sec : if timeflag=3 then gosub delay3sec
```

```
if timeflag=3 then gosub delay3sec : if timeflag=3 then gosub delay3sec
if timeflag=10 then gosub delay10sec : if timeflag=10 then gosub delay10sec
if timeflag=10 then gosub delay10sec : if timeflag=10 then gosub delay10sec
if timeflag=10 then gosub delay10sec : if timeflag=10 then gosub delay10sec
if timeflag=30 then gosub delay30sec : if timeflag=30 then gosub delay30sec
if timeflag=30 then gosub delay30sec : if timeflag=30 then gosub delay30sec
if timeflag=30 then gosub delay30sec : if timeflag=30 then gosub delay30sec
if timeflag=30 then gosub delay30sec :

if z<=93 then goto loop
bitti:
gosub delay
? "Wait 30 seconds to finish the experiment"
gosub delay
gosub back Monochromator will be set to the initial energy value
close #1 : close #3 : stop
read dbs$+".dat",d : print d.time$
if not yesnobox("Okey?") then goto start
stop
bosoku:
gpibwrite(8,"OUTR? 1") : abc$=gpibread$(8) : gpibwrite(8,"OUTR? 2") :
jbc$=gpibread$(8)
return
ttl:
gpibwrite(8,"AUXV 1,1.4") : gpibwrite(8,"AUXV 1,0.8")
return
sensita: : gpibwrite(8,"SENS 26") : sensflag=26 : return
sensitb: : gpibwrite(8,"SENS 25") : sensflag=25 : return
sensitc: : gpibwrite(8,"SENS 24") : sensflag=24 : return
sensitd: : gpibwrite(8,"SENS 23") : sensflag=23 : return
sensite: : gpibwrite(8,"SENS 22") : sensflag=22 : return
sensitf: gpibwrite(8,"SENS 21") : sensflag=21 : return
sensith: gpibwrite(8,"SENS 20") : sensflag=20 return
sensitk: gpibwrite(8,"SENS 19") : sensflag=19 : return
```

```
sensitl: gpibwrite(8,"SENS 18") : sensflag=18 : return
sensitm: gpibwrite(8,"SENS 17") : sensflag=17 : return
sensitn: gpibwrite(8,"SENS 16") : sensflag=16 : return
sensito: gpibwrite(8,"SENS 15") : sensflag=15 : return
sensitp: gpibwrite(8,"SENS 14") : sensflag=14 : return
sensitr: gpibwrite(8,"SENS 13") : sensflag=13 return
sensits: gpibwrite(8,"SENS 12") : sensflag=12 return
sensitt: gpibwrite(8,"SENS 11") : sensflag=11 : return
sensitab: gpibwrite(8,"SENS 10") : sensflag=10 : return
sensitac: gpibwrite(8,"SENS 9") : sensflag=9 : return
sensitad: gpibwrite(8,"SENS 8") : sensflag=8 return
sensitae: gpibwrite(8,"SENS 7") : sensflag=7 return
sensitaf: gpibwrite(8,"SENS 6") : sensflag=6 return
sensitag: gpibwrite(8,"SENS 5") : sensflag=5 return
shortw: gpibwrite(14,"V100,S") : gosub delay : gpibwrite(14,"G+"+d$+",S"): return
midw: gpibwrite(14,"V100,S") : gpibwrite(14,"G+"+d$+",S") : return
longw: gpibwrite(14,"V100,S") : gpibwrite(14,"G+"+d$+",S") : return
rem *********************************
tflag300msec: timeflag=0.3 : return
tflag1sec: timeflag=1 : return
tflag3sec: timeflag=3 : return
tflag10sec: timeflag=10 : return
tflag30sec: timeflag=30 : return
tcons300msec: gpibwrite(8,"OFLT 9") return
tcons1sec: oldflag=timeflag : gpibwrite(8,"OFLT 10") return
tcons3sec: oldflag=timeflag : gpibwrite(8,"OFLT 11") : return
tcons10sec: oldflag=timeflag : gpibwrite(8,"OFLT 12") : return
tcons30sec: oldflag=timeflag :gpibwrite(8,"OFLT 13") return
back: gpibwrite(14,"V120,S") : gpibwrite(14,"G-7208,S") :return
rem ---------------------------------
delay0: t=time delay01:if time-t<500 then goto delay01 : return
delay: t=time delay0a1:if time-t<1000 then goto delay0a1 : return
rem --------------------------------------
delay3msec: t=time : delay111:if time-t<1000 then goto delay111: return
```

```
delay1sec: t=time : delay1sa:if time-t<1000 then goto delay1sa
return
delay3sec: t=time : delay1:if time-t<3000 then goto delay1 : return
delay10sec: t=time : delay133:if time-t<10000 then goto delay133 : return
delay30sec: t=time : delay1a1:if time-t<30000 then goto delay1a1 : return
delay4: t=time : delay5:if time-t<6000 then goto delay5 : return
delay2: t=time: delay5ed:if time-t<3 then goto delay5ed : return
delayshort: t=time : delayshrt:if time-t<10000 then goto delayshrt : return
delaymidle: t=time : delaymid:if time-t<60000 then goto delaymid : return
delaylong: t=time : delayl:if time-t<150000 then goto delayl :return

arabek: t=time : delayl123:if time-t<6000 then goto delayl123 :return
fluxRead: flux file is to be read into y variable
dim y(94) : m=0 : read "D:\name ",oku
k=0 : okut: k=k+1 : y(k)=oku(k,3) :rem print "y(",k,")",y(k)
if k<94 then goto okut : return
```

APPENDIX B

COMPUTER PROGRAM FOR CALCULATION OF $\alpha(h\nu)$ SPECTRUM

This program was written by O. Goktas in ObjectBench software and is used to calculate absolute absorption coefficient from DBP yield spectrum. It calculates the absorption coefficient based on the procedure discussed in Chapter 2.

```
filecomment$="Comments about the data"
input "data file name",dbs$
input "tickness",d
format #1,energy["energy","eV"],alfa["absolute alfa","cm^-1 "], abstr["absolute tr", " "]
open #1,file="folder name\"+dbs$+".dat",desc$,overwrite
format #2,energy["energy","eV"],absalfa["absolute alfa","cm^-1 "], abstr["absolute tr",
" "]
 open #2,file="alfatr.dat",desc$,overwrite
format #3,energy["energy","eV"],alfalog["absolute alfa","cm^-1 "], abstr["absolute tr",
" "]
open #3,file="g123.dat",desc$,overwrite
open #3, graph= "alfa tr",overwrite

Rxf=0.41
Tx=0.05
gosub troku
gosub dbpoku
maxbul:
dim z(94)
temp=0
trmax=0
? "max bulunuyor"
```

```
k=0
kars:
k=k+1
t(k)=oku(k,4)
if t(k)>trmax then gosub degistir
rem print k,t(k)
if k<boyut then goto kars
? "trmax",trmax
absolutetr:
k=0
trfark=1000
tx=0.05
kkk2:
k=k+1
t(k)=t(k)*0.92/trmax

rem print k,t(k)
fark=abs(t(k)-tx)
if fark<trfark then gosub exbul
if k<boyut then goto kkk2
? trmax
? ex
? trfark
rem burdan sonra Ax=1-Tx-Rx formulunden absolute A
rem  bulunacak
Ax=1-Tx-Rxf
gosub absoltealfa
gosub alfahesapfront
gosub dosyayaz
rem **** absolute alfa hesaplaniyor*****
stop

alfahesapfront:
r2=0.10
```

```
dim alfa(boyutdbp)
k=0
hh:
k=k+1
alfa(k)=(1/d)*(ln(0.5*((1-r2)*(1+Alf(k)/T(k))+sqrt((1-r2)*(1-
r2)*(1+Alf(k)/T(k))*(1+Alf(k)/T(k))+4*r2))))
if k<boyutdbp then goto hh
return

degistir:
trmax=t(k)
return
troku:
m=0
? "transmission okunuyor"
read "*.*",oku
boyut=oku.rows
? boyut
input akl$
dim t(boyut)
dim z(boyut)
k=0

okut:
k=k+1
t(k)=oku(k,4)
rem print k,t(k)
if k<boyut then goto okut
return

dbpoku:
? "DBP file  okunacak"
read "c:\OB\Data\absolutedeneme\*.*",okudbp
boyutdbp=okudbp.rows
```

```
? boyutdbp
input akl$
dim A(boyutdbp)
k=0

okut23:
k=k+1
A(k)=okudbp(k,5)
rem print k,A(k)
if k<boyutdbp then goto okut23
return

exbul:
trfark=fark
ex=k
return

absoltealfa:
dim Alf(boyutdbp)
? "absolute alfa hesaplanacak"
k=0
c=ex
okut23c:
k=k+1
Alf(k)=A(k)*Ax/A(c)
rem print k,Alf(k)
if k<boyutdbp then goto okut23c
return

dosyayaz:
k=0
kkk123:
k=k+1
energy=okudbp(k,1)
```

```
absalfa=Alf(k)
abstr=t(k)
alfa=alfa(k)
write #1
alfalog=log(alfa(k))
write #2
write #3
if k<boyutdbp then goto kkk123
return
```